![Tomas Bata University in Zlín — Centre of Polymer Systems]

Doctoral Thesis

Dispersion systems based on nanoparticles

Disperzní systémy na bázi nanočástic

Author: Ing. Eva Korábková

Degree programme: P3924 Material Sciences and Engineering

Degree course: 3911V040 Biomaterials and Biocomposites

Supervisor: doc. Ing. Věra Kašpárková, CSc.

Consultant: Ing. Lucie Urbánková, Ph.D.

Zlín, August 2023

ACKNOWLEDGMENT

CONTENT

ABSTRACT

Colloidal systems play an important role in various industrial fields. As these systems are usually unstable, considerable effort is devoted to their stabilization by suitable stabilizers. A wide range of substances is used for this purpose; however, due to the growing need to protect the environment, attention is increasingly focused on materials from renewable natural sources and materials showing biocompatibility with living systems. In this context, nanocellulose is considered one of the new potential candidates for the development of materials and products towards a more sustainable future. With the growing development of nanotechnology, nanocellulose has emerged as a very interesting material. Due to its remarkable properties, ecological nature, and easy availability, it is considered one of the most important "green" materials of the modern age.

Following the issue of stabilization of dispersion systems, the doctoral thesis is devoted to cellulose nanoparticles and their ability to stabilize colloidal dispersions. Specifically, two types of dispersion systems are studied here. The first type are classical dispersions, where the Pickering emulsions composed of a combination of titanium dioxide particles and cellulose nanoparticles are studied. Such systems could be used, for example, in UV protection products. The second type of studied systems includes conducting polyaniline-based colloidal dispersions prepared by polymerization in the presence of two types of cellulose nanoparticles, namely cellulose nanocrystals or nanofibers. In the next step, the work focused on the use of these systems for the preparation of Pickering emulsions and thin conducting films with potential applications in biomedicine.

Key words: *nanocellulose, polyaniline, Pickering emulsions, colloidal dispersion, stabilization*

ABSTRAKT

Koloidní systémy hrají významnou roli v řadě průmyslových odvětví. Jelikož se obvykle jedná o nestabilní systémy, je značné úsilí věnováno jejich stabilizaci pomocí vhodných stabilizátorů. Ke stabilizaci koloidních systémů lze použít širokou škálu látek, avšak vzhledem k rostoucím potřebám společnosti a nutnosti ochrany životního prostředí se pozornost stále více upírá na materiály z obnovitelných přírodních zdrojů a na materiály vykazující biokompatibilitu s živými systémy. V této souvislosti je nanocelulóza považována za jeden z nových potenciálních kandidátů pro vývoj materiálů a produktů směrem k udržitelnější budoucnosti. S rostoucím rozvojem nanotechnologií se nanocelulóza ukázala jako velmi zajímavý materiál. Díky svým pozoruhodným vlastnostem, ekologické povaze a snadné dostupnosti je považována za jeden z nejvýznamnějších „zelených" materiálů moderní doby.

V návaznosti na problematiku stabilizace disperzních systémů se dizertační práce věnuje nanocelulózovým částicím a jejich schopnosti stabilizovat koloidní disperze. Konkrétně jsou zde studovány dva typy disperzních systémů. Prvním typem jsou klasické koloidní disperze, kde je studována příprava Pickeringových emulzí využívající ke stabilizaci kombinaci částic oxidu titaničitého a částic nanocelulózy. Takové systémy by mohly najít uplatnění například v přípravcích na ochranu proti UV záření. Druhý typ studovaných systémů zahrnuje vodivé koloidní disperze na bázi polyanilinu připravené polymerací ve vodném prostředí využívající ke stabilizaci dva typy nanocelulózových částic, a to celulózové nanokrystaly nebo nanofibrily. V dalším kroku se práce soustředila na využití těchto systémů pro přípravu Pickeringových emulzí a tenkých vodivých filmů s potenciálními aplikacemi v biomedicíně.

Klíčová slova: *nanocelulóza, polyanilin, Pickeringovy emulze, koloidní disperze, stabilizace*

1. BACKGROUND

The field of nanotechnology is one of the most exciting and dynamic areas of science today. Nanotechnology deals with the production and use of materials of different types at the nanoscale level in various fields, such as medicine, the automobile industry, electronics, energy storage, catalysis, cosmetics, biotechnology, and environmental applications [1–3]. Nanomaterial is currently defined by the European Commission (2011/696/EU) as a *natural, incidental, or manufactured material containing particles, in an unbound state or as an aggregate or as an agglomerate and where, for 50 % or more of the particles in the number size distribution, one or more external dimensions is in the size range 1 nm – 100 nm.* Nanoparticles (NPs) are the basic component in the production of nanostructures [4], and according to the International Organization for Standardization (ISO) (ISO/TS 80004-2:2015), they are defined as an object with three dimensions below 100 nm. However, the definitions of nanomaterials and nanoparticles are not completely uniform. They vary from organization to organization and continue to be an area of active scientific and political debate [4–6]. Because of their size, NPs have high surface-to-volume ratios, so they exhibit very specific physical and chemical properties which make them suitable candidates for various applications [1]. Compared to conventional materials, the properties of nanoscale materials can impart new material properties and biological behaviour [7,8]. In recent years, more attention has been focused on nanoscale bio-based materials. In the field of nanotechnology, nanocellulose has emerged as a highly interesting biomaterial and is considered one of the most promising materials [9].

The primary goal of this doctoral thesis is to investigate the ability of cellulose nanoparticles, whether they are natural or modified, to stabilize colloidal dispersions, as well as to research systems derived from them. Thus, this work advances the knowledge of the behaviour of cellulose nanoparticles, a topic that is currently being investigated by many scientists.

2. NANOCELLULOSE

Cellulose is the most abundant renewable polymer consisting of glucose units linked by β-(1-4) glycosidic bonds (Fig. 1) [10,11]. This naturally occurring polysaccharide excels in extraordinary properties such as large bioavailability, biodegradability, high biocompatibility, sustainability, and low price. These properties make it a promising candidate for use in biocompatible products [12,13]. In addition, cellulose contains a significant amount of hydroxyl groups with a good affinity to various polymers, including conducting polymers [12–14].
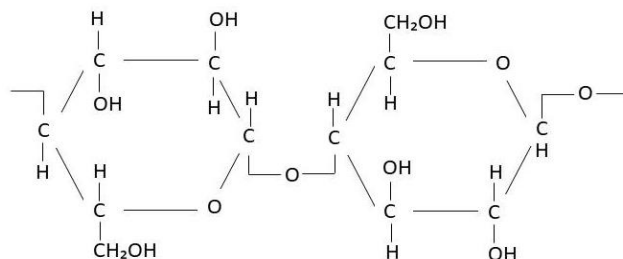
Figure 1 Chemical structure of cellulose.

In recent years, interest has focused on nanocellulose, especially for its interesting properties and wide range of possible applications [15]. Cellulose can be converted to nanocellulose using various approaches, such as mechanical, chemical, and enzymatic treatments (Fig. 2) [16]. Three main types of nanocellulose include, (1) cellulose nanocrystals (CNC) also called nanocrystalline cellulose, cellulose (nano) whiskers, rod-like cellulose microcrystals; (2) cellulose nanofibrils (CNF) also known as nanofibrillated cellulose (NFC), microfibrillated cellulose (MFC), cellulose nanofibers; and (3) bacterial cellulose (BC) or microbial cellulose [17]. It should be mentioned that in the literature, the above-given classification and designation of nanocelluloses are not unequivocally used, therefore, several examples of the same material differing in the name are given above. Each type of nanocellulose excels in specific properties that determine its future application. In general, the properties of nanocelluloses mainly depend on the fabrication route, processing conditions, the source of cellulose, and the subsequent functionalization of the surface [18,19]. The attractive properties of nanocellulose include outstanding mechanical properties, biocompatibility, adaptable surface chemistry, great optical properties, and primarily compatibility with a broad range of materials such as polymers, proteins, and/or cells. Due to these properties, nanocellulose has enormous potential in many applications [20]. In this context, the use of nanocellulose in the field of biomedicine is particularly interesting. Because some tissues respond to electrical fields and stimuli [21], conductivity is considered an important characteristic in biomedical applications. Therefore, it could be advantageous to combine biocompatible nanocellulose with electrically conducting polymers in the development of biomedical materials. In addition to

these applications, the use of nanocellulose in cosmetics is also interesting. Especially in the case of topical applications, nanocellulose can be used as carriers for UV-blocking products [22].
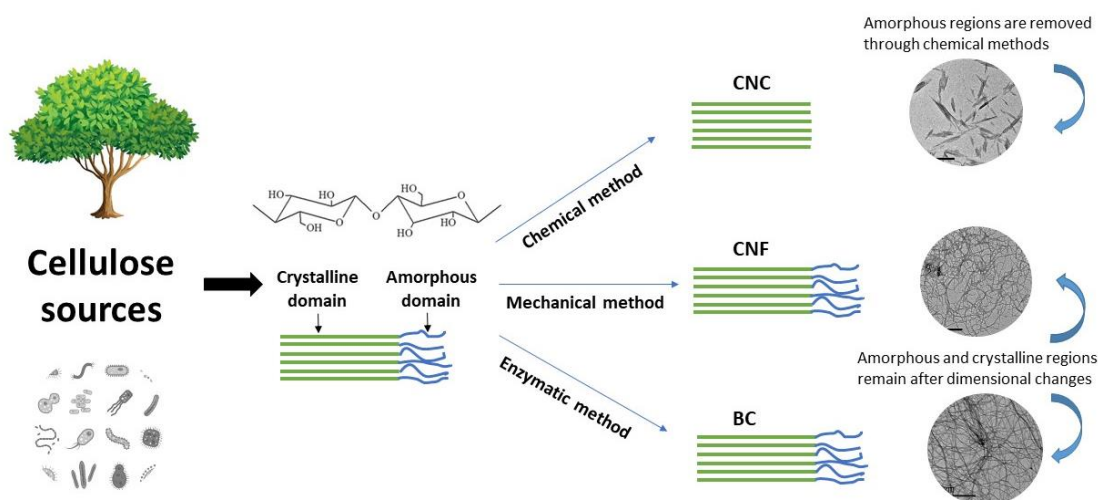
Figure 2 General process for the isolation of cellulose nanocrystals (CNC), cellulose nanofibers (CNF), and bacterial cellulose (BC) from cellulose sources. TEM micrographs adapted from [23]*.*

2.1 Cellulose nanocrystals

Cellulose nanocrystals (CNC), as illustrated in Fig. 3a, have a rod-shaped structure (length ~ 100–250 nm and diameter ~ 5–70 nm) that tapers at the end of the crystal. During CNC production, the amorphous regions of cellulose are removed which leads to highly rigid nanomaterial with high crystallinity [24]. CNC can be prepared by hydrolysis with sulfuric or hydrochloric acids or *via* oxidation with strong oxidizing agents such as 2,2,6,6-tetramethylpiperidine-1-oxy radicals (TEMPO) or ammonium persulfate (APS). During the hydrolysis with sulfate acid, charged sulfate ester groups ($-OSO_3H$) are introduced onto the cellulose surfaces, which contribute to the electrostatic stabilization of the CNC in an aqueous suspension. The disadvantage of this method is the high consumption of sulfuric acid and the high costs of its recycling. Similarly, hydrochloric acid can be used. TEMPO-mediated oxidation substitutes C_6-hydroxyl groups with C_6-carboxyl groups on cellulose crystal surfaces [25–28]. Correspondingly to acid hydrolysis, TEMPO-mediated oxidation uses harmful agents such as hydrazine or sodium borohydride ($NaBH_4$), which show toxicity and generate a lot of chemical waste [29]. A more energy-efficient method for obtaining CNC is based on the oxidation of cellulose materials with APS, which exhibits low long-term toxicity, high solubility in water, and a favourable price. The preparation of highly crystalline CNC according to Leung et al. [30] *via* oxidation with APS produces nanocellulose with –COOH groups at the surface and higher thermal stability than

10

traditional hydrolysis-produced CNC [31]. Due to the carboxyl groups on the CNC surface, the nanocellulose prepared by this process is referred to as carboxylated cellulose nanocrystals (cCNC) [29].

2.2 Cellulose nanofibers

Cellulose nanofibers (CNF)[1], also called microfibrillated cellulose (MFC) or nanofibrillated cellulose (NFC), excels in low-density and high mechanical properties [32]. It contains very long cellulose nanofibers with a length of ~ 1–10 μm and a diameter of ~ 5–60 nm (Fig 3b). The longer fibers of the CNF compared to the shorter rod-like CNC are due to the presence of an amorphous region in the CNF which results in different shapes of fibrils starting from cylindrical to flat ribbon-like structures. The production of CNF requires a lot of mechanical energy but is less demanding concerning the use of chemicals compared to CNC. CNFs can be produced in several different ways [24] such as high-pressure homogenization or other mechanical processes, which can be used individually or in combinations. However, the disadvantage of the process is the high consumption of energy. In this context, some pretreatments of the starting material are included in the CNF manufacture to reduce the size of fibers before homogenization. These pre-treatments can be mechanical, such as refining or cryo-crushing, biological which includes enzymes, or chemical employing alkali [32].

2.3 Bacterial cellulose

Bacterial cellulose (BC) is an extracellular polysaccharide produced by some bacteria such as the genera *Gluconacetobacter* (formerly *Acetobacter*), *Agrobacterium, Aerobacter, Achromobacter, Azotobacter, Rhizobium, Sarcina,* and *Salmonella*. Although the molecular formula of BC is the same as that of plant cellulose, its physical and chemical properties are different. Compared to plant cellulose, BC has a high purity and exhibits a higher degree of polymerization and crystallinity resulting in a very high elastic modulus. Moreover, BC also exhibits higher tensile strength and water-holding capacity than plant cellulose [33]. In terms of morphology, BC shows a characteristic ribbon-like nanofiber structure (Fig. 3c) with a diameter of ~ 20–100 nm. In addition, BC nanofibers are about 100 times thinner than plant cellulose fibers [24,33]. Considering the challenging large-scale production and commercialization of the BC, the use of CNC or CNF appears to be a more attractive alternative [14,34].

---

[1] *Cellulose nanofibers are abbreviated differently in literature – we adopted CNF in this thesis.*
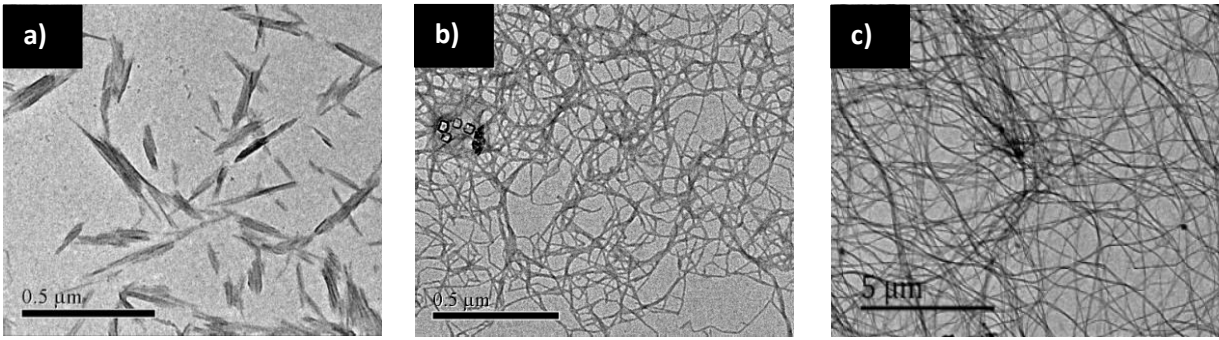
Figure 3 TEM images of (a) CNC, (b) CNF, and (c) BC [23].

3. COLLOIDAL DISPERSIONS

Disperse system refers to a two-phase system with one substance (dispersed phase) distributed throughout the second substance (continuous phase). There are two main approaches to the classification of dispersion systems: 1) the nature of the dispersed and continuous phases (Tab. 1), and 2) the size range of dispersed particles/droplets [35,36]. As far as particle/droplet size is concerned, dispersions are generally classified as molecular dispersions (< 1 nm), colloidal dispersions (1 nm − 1μm), and coarse dispersions (> 1μm) [37]. The latter classification is important due to the different behaviour of these systems in a given colloidal range. For example, coarse dispersions are more prone to sedimentation than colloidal dispersions due to their greater particle size and deficiency of Brownian motion [35]. Nevertheless, even systems with particle sizes outside the colloidal range exhibit many of the properties of colloidal dispersions [38,39].

Dispersion systems are of great importance for various applications; especially colloids play an essential role in our daily life and industry. The doctoral thesis, therefore, further focuses on the topics related to colloidal dispersions.

Table 1 Types of disperse systems [36].

Dispersed phase	Dispersion Medium	Type
Solid	Liquid	Suspension
Liquid	Liquid	Emulsion
Liquid	Solid	Gel
Liquid	Gas	Aerosol
Gas	Liquid	Foam
Solid	Solid	Composite

In colloid science, colloids can further be classified into two groups, lyophilic and lyophobic. Examples of lyophilic dispersions are surfactant micelles or protein solutions. Lyophobic dispersions include emulsions, foams, suspensions, or aerosols [38]. Lyophilic colloidal dispersions are thermodynamically stable systems that form spontaneously in contact with the phases due to the affinity of the dispersed phase for the dispersion medium. On the other hand, lyophobic colloids are thermodynamically unstable and arise through the input of

mechanical energy. They can be prepared using two approaches 1) dispersion methods including the breakdown of larger particles into particles of colloidal dimensions with a colloid mill or ultrasound; and 2) condensation methods involving chemical reactions, in which colloidal particles are formed by aggregation of smaller particles. In the case of dispersion methods, the particles will tend to reunite, which can be prevented by the addition of a stabilizing agent, for example, a surfactant [38,39].

3.1 Emulsions

Emulsions are an important class of dispersed systems with a wide range of applications, which are composed of two immiscible liquids [40,41]. Generally, the formation of emulsions requires using of mechanical force to break up large droplets of the dispersed phase in the continuous phase [42]. There are several emulsification methods, such as simple shaking, mixing with rotor-stator systems, liquid injection through porous membranes, or high-pressure homogenizers and ultrasound generators [43]. Emulsions can generally be classified as oil-in-water (O/W) or water-in-oil (W/O) emulsions, depending on whether the dispersed phase is oil or water, respectively. In addition to these simple emulsions, there are other types of multiple emulsions such as oil-in-water-in-oil (O/W/O) or water-in-oil-in-water (W/O/W) emulsions. Furthermore, water-in-water (W/W) or oil-in-water-in-water (O/W/W) emulsions can exist [44]. Since emulsions are thermodynamically unstable systems, it is necessary to stabilize them by adding a third substance, an emulsifier, which acts as an emulsion stabilizer [45]. One of the most important factors determining not only the stability of the emulsion but also its physical and chemical properties is the choice of a suitable stabilizer [44]. There are many different stabilizers such as surfactant molecules, polymers, proteins, or particles [46] of which surfactants are the most common. Due to their amphiphilic structure, surfactants can adsorb to the surface of freshly formed droplets during homogenization, and stabilize the droplets by reducing the surface tension between oil and water and simultaneously covering them with a thin film preventing aggregation [43–45,47]. For surfactants, the hydrophilic-lipophilic balance (HLB) system serves as a guide for their selection [48].

3.2 Pickering emulsions

A special type of emulsions are the Pickering emulsions (PE), which use solid particles for the stabilization of emulsion droplets. Various particles, such as starch [49,50], silica [51,52], calcium carbonate [53,54], titanium dioxide [55–57], or organic particles [58] can be used to stabilize Pickering emulsions, and their diversity allows the preparation of emulsions with custom features and functions [59]. In practice, effective Pickering stabilization can be achieved using particles whose average size is at least an order of magnitude smaller than the size

of the emulsion droplets. For this reason, nanoparticles are needed to stabilize submicrometer droplets [60].

Compared to other stabilization mechanisms, stabilization by solid particles offers many advantages, such as high stability against coalescence and Ostwald ripening [50]. Pickering emulsions are also characterized by low toxicity and excellent skin compatibility compared to conventional surfactant-stabilized emulsions, which sometimes show negative effects on the skin, often demonstrated by their irritation. In many cases, Pickering emulsions are biologically compatible and environmentally friendly [61–63]. These special types of emulsions are considered promising systems in the field of biomedicine, food, cosmetics, and many others [41]. Moreover, Pickering emulsions, which are sensitive to external stimuli (e.g. temperature, pH, or light), have an interesting use [62].

3.2.1   Mechanism of stabilization

The mechanism of stabilization by solid particles is completely different from the mechanism of stabilization by surfactants (Fig. 4). The precondition for particles to stabilize droplets is their wetting by both phases (oil/water). The adsorbed particles then form a steric (or electrostatic) barrier between the oil droplets and can accumulate irreversibly on the interface, which leads to effective stabilization [41,59]. By theory, the strength of adsorption can be expressed using desorption energy ΔGd, which represents the energy required to remove the spherical particle of radius r and contact angle θ from the oil/water interface with interfacial tension γ_{ow} and is defined by equation (1). In Pickering emulsions, the value of this energy is very high and therefore adsorption of particles at the interface is almost irreversible, which makes Pickering emulsions more stable compared to conventional emulsions [64].

$$\Delta G_d = \pi r^2 \gamma_{ow}(1 - |cos\theta|)^2 \qquad (1)$$

The location of the solid particles at the interface between the oil and water phases is determined by the contact angle (also referred to as a wetting angle) [59], and according to the so-called Finkle's rule, depending on the contact angle, it is possible to predict which type of emulsion will be formed [65]. If the contact angle is larger than 90°, the particles will stabilize W/O emulsions, while at a contact angle of less than 90°, the O/W emulsions will be stabilized [41,59]. In addition, for strongly hydrophilic particles, a large part of their volume remains in the water phase and therefore cannot provide a sufficient barrier to hinder droplet coalescence. Similarly, for strongly hydrophobic particles, a large part of their volume resides in the oil phase leading to less protection for droplet coalescence.

An alternative method how to improve emulsion stability may be using a combination of stabilizers, which can be incorporated into the emulsion by

various approaches such as co-adsorption, complexation, or layer-by-layer method. An interesting approach is the layer-by-layer (LbL) method, which consists of the rapid adsorption of a stabilizer with an electric charge on the droplet surface during homogenization and forming a "primary" emulsion followed by the addition of a second, oppositely charged stabilizer which adsorbs on the droplet and forms a "secondary" emulsion containing droplets coated with a bilayer interface formed through electrostatic attraction. This process can be repeated several times to form a series of layers around the droplets that can improve their stability [66,67]. This method allows the gradual adsorption of various components such as nanoparticles, proteins, or enzymes because the growth of the layer can be controlled not only by their electrostatic attraction but also by other forces, such as hydrogen bonding or hydrophobic interactions [68].
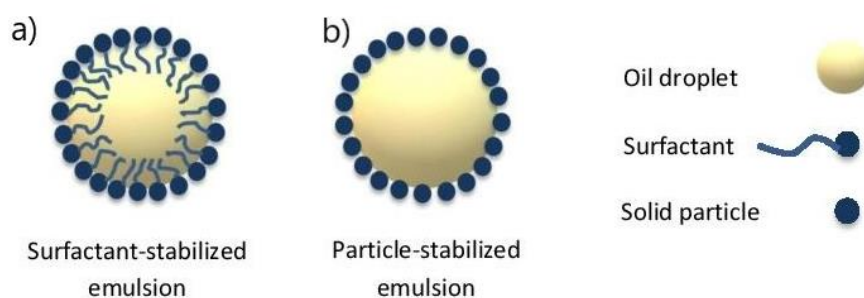
Figure 4 Schematic diagram of an O/W emulsion droplet showing different interfacial stabilization by a) surfactant, and b) solid particles.

3.2.2   Factors influencing the stability of Pickering emulsions

The stability of Pickering emulsions lies in the compact arrangement of solid particles on the surface of the emulsion droplets preventing their collision and agglomeration. Simultaneously, particles adsorbed on the surface of the droplets increase the repulsive force between the droplets, thereby improving emulsion stability. The stability of Pickering emulsions can be evaluated using various techniques such as microscopy, particle size analysis, zeta potential, high-speed centrifugation, conductivity, turbidity, and rheological analysis [69].

The stability of PE mainly depends on the properties of the particles and the properties of the used oil and aqueous phases [70]. The key parameters influencing the stability are 1) the wettability of the particles reflecting their hydrophilicity or hydrophobicity [71] and 2) the size, morphology, and concentration of the particles used for stabilization. Generally, the particles used to stabilize emulsions should be smaller than the target emulsion droplet size. Additionally, the adsorption time at the interface increases with growing particle size causing an increase in final droplet size [72]. The concentration of solid particles has also an important effect on the stability of Pickering emulsions. A higher concentration of solid particles causes more particles to be adsorbed at the interface leading to more effective prevention of droplet aggregation [73]. On the other hand, at a low concentration of particles, coalescence and the destruction

of the emulsion droplets occur earlier before the particles can stabilize them. However, a high concentration of particles does not always lead to a dense coverage of the surface of the emulsion droplets, and on the contrary, a weak coverage does not necessarily cause poor stability of emulsions [72]. Particle morphology also greatly affects the stability of emulsions. Although spherical particles are the most studied, stabilization with ellipsoidal particles (e.g. polystyrene particles), dimer particles, flake-like particles (laponite clays), layered double hydroxides or graphene oxides, and rod-like particles (carbon nanotubes, cellulose nanocrystals, silica nanowires) has been reported [74].

Oil type and volume fraction are other important factors affecting emulsion stability [75]. In general, the type of oil affects the interfacial tension of the oil-water interface, and can also affect the interactions with the particles [70]. Here, the main variables are the viscosity and polarity of the oil phase. The very high viscosity of the oil can reduce the fluidity of the droplet interface preventing the adsorption of particles on it, as well as slowing down the adsorption rate leading to the formation of large droplets [69]. In addition, the oil/water ratio can affect the type of emulsion. Changes in the O/W ratio at constant particle wettability or with progressive changes in particle wettability can then cause catastrophic phase inversion [70,76].

Particle charge, salt concentration, and pH can also dramatically change the stability of emulsions. The pH of the system changes the surface charge of particles and thus the electrostatic interaction between them and regulates the adsorption behaviour as well as the barrier created at the oil-water interface [75]. Furthermore, the presence of salt in the aqueous phase of the emulsion will cause an electrostatic shielding effect on the particles leading to a change in the surface charge of the particles and adsorption at the interface, which will affect the stability of the emulsion [75]. Thus, the type and stability of Pickering emulsions can be modulated by controlling and/or adjusting the pH and ionic strength [70].

In summary, the selection of a suitable stabilizer is a critical factor in the preparation of Pickering emulsions and simultaneously there are many factors affecting their stability. Therefore, in the preparation of Pickering emulsion, a more detailed experiment should be carried out to find the best formula [69,77].

3.2.3   Cellulose nanoparticles as an emulsion stabilizer

A variety of cellulose particles can be used to stabilize emulsion systems, of which CNC shows high efficiency in stabilizing interfaces [78]. CNCs were shown to facilitate the formation of O/W emulsions without the addition of surfactants, which is attributed to their partially amphiphilic character. Despite the overall hydrophilicity of the CNCs, the edges of nanocrystals are hydrophobic, allowing adsorption at the oil-water interface. The hydrophilic nature of the CNC predetermines its better performance in the stabilization of O/W emulsions. However, after suitable surface functionalization, cellulose can also stabilize emulsions with a continuous oil phase [79]. According to Andersen et al., it is

possible to adjust the hydrophobicity of cellulose fibers using several procedures, such as silylation [80] or using quaternary ammonium salts [26]. As for specific applications, Wen et al. prepared emulsions containing D-limonene stabilized by CNC [81], Mikulcová et al. studied emulsions containing components of essential oils stabilized by CNC and CNF (designated MFC in the publication) [82] and the same authors prepared in their next study O/W pH-responsive emulsions stabilized by cCNC containing carboxyl groups on the surface [83]. CNC as an emulsion stabilizer was also used in [26,84–89].

The CNF (designated MFC in the publication) stabilized emulsions prepared by Winuprasith and Suphantharika showed that the stability of the emulsions increased with decreasing fiber size and increasing CNF concentration [90]. Xhanari et al. investigated the emulsions prepared with CNF (designated MFC in the publication) of relatively low hydrophobicity and concluded that the main mechanism preventing the coalescence of emulsion droplets is network formation [91]. Similarly, Mitbumrung et al. revealed that CNF (designated NFC in the publication) stabilized the emulsions by adsorption at the oil-water interface, forming a steric barrier that provided electrostatic repulsion. Moreover, a three-dimensional network in the continuous phase was formed [92]. In another study, water-in-toluene emulsions stabilized solely by hydrophobized CNF (designated MFC in the publication) were investigated. The emulsions showed excellent stability which increased with growing CNF concentration [80].

Although the use of BC as a stabilizer is limited by low production capacity, it has been employed in several studies. For example, Yan et al. dealt with the synthesis of BC and bacterial cellulose nanocrystals (BCN) and proved their ability to stabilize olive oil Pickering emulsions. In addition, BCN was more sensitive to changes in pH and ionic strength than BC, revealing better colloidal properties of BC [93]. A similar conclusion was drawn by Paximada et al., who used different types of cellulose (hydroxypropyl methylcellulose, carboxymethyl cellulose, and BC) to stabilize O/W emulsions. Correspondingly to the previous study, BC emulsions were not affected by changes in pH, temperature, or ionic strength, unlike emulsions prepared with the remaining two cellulose polymers. Overall, emulsions with BC showed the highest stability compared to emulsions with other used celluloses [94]. Further studies with BC as an emulsion stabilizer were also performed [95–98].

3.2.4 Pickering emulsions for topical applications

Pickering emulsions can be used in many fields including pharmaceutics and cosmetics in topically applied products. Here, they gradually substitute traditional surfactants that cause skin irritation and other adverse side effects [99–101].

In topical applications, Pickering emulsions can act as platforms for skin photoprotection [102]. Since sunscreens are emulsion-based products [103], physical UV filters can be directly used as emulsion stabilizers [104]. Among physical UV filters, titanium dioxide (TiO_2) and zinc oxide (ZnO) are widely used

[105]. The study by Frelichowska et al. suggests that Pickering emulsions have better adhesion to the skin compared to classical emulsions [106], which would lead to better skin protection. In another study, Lee et al. prepared stable O/W Pickering emulsions stabilized by hydrophobically modified cellulose nanofibers hybridized with ZnO nanoparticles ($HCNF_{ZnO}$) and demonstrated remarkable UV blocking due to the synergy of this complex with chemical UV filter, avobenzone. In addition, O/W Pickering emulsions showed 6.6 times higher excellent water resistance compared to conventional emulsions [107]. Other stable Pickering emulsions with high SPF values and a suitable ratio of UVA/UVB protection were prepared using the combination of three multifunctional solid particles (ZnO, TiO_2, starch) and green coffee oil, where the combination of starch with physical UV filters led to a synergistic increase in the SPF value (around 2 fold) [102]. Bordes et al. also focused on the preparation of Pickering emulsions for surfactant-free sunscreen creams. In this study, C_{12}-C_{15} alkyl benzoate, an ingredient commonly present in commercial sunscreens, served as the oil phase, and inorganic nanoparticles (NPs) (TiO_2 and/or ZnO) were used as UV filters. The results showed that ZnO NPs were able, in certain formulations, to stabilize emulsions, but silica-coated TiO_2 NPs were ineffective as a stabilizer. However, the TiO_2/ZnO NPs mixture led to stable Pickering emulsions with a photoprotective effect similar to the surfactant-based sunscreen cream with an *in vitro* SPF of about 45 [99]. Terescenco et al. described the textural properties of Pickering emulsions stabilized with three different types of particles (TiO_2, SiO_2, and ZnO) compared with conventional emulsions stabilized by surfactants for topical use. The results of the study show that particle-stabilized emulsions cause a less glossy and greasy texture than surfactant-stabilized emulsions, which leads to better spreadability of the formulation [108]. Although the research focused on particle-stabilized emulsions for UV protection is still in its infancy, published studies promise good future applications of these systems.

Due to the hydrophilic character of TiO_2 particles [109], the preparation of commercially usable emulsions stabilized only by unmodified TiO_2 for cosmetic applications is still a challenge [110]. Therefore, hydrophobically modified TiO_2 particles or TiO_2 in combination with another substance are often used. Although particle surface modifications have demonstrable advantages [111], their implementation is usually not possible without the use of surfactants and organic solvents, which are often not environmentally friendly [110].

Surface modification may also affect other surface properties of the particles, which may be undesirable in applications where these parameters are important [112]. In addition, a study by Wang et al. revealed that emulsions stabilized with surface-modified TiO_2 nanoparticles exhibited worse UV protection than emulsions stabilized with untreated TiO_2 nanoparticles [110]. In this context, it could be advantageous to combine TiO_2 with cellulose nanoparticles, which have already demonstrated (in earlier studies) the ability to form stable emulsions, and in addition, represent environmentally friendly stabilizers.

4. CONDUCTING POLYMERS

The term conducting polymer (CP) refers to a large class of materials that can conduct electrical charge [113]. The electrical conductivity of polymers has been studied for over 60 years [114]. Polyacetylene was the first electrically conducting polymer discovered in 1977 [115], other conducting polymers such as polypyrrole (PPy), polythiophene (PT) and polyaniline (PANI) have been developed over the last 30 years [114,116]. These materials typically exhibit electrical and optical properties that are comparable to metals and semiconductors, while retaining some of the advantages of conventional polymers [116]. Although the very first papers on conducting polymers were published more than 30 years ago, the importance and interest in these materials are constantly growing [117,118].

The electrical conductivity of CPs is based on the presence of conjugated double bonds along the polymer backbone, which allows charge carriers to move freely; however, conjugated double bonds do not result in highly conducting polymer materials. To achieve high conductivity, a doping process is used [119]. By doping, the conductivity of undoped polymers (10^{-6}–10^{-10} S cm^{-1}) can be increased by 10 orders of magnitude or more [119]. For example, polyacetylene doped with iodine achieved a conductivity higher than 10^4 S cm^{-1} [120,121], which is similar to the conductivity of lead at room temperature ($4.8 \cdot 10^4$ S cm^{-1}) [119]. The dopant´s role is to add or remove electrons from CPs. Thus, dopants are integrated as counter ions into CPs when the CPs are oxidized or reduced. Doping can be classified into two types. P-doping occurs when the polymer backbone is oxidized, whereas the reduction of the polymer backbone occurs by n-doping [122]. The conductivity of CPs usually increases with increasing dopant concentration. Available doping methods include electrochemical or chemical doping, photo-doping, non-redox doping, and charge-injection doping, with the first two procedures being the most commonly used [119].

Conducting polymers can be classified according to various criteria, of which the most important criterion relates to the type of movement of the electric charge, which depends on the chemical structure of the polymer [114]. If the conductivity is given only by ionic mobility, they are ion-conducting polymers [113]. Polymers with redox-active species exhibit electronic conductivity and are referred to as electrically conducting polymers (ECPs). This group of CPs further includes redox and conjugated polymers, which differ according to the mechanism of electron transfer. The electron transfer by electron hopping is typical for redox polymers, such as poly(vinylferrocene). The conjugated polymers, on the other side, show the extended π-conjugated system leading to the creation of charge carriers with the ability to move in delocalized π-systems after doping. Conjugated polymers thus show higher conductivity compared to redox polymers [113,116]. Polypyrrole (PPy), polyaniline (PANI), and poly(3,4-ethylenedioxythiophene) (PEDOT) are examples of conjugated

polymers of which PANI is the most studied one and is used in the thesis [123,124].

4.1 Polyaniline

Polyaniline is a homopolymer with a *p*-linked phenylene amine imine structure (Fig. 5) characterized by easy synthesis and high environmental stability [125–127]. Depending on the degree of oxidation, PANI can exist in the form of salt or base. The oxidation states are given by a combination of benzenoid (amine N) and quinoid (imine N) rings. Three oxidation forms of PANI include leucoemeraldine (fully reduced, emeraldine (partially oxidized), and perningraniline (fully oxidized form), of which the emeraldine salt is the only conducting form of PANI [128–130]. Green emeraldine salt is an essential stable form of polyaniline with a typical conductivity in the range of $10^{-1}-10^{1}$ S cm^{-1}, which is usually formed by oxidation aniline, for example in the form of the hydrochloride or sulfate. Treatment of the protonated emeraldine salt with alkali produces a blue non-conducting emeraldine base with conductivity $10^{-10}-10^{-8}$ S cm^{-1}. Oxidation of emeraldine gives protonated blue pernigraniline, whose base is violet. Alternatively, by reduction of emeraldine, colorless, non-conducting leucoemeraldine can be obtained [131].
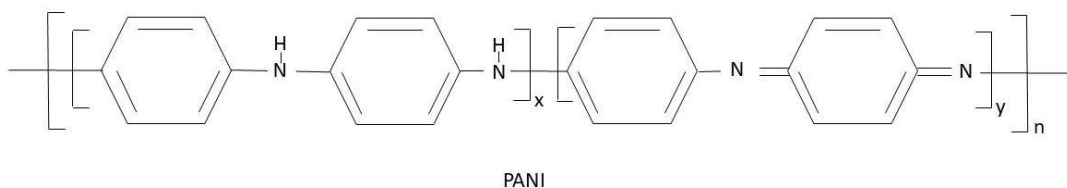
PANI

Figure 5 Chemical structure of polyaniline (PANI).

4.1.1   Synthesis

PANI can be synthesized by chemical or electrochemical polymerization [132]. In the case of chemical synthesis, polyaniline is typically prepared by the oxidation of aniline with ammonium peroxydisulfate in an acidic aqueous medium with high initial acidity of the reaction medium, pH < 2.5. In addition to ammonium peroxydisulfate, salts of iron (III), cerium (IV), silver (I), or dichromates can be used as oxidants, of which the highest yields and conductivity are obtained with peroxydisulfate [133]. Standard polymerization according to the protocol given by IUPAC is based on mixing 2.59 g of aniline hydrochloride dissolved in water to 50 mL of solution with 5.71 g of ammonium peroxydisulfate also dissolved to 50 mL of solutions at an ambient temperature close to 20 °C. The reaction product (solid powder) is separated on a filter followed by rinsing with 0.2M hydrochloric acid and then with acetone or methanol and dried in air at room temperature or in a desiccator. In this way, 2 g of polyaniline hydrochloride powder in the conducting, emeraldine form is obtained [134]. Many studies further describe the polymerization of aniline in micelles [135,136],

in reverse micelles [137,138], or in emulsions [139,140]. Interesting studies describe the enzymatic polymerization of aniline using chitosan as a steric stabilizer and toluenesulfonic or camphorsulfonic acids as doping agents [141]. In many applications, it is essential to produce polymers in the form of thin films. The synthesis of PANI films will be discussed in a separate chapter.

4.1.2   Morphology

Depending on the synthesis conditions, different PANI morphologies arise comprising globules, nanofibers, or nanotubes [133]. The creation of individual morphologies consists of three steps: 1) the formation of the nucleates, 2) their organization or self-assembly, and 3) the growth of PANI chains from the nucleates [142]. Globules, sometimes also referred to as granules, are the most typical morphologies of PANI formed during the oxidation of aniline under strongly acidic conditions, at pH < 2.5 (Fig. 6a) [133,142]. The size of globules ranges from tens to several hundreds of nanometers [143]. The growth of globular structure starts from the phenazine-like oligomers (nucleates) formed during the oxidation of aniline which is insoluble in the reaction mixture. They separate and form random aggregates acting as initiation centers for the further growth of PANI chains forming a body of the globules [133]. Nanofibers, also called nanowires, are objects with a diameter of tens of nanometers with a high aspect ratio. They are usually branched and produce more complex hierarchical structures [133,142]. Nanofibers are formed when aniline nucleates produce stacks stabilized by interactions between phenazine-like oligomers, and PANI chains then grow at the right angle from the single stack of nucleates and produce the body of nanofibers. By adsorption of any free nucleates on the nanofibers, branches are formed. Another form of PANI with a diameter of tens to hundreds of nanometers are nanotubes. Nanotubes differ from nanofibers by the presence of the inner cavity with a diameter of 10–150 nm (Fig. 6b) [142]. The mechanism of nanotube formation assumes the existence of the template [133]. Nanotubes are formed by the oxidation of aniline initiated at low acidity, pH > 3.5, and terminated at high acidity, pH < 2.5, where low acidity ensures the formation of aniline oligomers in sufficient amount, while high terminal acidity is essential for the PANI formation [142]. When the oxidation is stopped at the phase of oligomer formation, additional morphologies are formed. For example, in oxidation under alkaline conditions, microspheres displaying an opening or small-and-large sphere snowman-like morphology are obtained (Fig. 6c). Conversely, in oxidation under mildly acidic conditions, the aniline phenazine-like oligomers self-assemble to form flower-like morphologies or hairy microspheres similar to rambutan [133]. In addition to the mentioned morphologies, other structures such as flakes, ribbons, or nanobelts can be obtained by tuning the pH profile during the oxidation of aniline [142].
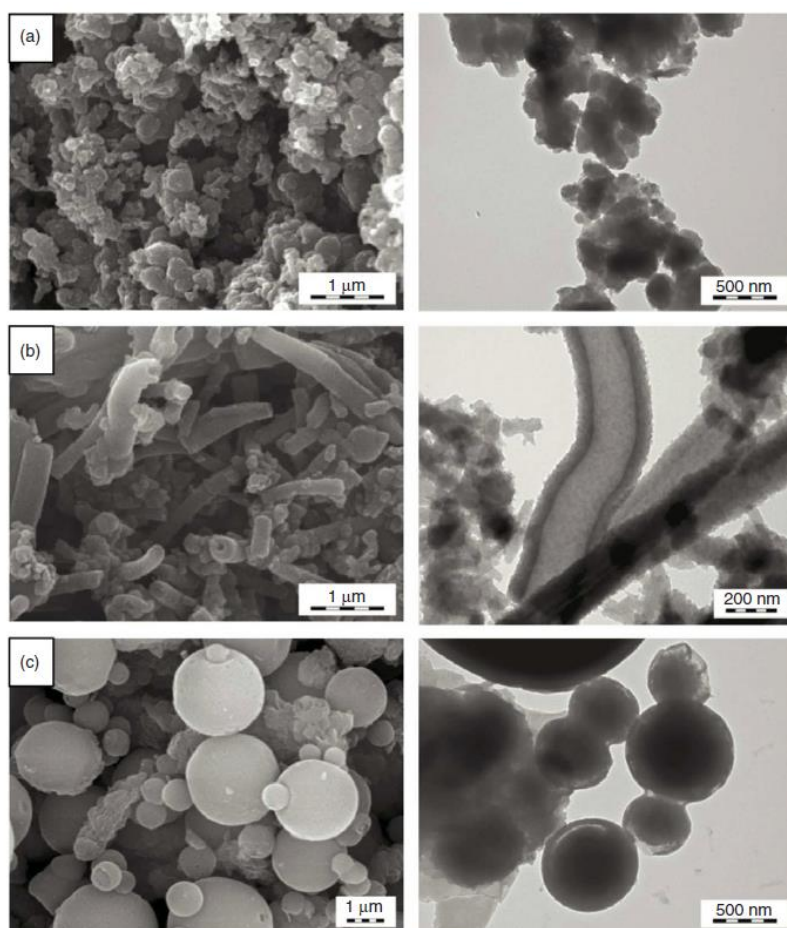
Figure 6 SEM (left) and TEM (right) images of a) globules, b) nanotubes, and c) microspheres [133].

4.1.3 Applications

Polyaniline can be produced in several application forms (Fig. 7). As mentioned above, under standard polymerization of aniline, PANI is obtained in the form of a powder. Polyaniline powder has an extremely low solubility [144] making it difficult to process and use [133]. Therefore, PANI powder is frequently applied as a part of conducting composites similar to carbon black [133]. Thin films and coatings are more exploitable application forms of PANI. The thin films are formed on the surface of a material by immersing it in the reaction mixture containing PANI precursors [133]. Colloidal dispersions are another important application form of PANI. In general, colloidal conducting dispersions result from the preparation of CPs in the presence of a suitable stabilizer. Many different substances, such as water-soluble polymers, functional polymers, block and graft copolymers, particles, polymer latexes, or surfactants can be used as stabilizers. Colloidal dispersions are important modifications of conducting polymers that improve their processing properties and allow for more advanced applications [131,145]. Recently, researchers have focused on the preparation of new types of polyaniline forms, these including hydrogels [146], aerogels [147], or cryogels [148].
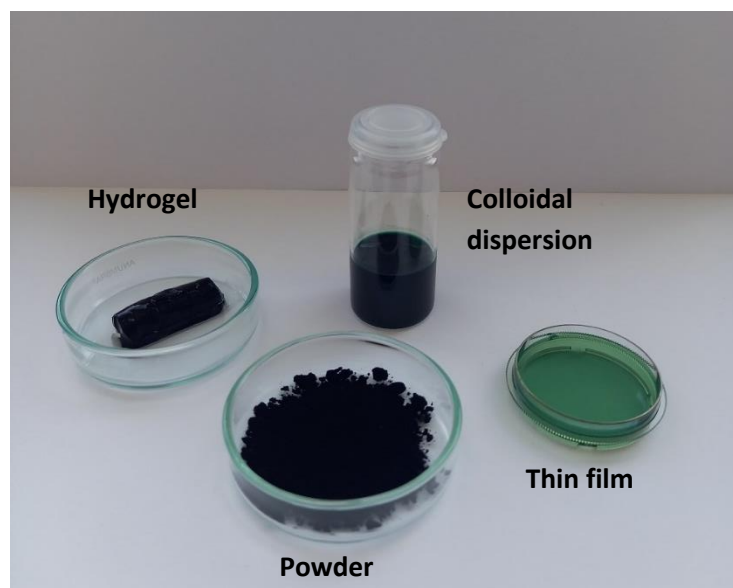
Figure 7 Various forms of polyaniline.

Polyaniline finds a wide range of practical applications, from electronics to biomedical engineering. For example, PANI is extensively used in electrochemical energy storage and conversion technologies, such as supercapacitors, rechargeable batteries, and fuel cells [149]. Due to the presence of stable redox states, PANI can be used as a medium for storing primary energy [133]. In recent years, PANI has attracted attention as a promising anti-corrosion material with a remarkable ability to protect various metals, including aluminium, mild steel, copper, and stainless steel [150]. Furthermore, due to its electrical conductivity and biocompatibility, PANI is a promising material in biomedical applications [151]. The conductivity of PANI is critical for the transmission of electrical signals in biological systems. Such materials allow cells or tissues cultured on conducting surfaces to be stimulated by an electrical signal, which is crucial, especially in tissue engineering of electro-sensitive tissues [152,153]. The use of PANI in scaffolds with potential application in bone regeneration [154] or muscle regeneration [155] has been reported in this context. Due to its nature, PANI is one of the most promising polymers for application in biosensors [156] or bioactuators [157–159].

5. CONDUCTING COLLOIDAL DISPERSIONS

The concept of the preparation of colloidal particles relies on the presence of a stabilizer, for example, a polymer, in the reaction mixture [160]. First, the adsorption of the aniline oligomer on the stabilizer chains occurs followed by stimulation of chain growth and nucleus formation. Then other oligomers and new chains are formed near the nucleus and a colloidal particle grows. The diameters of the colloidal particles usually range from 200 to 400 nm [133,160]. The particles can be uniform in size or polydisperse with different morphologies from

spheres to extended objects with a high aspect ratio [142]. Colloidal PANI has been studied by many researchers and research groups. Currently, the PANI colloids were prepared in the presence of various types of stabilizers that control their future application. For example, Gonçalves et al. prepared colloidal PANI-GA (gum Arabic) dispersions with excellent biocompatibility suitable for biological and biomedical applications. Thanks to easy synthesis and the sustainability of GA, this nanocomposite is promising for the development of clinically safe devices, thus expanding the possible applications of the composite [161]. In another study, Bober et al. prepared PANI–silver colloids stabilized by gelatine for application in regenerative medicine or biosensing [162]. Anticorrosive coatings based on PANI-Zn colloids stabilized with N-poly(vinylpyrrolidone) (PVP), or colloidal SiO_2 were studied by Boshkova et al. The authors reported that SiO_2-based products have better colloidal stability than products containing PVP. The main benefit of the PANI-Zn/SiO_2 hybrid coating over Zn alone was improved corrosion resistance in the model medium (5% NaCl solution, pH 6.7) [163]. Similar results were reported by Kamburova et al. who studied colloidal suspension of PANI-SiO_2 incorporated into zinc-based coatings for corrosion protection [164]. Kebiche et al. focused on the metal incorporation into PANI nanostructures based on the use of palladium/tin (Pd/Sn) colloids. Conducting polymer-metal nanocomposites are a new class of materials combining the mechanical, optical, and electrical properties of CPs with magnetic properties and high electrical conductivity of metallic inclusions that can be used in electronics, sensors, photovoltaic cells, memory devices, protective coatings against corrosion or supercapacitors [165].

Another interesting group of substances that can be advantageously used to stabilize conducting colloidal dispersions are biopolymers. Cellulose derivatives, such as ethyl(hydroxyethyl)cellulose (EHEC) [166] and hydroxypropylcellulose (HPC) [167], proteins albumin [168] and gelatin [162] have been used for the synthesis of colloidal PANI. Recently, Kašpárková et al. prepared PANI colloids using biocompatible polysaccharides, sodium hyaluronate (SH), and chitosan as stabilizers. Both polysaccharides improved the biocompatibility of CPs and can be used to stabilize conducting colloids, especially for biological applications [169]. Nanoparticles of PANI stabilized with pectin were successfully synthesized by Anbalagan et al. [170]. In the case of PPy-based composite colloids, their synthesis was accomplished using xanthan gum [171]. The benefit of using biopolymer stabilizers for CPs lies not only in improving the processability of the resulting conducting composite but also in providing biocompatibility for potential biomedical applications [170].

5.1 Synthesis of conducting colloids

Although conducting polymers are typically polymerized in an aqueous medium, it may be more advantageous in some cases to prepare CPs in a non-aqueous, organic medium, for example, to incorporate a material insoluble in the aqueous phase.

5.1.1 Polymerization in aqueous media

Dispersion polymerization is one of the possibilities to prepare a colloidal form of CPs. PANI and PPy are commonly synthesized by oxidative polymerization of their monomers (i.e. aniline and pyrrole) in an aqueous acidic medium in the presence of oxidizing agent (most frequently ammonium persulfate (APS) for PANI, and ferric chloride ($FeCl_3$) for PPy) and steric stabilizer [131]. The preparation of colloidal PANI according to the protocol of IUPAC in the presence of PVP as a stabilizer consists in dissolving 259 mg of aniline hydrochloride (AH) in 5 ml of an aqueous solution of PVP (40 g l^{-1}). The addition of 5 mL of an aqueous solution containing 571 mg of APS under brief stirring starts the polymerization, which is carried out at room temperature close to 20 °C. The reaction is completed within a few minutes [172]. In the case of PANI, the mixture gradually turns blue, indicating the formation of a protonated, pernigraniline, which at the end of the polymerization changes to the final, protonated green emeraldine salt [131]. The principles leading to the formation of PANI or PPy are analogous and consist of the spontaneous attachment of oligomers formed *via* the oxidation of monomers in an acidic medium to a stabilizer, creating thus a nucleus for the PANI (or PPy) growth [131,173]. The dispersion polymerization method is characterized by typical features: a) the monomer is miscible with the reaction medium (as opposed to emulsion or suspension polymerization); b) the polymer formed during the polymerization is insoluble under the same conditions; and c) the macroscopic precipitation of the polymer is prevented by the presence of a stabilizer. Compared to monomers, such as styrene or methyl methacrylate, PANI and PPy are not soluble in their respective monomers and the polymerization can take place in the aqueous phase [131].

Another approach for producing colloidal CPs is emulsion polymerization [174]. In this method, the monomer, oxidant, and surfactant-based stabilizers are all added to the solvent (water) at the same time, resulting in the formation of micelles [175]. Surfactants play an important role in this process because they allow micelles to form, creating thus polymerization loci for particle nucleation, and stabilize the particles [176]. The monomers polymerize inside the micelles, where they are trapped in a localized environment caused by surfactant encapsulation, forming thus stable colloidal dispersions (Fig. 8) [175].
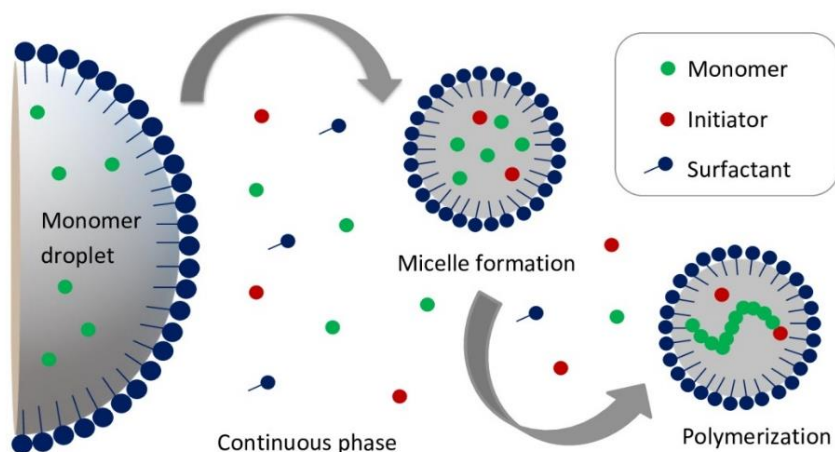
Figure 8 Schematic representation of emulsion polymerization.

5.1.2 Polymerization in non-aqueous media

The CPs can also be synthesized in a non-aqueous, organic environment. However, this procedure is far less common and the preparation of PANI colloids in organic media was only recently described by [177]. In this study, PANI colloids were synthesized in the organic phase of chloroform or xylene in the presence of a surfactant. The preparation route consisted of the oxidation of aniline hydrochloride (AH) with APS in 50 vol% water-organic solvents (chloroform or xylene) in the presence of sodium bis-(2-ethylhexyl) sulfosuccinate (AOT). The aqueous phase contained 0.1M AH, 0.125M APS, and 4 wt% AOT. Specifically, 50 mL of an aqueous solution of AH and AOT was mixed with 50 mL of an aqueous solution of APS. Finally, 100 mL of organic solvent was added. The reaction mixture was then stirred at room temperature for 1 hour. After the polymerization, the system was left at rest to separate into two phases. The organic phase contained PANI colloidal particles (~ 1 wt%), while residual reactants (APS) and by-products were collected in the aqueous phase. The resulting colloidal particles were globular and with a diameter of 50 nm. In contrast to colloids prepared in an aqueous medium, the organic PANI colloids do not frequently require purification (e.g. by dialysis). PANI colloids prepared in this way are suitable, for example, for printing applications [177]. In addition to this study, Lee et al. prepared nanocomposites based on bacterial cellulose (BC) and PANI using aniline interfacial polymerization in the presence of chloroform. The procedure involved dissolving aniline in 10 mL of chloroform and adding 10 mL of 1M HCl containing APS. The molar ratio of oxidant to aniline was 1.25:1. Never-dried BC was carefully placed above the organic phase and the reaction was performed at room temperature for 24 hours. The prepared BC-PANI composite was repeatedly washed with deionized water, methanol, and HCl to remove impurities and dried in a vacuum oven at 60 °C for another day. The study revealed that the polymerization started at the interface between the organic and aqueous phases within a few minutes. Interfacial polymerization is a

diffusion-controlled reaction so that the reaction can proceed overnight. The images revealed that PANI nanoparticles were densely arrayed along each fiber of BC. This BC-PANI nanocomposite could be used, for example, in biological or chemical sensors, and composite actuators [178].

5.2 Mechanism of stabilization of conducting colloids

Stability is an essential prerequisite for the application of conducting colloids [179]. Two aspects of PANI colloid stability must be considered, chemical and colloidal. Changes in the chemical structure of PANI cause a decrease in conductivity, which is reflected by the changes in the optical spectra, whereas colloidal stability is evaluated by the changes in particle size and is influenced by the properties of the stabilizer used in polymerization [180].

The stabilization mechanism of conducting colloidal dispersions is determined by the type of stabilizer used, which can be a surfactant, polymer, or solid particle.

5.2.1 Colloidal dispersions with surfactants

Surfactants represent a unique class of chemical compounds with molecules consisting of a hydrophilic head group interacting with an aqueous medium, and a hydrophobic chain [181]. The surfactants influence the preparation of CPs in three ways: 1) the presence of surfactant micelles controls the distribution of the reactants between the micellar and aqueous phases leading to a change in the site and course of the polymerization, 2) anionic surfactants can act as counterions for CP polycations, and 3) the hydrophobic part of the surfactant molecules can adsorb on the produced CP, thereby making the surfactant a part of the resulting material [182]. According to Stejskal et al., surfactants (anionic, cationic, or non-ionic) can be used as colloid stabilizers [182].

If polymerization occurs directly in the surfactant micelle, the reaction kinetics, selectivity, and reaction yield depend on the location of the reactants in the micelles. The site of incorporation of a solubilized substance relates to its chemical nature; the non-polar, highly hydrophobic substances are situated in the hydrocarbon core of the micelles, whereas polar or surface-active molecules are solubilized at the micelle–water interface (Fig. 9) [135]. In the case of polymerization of aniline in an acidic aqueous medium in the presence of sodium lauryl sulfate (SDS), formed aniline cations adsorb on the micellar surface by electrostatic interaction with anionic SDS molecules that are fully exposed to the aqueous phase [183].

The most common mechanism of stabilization of colloidal PANI is thus the solubilization of aniline monomers at the micelle-water interface, with some of them being adsorbed on the micelle surface and some of them also existing in the aqueous phase. Solubilized aniline polymerizes by APS oxidant present in the aqueous phase. The reaction occurs mainly at the micelle-water interface as the APS cannot penetrate the micellar surface. Aniline molecules originally present

in the aqueous phase are then gradually incorporated into the hydrophobic core of micelles as they grow into dimer, trimer, and tetramer with increased hydrophobicity. After the reaction is completed, produced PANI particles are stabilized by electrostatic repulsive interactions through adsorbed and incorporated SDS molecules [135].

Examples of surfactants used to stabilize conducting colloids include sodium dodecylbenzenesulfonate (SDBS) [184–186] or dodecylbenzenesulfonic acid (DBSA) [183,187] both used to prepare colloidal PPy dispersions. Here, the polymerization of pyrrole and formation of PPy occur within the surfactant bilayer. Studies also report on the polymerization of PANI in the presence of DBSA [188] or nonionic surfactants [189]. In this case, the surfactant is attached by protonation of its anionic group to the positively charged imine nitrogen of PANI. However, other possible mechanisms of CP polymerization in the presence of surfactants are reported, such as the adsorption of their hydrophobic parts on the PANI molecule or the formation of bilayers of the bound and redundant surfactant [131].
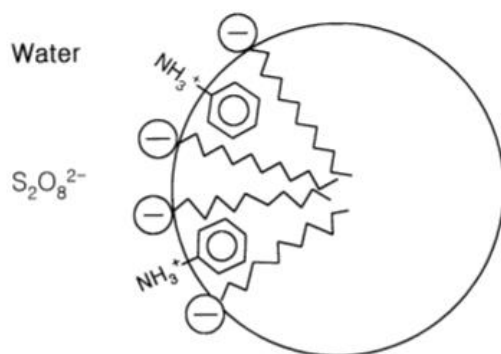
Figure 9 Scheme of aniline incorporation into the SDS micelle in HCl environment [135].

5.2.2   Colloidal dispersions with polymer stabilizer

The PANI chain can easily interact with many various water-soluble polymers such as poly(vinylalcohol) (PVA), poly(acrylamide) (PAM), and poly(ethylene) oxide (PEO). Although PEO is one of the most commonly used water-soluble polymers, data on its effectiveness as a stabilizer are inconsistent. It was found that the high-molecular-weight ($>10^5$ g mol^{-1}) PEO can act as a stabilizer, whereas the low-molecular-weight polymer cannot [131]. In addition to these stabilizers, the use of poly(2-acrylamido-2-methyl-1-propanesulfonate) (PAMPSA) has been also reported [190]. Another frequently used water-soluble polymer is PVP, which has been used to stabilize CPs in [160,191–194].

The mechanism of formation of colloidal PANI particles stabilized with polymers consists of the production of low molecular weight oligomers in an acidic environment during aniline oxidation, followed by their spontaneous attachment to the stabilizing polymer creating a nucleus for the PANI growth (Fig. 10) [195]. Then the formation of new oligomers and polymerization

proceeds and the colloidal PANI particle further grows [172]. The steric stabilizer on the surface of the colloidal particles forms a protective shell and prevents their aggregation [196].

Figure 10 Colloidal PANI particles stabilized by a polymer [195].

In addition to the above-listed polymers, another group of polymer stabilizers includes polymer latexes. For example, Beadle et al. prepared a series of PANI-copolymer latex composites by chemically polymerizing aniline in the presence of a film-forming chlorinated copolymer latex [197]. Also, Terlemezyan et al. polymerized aniline in the presence of latex particles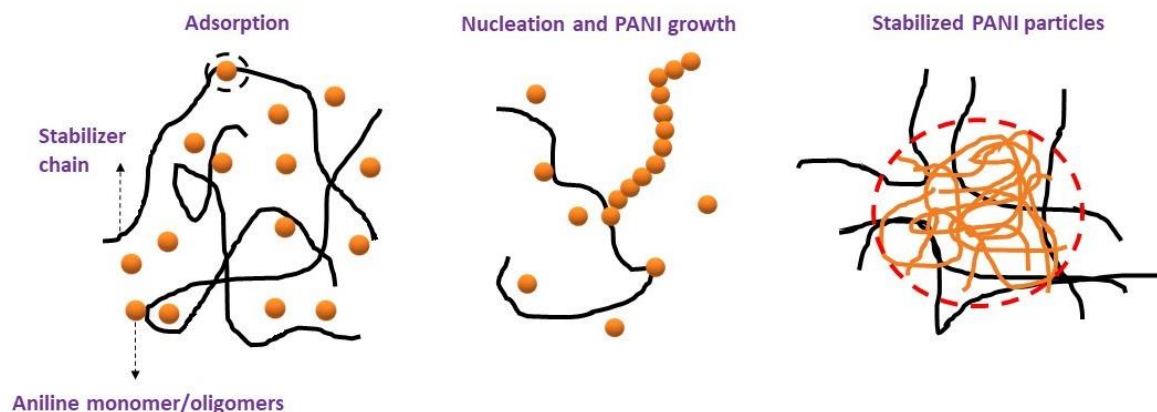 to prepare composite materials [198]. Later, Xie et al. prepared conducting composites composed of aniline and poly(butadiene-*co*-styrene-*co*-2-vinylpyridine) (PBSP) [199]. Similarly, Lei et al. prepared PANI-coated polystyrene latex suspension stabilized by PVP [200]. The preparation of PPy in the presence of latex particles also led to stable composite systems [201–203].

5.2.3   Colloidal dispersions with solid particles

The mechanism of formation of colloidal PANI in the presence of solid particles as a stabilizer was described in the works of [131,172,204]. At the beginning of polymerization, a solid stabilizer such as silica is present in the reaction mixture (Fig. 11a). During the polymerization process, aniline oligomers are formed (Fig. 11b) and they are attached to the stabilizer either by chemical grafting or physical adsorption (Fig. 11c). The particles of the stabilizer are partly or fully covered with PANI and simultaneously PANI nucleates are formed, which grow during the polymerization process, and dispersed CP particles are created (Fig. 11d). Some solid particles may still be free and not attached to the dispersed particles (Fig. 11d). The resulting particles have a raspberry structure that results from aggregation. Compared to the density of most organic polymers $(1.0 \pm 1.3$ g cm^{-3}) that are used to stabilize conducting colloidal dispersions, the density of inorganic particles is much higher, specifically, in the case of silica, which exceeds 2.1 g cm^{-3}. As a result, PANI colloids stabilized with inorganic

particles show a higher density compared to systems stabilized with organic polymers [205].
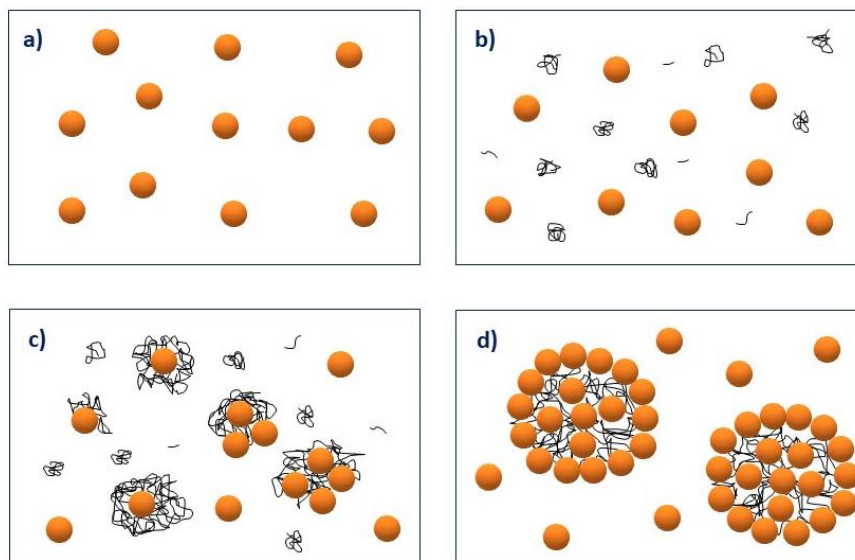
Figure 11 Formation of PANI colloidal particles in the presence of solid particles as a stabilizer [131].

One of the frequently used stabilizers for conducting PANI and PPy colloids is ultra-fine colloidal silica. Gill et al. used these particles to prepare PANI-silica colloidal composites [206,207]. Also, Stejskal et al. polymerized aniline in the presence of ultrafine colloidal silica particles [208]. Silica particles have also been used for PPy colloids [209–211]. Not only silica particles have proven to efficiently stabilize PANI and PPy colloids. Successful polymerization of aniline or pyrrole was also performed in the presence of tin oxide [212], manganese oxide [213], and zirconium dioxide [214]. In recent years, interest has focused on bio-based particulate stabilizers such as cellulose nanoparticles discussed below.

5.3 Application of conducting colloids with cellulose nanoparticles

Nanocellulose-based conducting materials have attracted tremendous attention. The presence of abundant hydroxyl groups on the nanocellulose surface enables direct interaction with the functional groups of conducting polymers (e.g. amine groups of aniline or –NH in the pyrrole ring) [215–217]. Conducting polymer/cellulose materials thus combines the properties of both components, i.e. the electrical and chemical properties of the conducting polymer and the strength, flexibility, and available surface area of the cellulose particles [218]. Similarly to classical dispersions, also conducting colloidal dispersions can be prepared with all types of cellulose nanoparticles.

In the case of the combination of CNC with conducting polymers, several studies have been reported to deal with this topic. A typical procedure for the

preparation of CNC-PANI colloids is the oxidative polymerization of aniline (or pyrrole) *in situ* in the presence of CNC. Razalli et al. synthesized a conducting biocompatible nanocomposite of CNC-PANI. FTIR spectra confirmed the incorporation of CNC into the nanocomposite. However, aggregation of PANI particles was observed with the growing aniline concentration [216]. Abdi et al. developed a sensitive electrochemical biosensor containing a nanocomposite of CNC-PANI [219]. Latonen et al. prepared conducting ink based on CNC and PANI in a water-glycerol solvent system. The resulting CNC-PANI nanoparticulate ink was stable and exhibited high electrical conductivity [220]. CNCs were also used to prepare self-healing conducting hydrogels with PANI coated on the surface of polycarboxylic multi-branched cellulose nanocrystals (multi CNC-PANI) [221] or porous cellulosic aerogel substrate for layer-by-layer (LbL) assembly of supercapacitor electrodes [222]. Al-Dulaimi et al. prepared conducting PPy-CNC nanocomposite *via* deposition of pyrrole monomers on the CNC surface by electrostatic attractions between the sulfate groups of CNC and the amine group of pyrrole [223]. Chemical polymerizations leading to the formation of CNC-PPy were performed also by [224] and [225].

Similarly to CNC, CNF-PANI colloids can be synthesized by the oxidation of aniline (pyrrole) *in situ* in the presence of CNF. Wang et al. described a simple method to obtain a conducting film with excellent conductivity of 104.7 S m^{-1} and stability by using aqueous dispersions of PANI composite stabilized with cellulose nanofibers [226]. Luong et al. prepared CNF-PANI (NFC/PANI in the publication) suspensions which were used for the production of CNF-PANI paper-based composite materials. The CNF-PANI exhibited good mechanical properties and high conductivity, which presumes its use in flexible electrodes, antistatic coatings, or electrical conductors [227]. PANI-modified CNF was prepared by Auad et al. as reinforcement of a smart polyurethane [228]. Nanocomposites of CNF-PANI were also synthesized by Silva et al. who reported on the good thermal stability of the material due to PANI acting as a protective barrier against cellulose degradation [229]. Correspondingly, He et al. demonstrated increased thermal stability of CNF caused by the addition of PANI [230]. Electrically conducting nanocomposites of CNF were further successfully produced by Mattoso et al. with potential use in sensors, antistatic, and anticorrosive nano-coatings [231].

CNFs were also used in combination with PPy. For example, an electrically conducting composite of CNF (MFC in the publication) and PPy was synthesized by [232]. In the study of Bober et al. flexible free-standing composite films of CNF-PPy and CNF-PPy-Ag (NFC/PPy and NFC/PPy-Ag in the publication) were synthesized *via in situ* one-step chemical polymerization [233]. Furthermore, flexible, nano-papers based on CNFs with PEDOT:PSS (polystyrene sulfonate) and/or PPy were prepared. Synergies between PEDOT:PSS and PPy resulted in highly conducting and thermally stable materials [234]. Bideau et al. synthesized a composite film based on TEMPO-oxidized cellulose nanofibers (TOCN), PVA,

and PPy. The synthesis led to induced adsorption of PPy on the surface of the TOCN and the composites showed effectiveness against gram positive *Bacillus subtilis* and gram negative *Escherichia coli* strains [235].

The use of BC to stabilize conducting colloidal dispersions has also been reported by several researchers. Lee et al. prepared BC-PANI composite particles by interfacial polymerization of aniline in the presence of chloroform. In the resulting composite, nanoparticles were densely arranged along each fiber of BC and their electrical conductivity reached up to 3.8×10^{-1} S cm^{-1} [178]. Müller et al. prepared BC-PANI composite coatings with electrical conductivity of 0.9 S cm^{-1} and good mechanical properties [236]. Analogous studies were reported by [237–239]. Bacterial cellulose has also been successfully used in the preparation of PPy-based composites and membranes [240–244].

6. CONDUCTING THIN FILMS

Thin films are layers of material formed on a solid support (substrate) either directly by a physical process or *via* a chemical and/or electrochemical reaction [245]. In connection with CPs, it is an alternative strategy for their processing [172]. Stable conducting thin films are interesting research subjects and are widely used in many applications including optics, sensors, biomedical devices, etc. [246].

6.1 Synthesis of thin films

Thin films of PANI can be prepared chemically or electrochemically [247]. Electrochemical polymerization allows to control of the area and thickness of the resulting film [248]; however, this method requires the use of a conducting surface [249] and the resulting films are thinner compared to films prepared by chemical oxidation [250]. Chemical polymerization, therefore, represents a more general approach to the preparation of thin films [133].

6.1.1 Chemical synthesis

The chemical method includes oxidative chemical polymerization of aniline in an acidic aqueous medium with ammonium persulfate (APS) as an oxidizing agent [251]. Essentially any substrate present in the reaction mixture can be coated with a PANI film of submicrometre thickness [172]. The PANI film formation mechanism involves three steps: 1) adsorption of aniline oligomers at the interface (oligomers are more hydrophobic than the aniline cations and tend to separate from the aqueous medium, for example by adsorption on available surfaces), 2) stimulation of chain growth by oligomers and nucleus formation (the first surface-anchored PANI chain forms a nucleus of the future film), and 3) growth of other chains due to the auto-acceleration mechanism close to the nucleus. The chains then extend along the surface and, are preferably oriented perpendicularly

for steric reasons (Fig. 12A) [160], resulting in a brush-like structure [133]. Depending on the reaction conditions, the film thickness varies from 100 to 400 nm. Many surfaces including polystyrene Petri dishes, glass, or metals can be used as substrates for coating with a conducting thin film. The selection of a suitable surface plays an important role in the formation of a PANI film. The films are more uniform on hydrophobic surfaces, whereas on hydrophilic substrates they have a globular structure [133]. Moreover, it was reported that the conductivity of films prepared on hydrophobic substrates might be higher compared to films prepared on hydrophilic substrates such as glass [252], which is explained by the different organizations of PANI chains [253,254].

Besides standard chemical polymerization, dispersion polymerization can be used to prepare thin PANI films. This procedure involves adding a suitable steric stabilizer to the commonly used reaction mixture that contains aniline (aniline hydrochloride) and an oxidant [131,255]. The presence of a stabilizer that prevents macroscopic precipitation of the PANI results in a different morphology of the films and their surface roughness is significantly reduced [256]. The principles of film formation by dispersion polymerization are similar to the formation of colloidal particles [255] discussed in Chapter 5. Dispersion films are thinner than PANI films prepared without stabilizers, which is due to the absence of PANI precipitate [256]. The organization of PANI chains on the film surface is also different and the chains do not show a brush structure, but lie loosely twisted on the substrate (Fig. 12B) [256].
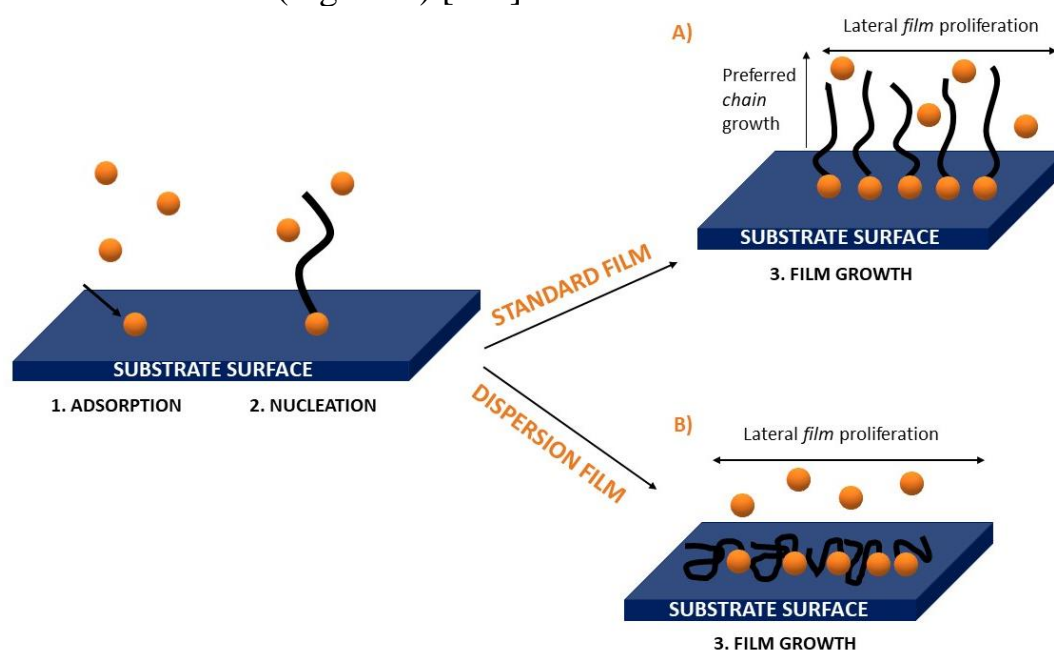

Figure 12 The model of PANI film formation.

6.1.2 Electrochemical synthesis

Conducting films can be easily prepared by electrochemical oxidation of monomers on the surface of the electrode [257]. The choice of electropolymerization conditions, especially the applied potential and current,

critically influences film formation. The applied potential should be high enough to oxidize and polymerize the monomer, but simultaneously low enough not to cause undesirable corrosion. The polymerization solution consists of the monomer, solvent, and supporting electrolyte [249].

The principle of the electrochemical synthesis of PANI consists of the oxidation of aniline in electrolyte solutions [133]. The oxidation of the monomer produces free radicals, that adsorb on the electrode surface and can subsequently undergo a reaction resulting in the desired thin films [258]. This reaction produces an oligomer, which is then oxidized to form a polymer chain. The polymerization process is influenced by various factors including the nature of the doping anion, pH and composition of the electrolyte, electrode material, temperature, and others [259]. PANI can be synthesized by one of three electrochemical methods: 1) the potentiostatic technique based on the application of a constant potential, 2) the galvanostatic technique that applies a constant current, and 3) the potentiodynamic technique in which current and potential differ [259]. Regardless of the method used, the reactor vessel consists of a three-electrode assembly (Fig. 13), namely a working electrode (the substrate to be coated), a reference electrode (usually Ag/AgCl), and an auxiliary electrode or counter-auxiliary electrode (commonly platinum electrode) [249,259]. Similarly to the chemical method, PANI film forms under sufficient acidity in the reaction medium. Higher pH values result in the synthesis of undesirable short oligomers [259]. Therefore, the electropolymerization of aniline is conducted in aqueous solutions containing inorganic acids such as sulfuric, perchloric, nitric, or phosphoric acids; the organic acids such as p-toluenesulfonic acid; or the aqueous solutions of polymeric acids, such as poly(styrenesulfonic acid) or poly(2-acrylamido-2-methyl-1-propanesulfonic acid) [133]. The electrochemical synthesis provides a polymer characterized by a high degree of purity [250] and is considered a method of green chemistry since the oxidation of the monomer is induced by voltage or current [258].
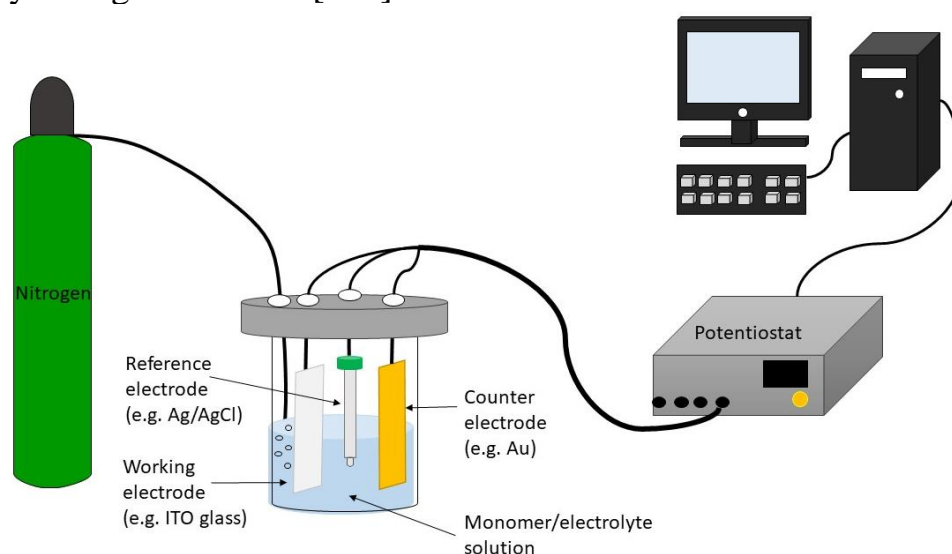

Figure 13 A schematic of the electrochemical synthesis set-up.

6.2 Deposition of Thin Films

In connection with a wide range of thin film applications, several deposition methods have been developed to optimize film properties [260]. Techniques used for the deposition of thin films include chemical and physical methods [251]. Chemical methods of PANI thin film deposition include

- Bulk chemical polymerization (discussed above). Most of the conducting polymers including PANI can be spontaneously deposited as a thin film on various substrates during polymerization [251].
- Chemical vapor deposition (CVD) involves exposing the substrate to volatile precursors, which react and/or decompose on the surface of the substrate to form a thin film deposit [261]. Traditionally, heat is used as an energy source in these processes, which limits the types of substrates that can be used. Especially temperature-sensitive substrates must be avoided [262].
- Plasma-enhanced chemical vapor deposition (PECVD) enables the deposition of films at lower temperatures using plasma. During this process, the source gas is ionized by the energetic electrons generated in the plasma [263]. The deposition rate is typically higher and easier to control because plasma-activated precursors are more reactive [262].
- Langmuir-Blodgett (LB) technique excels for its simplicity, low cost, and ability to change the parameters of the film [264,265]. The principle of the method is the formation of a single layer of molecules on the surface of the liquid (water), which is then transferred to the substrates. Using multiple repetitions, thin layers with a controlled molecular thickness on substrates can be deposited.
- Layer-by-layer (LbL) self-assembly technique consists of the formation of an ultrathin film on a solid support using alternating exposure to positive and negative species with spontaneous deposition of the oppositely charged ions [266].
- Spin coating technique is a simple procedure with the possibility of mass production [267]. This method consists of 1) deposition of material on the turntable; 2) spin up; 3) spin off and evaporation that occurs throughout the process [268]. The thickness of the film depends mainly on the angular speed of spinning, and concentration of the solution and the solvent [261].

Among physical methods, the following can be listed

- Thermal evaporation technique represents one of the most popular techniques for its simplicity and good control of thin film parameters [269]. In this method, the material is heated to a high temperature using very low pressure in extremely clean conditions where it evaporates. Subsequently, the vapour is allowed to condense on the target substrate, together with the gaseous fraction and the solid residue [270].

- Sputtering is based on the ejection of atoms from the surface of the material by bombardment with energetic particles. The sputtered atoms can be further condensed on the substrate to form a thin film [270].

Another well-known deposition strategy is the electrochemical growth of PANI thin films *via* galvanostatic, potentiostatic, or voltammetric techniques [271] discussed in the previous chapter. Although very thin films with excellent control over their morphology can be deposited in this way, the deposition is limited to conducting surfaces [264,272].

6.3 Application

The thin films of conducting polymers are used in different applications. Specifically, PANI films can be used in gas [273,274], chemicals [275] and pH sensors [276], supercapacitors [277,278], electrochromic devices [279], solar cells [280], batteries [281,282], and protection of metal surface from corrosion [283], etc.

As already mentioned, polyaniline is an excellent candidate for applications in biomedicine [151]. In the context of biomedical applications, cell proliferation on the surface of a conducting film is essential. Liu et al. investigated the cellular biocompatibility of a PANI film prepared *via* electroless surface polymerization. The study revealed that the film enabled cell proliferation, and thus could be applied as a surface coating to culture neuronal cells for tissue regeneration [284]. Wang et al. demonstrated that PANI films prepared by direct polymerizing deposition or a casting method were biocompatible and allowed cell attachment and proliferation [285]. One of the advantages of PANI is the simple modification of its surface, for example by reprotonation with various acids, the grafting of functional groups, and copolymerization with various co-monomers, etc. [148]. In this context, adhesion, proliferation, and migration of mouse embryonic fibroblasts on pristine PANI films, PANI films doped with sulfamic and phosphotungstic acids, and PANI films modified with PAMPSA were investigated. The results proved the ability of cells to adhere, proliferate and migrate both on pristine PANI films and films doped with sulfamic and phosphotungstic acids. The presence of PAMPSA, however, worsened the cell behaviour of the film [286]. Kašpárková et al. studied the cellular compatibility of PANI films prepared in the colloidal dispersion mode with poly-N-vinylpyrrolidon, sodium dodecylsulfate, Tween 20 and Pluronic F108 used as stabilizers. The results of the study pointed to a significant role of the stabilizers on the surface and electrical properties of the film as well as on their cellular compatibility. Compared to the other films, sodium dodecyl sulfate films showed high conductivity, good cell compatibility, and no harmful effects on human skin, and therefore appear to be the most promising in the field of biomedicine [287]. Recently, Jasenská et al. prepared PANI films with biocompatible polysaccharides, namely sodium hyaluronate (SH) or chitosan

(CH). The human induced pluripotent stem cells (hiPSC) used in the study were able to adhere and proliferate on the tested surfaces. Biological tests also demonstrated the ability of proteins to adsorb onto surfaces of the films and the absence of embryotoxic effects [288]. Another prerequisite for the application of materials in the field of biomedicine and biosensors is hemocompatibility [289]. Humpolíček et al. studied the hemocompatibility of pristine PANI films and the films modified with PAMPSA. The results proved that the functionalization of the films with PAMPSA hindered blood coagulation, reduced platelet adhesion capacity, and improved the stability of films under various pH, which opens the door for their applications in blood-contacting or collecting devices [290]. Also, Skopalová et al. studied the hemocompatibility of PANI films functionalized by substances with anticipated anticoagulant activity, namely sodium dodecylbenzenesulfonate (SDBS), 2-aminoethane-1-sulfonic acid (taurine) and N-(2-acetamido)-2- aminoethanesulfonic acid (ACES). This study revealed the absence of anticoagulation activity of the functionalized PANI films, which could be due to the low molecular weight of the compounds used for PANI functionalization. In addition to the proper functional groups in the substance used for the film modification, their sufficiently high molecular weight is crucial [289].

Several recent publications reveal a strong interest in the production of cheaper and more environmentally friendly electrically conducting films and composites. The combination of nanocellulose with conducting polymers brings many potential advantages, such as reducing dependence on non-renewable materials, biocompatibility, cheap production, and sustainability. Although nanocellulose itself is not a good conductor of electricity, it can serve as an eco-friendly and low-cost substrate in electrically conducting composites [215,291]. In addition, nanocellulose is intensively investigated in biomedicine [17] and appears to be a commercially available material with wide application potential.

7. AIMS OF WORK

The primary aim of the thesis is to increase knowledge about dispersion systems stabilized with solid particles, specifically cellulose (nano)particles. The particles are either combined with TiO_2 to form Pickering emulsions or utilized as a stabilizer for conducting PANI/cellulose composite colloids. The effort focuses on investigating and understanding the characteristics and behaviour of these classical and conducting dispersion systems. Particular emphasis is put on the formulation, production, and characterization of these systems, as well as the investigation of their biological properties. Intended applications of prepared colloidal systems are in the fields of biomaterials and cosmetics. The main goals of the work have been divided into following areas:

- The formulation of Pickering emulsions for skin photoprotection that are stabilized by a combination of **cellulose nanoparticles** and TiO_2, and the identification of a reliable and repeatable process for producing the emulsions at a lab scale.

    o A comprehensive examination of TiO_2 particle properties and behaviour under simulated *in vivo* and *in vitro* conditions. The information obtained here is critical for the successful integration of TiO_2 in the stabilizer layer of Pickering emulsions.

- Research into the ability of different types of **cellulose nanoparticles** to stabilize PANI in aqueous dispersion, with the goal of synthesizing PANI/cellulose ocomposite particles that can serve as 1) stabilizers of oil-in-water Pickering emulsions and 2) precursors for composite conducting films for potential biomedical applications.

8. EXPERIMENTAL

For clarity, the sections Experimental part, Result and discussion together with Summary of individual goals of the thesis are divided as follows:

a) **Study on TiO$_2$ particles:** based on the limited results of previous studies on the safety and properties of titanium dioxide (TiO$_2$) (nano)particles, a thorough study was conducted to investigate the behaviour of TiO$_2$ particles prior to their incorporation into Pickering emulsions. The study mimicked the *in vivo* conditions that occur after oral and dermal exposure to various forms of TiO$_2$ particles (rutile, anatase, and their commercial mixture) and investigated the physicochemical properties of the particles, including time-dependent agglomeration in simulated body fluids, human blood plasma, phosphate buffered saline (PBS) and media used for cell cultivation (DMEM).

b) **Study on cCNC/TiO$_2$-stabilized Pickering emulsions:** the follow-up study focused on the preparation of Pickering oil-in-water emulsions stabilized with pH-responsive carboxylated cellulose nanoparticles (cCNC) in combination with TiO$_2$ (a mixture of Rutile/Anatase). More specifically, the effect of formulation (ratio between cCNC and TiO$_2$) and preparation method (the Layer by Layer method *vs.* the conventional emulsification method) on the properties of final emulsions was studied. The emulsions could serve as platforms for skin photoprotection.

c) **Study on conducting colloidal systems:** the aim of the study was to develop three different types of conducting systems based on cellulose naoparticles – nanocrystals and nanofibers (CNC, CNF) and polyaniline (PANI). First and foremost, the study focused on the synthesis and characterization of PANI colloidal particles prepared by oxidative polymerization of aniline hydrochloride in the presence of CNC or CNF. The goal was to find a suitable composition of the reaction mixture that would results in stable colloids with favorable physico-chemical and biological properties. The colloids were then used to create other conducting systems for biological application, namely Pickering emulsions and thin films. The effect of the preparation process and formulation on the behaviour and properties of these systems was studied. In addition to physicochemical characterization, biological studies were also conducted.

8.1 Materials

8.1.1 Study on TiO$_2$ particles

Rutile 1 (Batch No. 120717/1) and Rutile 5 (Batch No. 120717/5) were the kind gift of Precheza a. s. (Přerov, Czech Republic). A mixture of Rutile/Anatase (Cat No. 634662-25G) and Anatase (Cat No. 637254-50G) were purchased from Sigma Aldrich (Taufkirchen, Germany).

Artificial saliva solution was prepared by dissolving 0.03 g $NaNO_2$, 0.2 g K_2CO_3, 0.5 g NaCl, and 4.2 g $NaHCO_3$ in 1 L water (Milli-Q filtration system, Merck, Darmstadt, Germany). The solution was adjusted to pH 6.8 with 1M NaOH or 1M HCl (all from Sigma-Aldrich, Taufkirchen, Germany). Simulated gastric fluid (SGF) (pH 1.2) was prepared by dissolving 1 g NaCl in 40 mL 1M hydrochloric acid. Milli-Q water was added to make a final volume of 0.5 L, and the solution was adjusted to pH 1.2 with 1M HCl. Similarly, simulated gastric fluid with pepsin (SGF^{Pepsin}) with pH 1.2 was prepared by the addition of 1.6 g pepsin (Sigma Aldrich, Taufkirchen, Germany) to 0.5 L of the SGF. Simulated intestinal fluid (SIF) with pH 6.8 was prepared by dissolving 6.8 g KH_2PO_4 in
77 mL 0.2M NaOH and adding water to make a final volume of 1 L. Then, the solution was adjusted to pH 6.8 with 1M NaOH or 1M HCl. For SIF with pancreatin (SIF^{Pancreatin}) with pH 6.8, pancreatin (Sigma Aldrich, Taufkirchen, Germany) was further added to the solution at a concentration of 10 g L^{-1}. Human blood plasma was obtained from healthy individuals *via* the Tomas Bata Regional Hospital in Zlín, after informed consent was signed. Finally, phosphate buffered saline (PBS), Dulbecco's modified eagle medium (DMEM), and DMEM supplemented with 10% calf serum (DMEM^{Serum}) were purchased from BioSera (Nuaille, France).

8.1.2 Study on cCNC/TiO$_2$-stabilized Pickering emulsions

Carboxylated cellulose nanocrystals (cCNC; 2.2 %) were prepared by oxidation of commercially available microcrystalline cellulose (Avicel PH101) with ammonium peroxydisulfate (APS; 98 %) (both supplied by Sigma Aldrich, Germany) according to procedure described in [30]. A mixture of Rutile/Anatase (Cat No. 634662-25G) was purchased from Sigma Aldrich (Taufkirchen, Germany). Caprylic/capric triglyceride (T) was acquired from AceTrade (Czech Republic). Sodium chloride (NaCl) was acquired from Mikrochem Trade (Slovakia). Calcium chloride (CaCl$_2$), hydrochloric acid (HCl), and sodium hydroxide (NaOH) were purchased from Ing. Petr Lukeš (Czech Republic).

8.1.3 Study on conducting colloidal systems

Ammonium peroxydisulfate (APS; 98 %), aniline hydrochloride (AH; reagent-grade ≥ 98 %), undecane, hydrochloric acid (HCl; 37 %), ethylene

glycol, and diiodomethane were acquired from Sigma Aldrich (Germany). Cellulose nanocrystals (CNC; 12.2 wt% in water) and cellulose nanofibers (CNF; 3 wt% in water) were purchased from Cellulose Lab (Canada). Caprylic/capric triglyceride (T) was acquired from AceTrade (Czech Republic).

8.2 Sample preparation

8.2.1 Study on TiO_2 particles

TiO_2 dispersions were prepared by homogenizing 0.05 g TiO_2 particles in 10 mL Milli-Q water for 30 min using a UP400S sonicator (Heielscher, Teltow, Germany) at a power of 400 W (24 kHz) and using an amplitude of 100 % with a cycle setting of 0.6 on an ice bath. The dispersions were then mixed with the tested simulated body fluids in concentrations specified in 8.3.1.

8.2.2 Study on cCNC/TiO_2-stabilized Pickering emulsions

Prior to preparation of Pickering emulsions, dispersions of cCNC and TiO_2 without an oil phase were studied as a part of the preformulation study. Compositions of the investigated samples are listed in Tab. 2. The dispersions were prepared by mixing cCNC and H_2O, then pH was adjusted to the desired value (0.1M HCl and/or 0.1M NaOH) and finally TiO_2 was added. The dispersions were left to equilibrate for 24 hours.

The oil-in-water (O/W) Pickering emulsions were prepared using tricaprylin/tricaprine (T) oil (dispersed phase), water (continuous phase), and a stabilizer made of carboxylated nanocrystalline cellulose particles (cCNC) and titanium dioxide (TiO_2, a mixture of Rutile/Anatase). The mass of the emulsions was fixed to 10 g, but the composition of individual emulsions changed, as shown in Tab. 3. Emulsions were prepared using two different methods. Specifically, the layer-by-layer (LbL) method and the conventional emulsification (CE) were used. Pickering emulsions were created using sonication (UP400S sonicator, Heielscher, Teltow, Germany) in both cases. Regardless the preparation method, the sonication parameters remained unchanged, namely an amplitude of 30 % and a cycle of 0.6.

In the LbL method, the cCNC dispersion was first mixed with demineralized water and oil, pH was adjusted to the required value and the system was sonicated for 2 min to prepare a primary emulsion. The selected amount of TiO_2 was added to the primary emulsion followed by a 2-min sonication, yilding the final Pickering emulsion (Fig. 14).

The CE method involved mixing cCNC dispersion with demineralized water, adjusting this dispersion to the required pH (again using 0.1M HCl and 0.1M NaOH), and adding the calculated amount of TiO_2. The mixture was then shaken by hand and left to stand for 24 hours. Finally, the calculated amount of oil was added to the mixture, followed by the 2-min sonication (Fig. 14).

The experiments also involved the preparation of emulsions containing electrolytes (in addition to all above mentioned ingredients). Specifically, NaCl ($27\ \mathrm{mmol\ L^{-1}}$ in the aqueous phase) or $CaCl_2$ ($3\ \mathrm{mmol\ L^{-1}}$ in the aqueous phase) were added. The concentration of electrolytes was chosen on the basis of previously conducted study [83]. In the case of the LbL method, salt was added before the first sonication as well as after the first and second sonications. In the CE method, the salt was always added after adjusting the pH, and before adding the TiO_2 particles.

Table 2 Composition of cCNC/TiO$_2$ dispersions.

Total stabilizer content [%]	cCNC:TiO₂ ratio	pH	O/W ratio
0.5	1:1; 3:2; 4:1	3; 4; 4.5; 5	20/80

Table 3 Composition of Pickering emulsions in preformulation study.

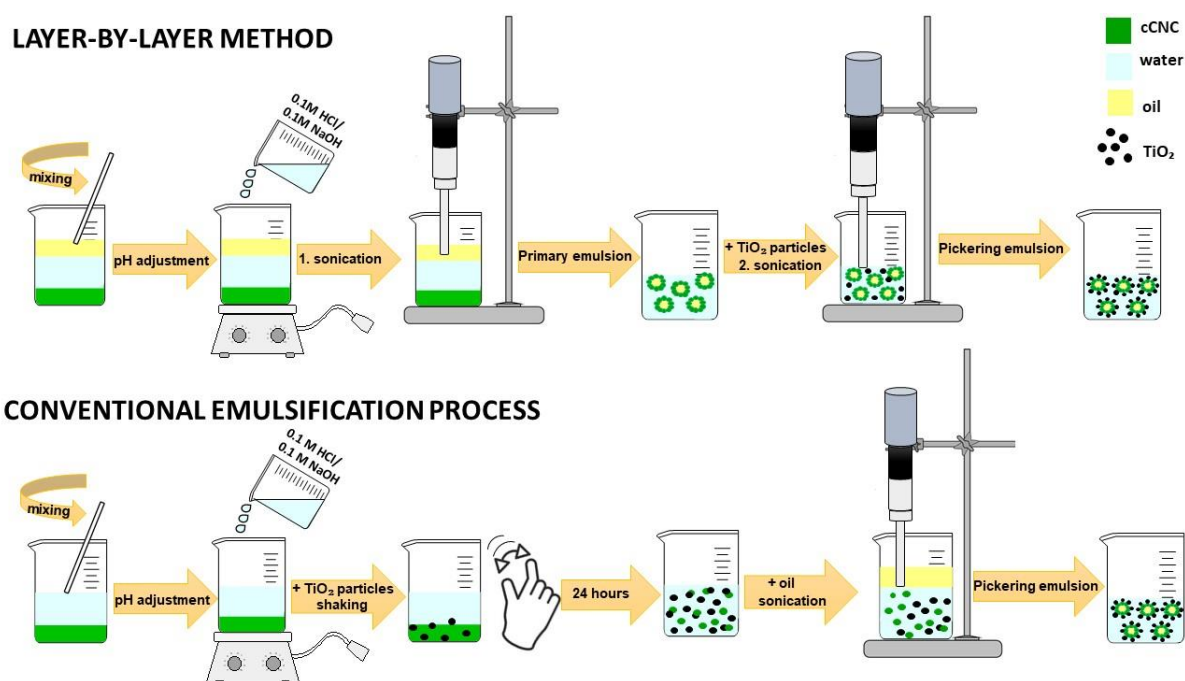| O/W ratio	Total stabilizer content [%]	cCNC:TiO₂ ratio		
10/90				
20/80	0.3	1:1	3:2	4:1
30/70				
20/80	0.5	n.p.	3:2	4:1
30/70				
20/80	0.7	n.p.	3:2	4:1
30/70				

n.p. not prepared

Figure 14 Schematic illustration of the formation of O/W Pickering emulsion.

8.2.3 Study on conducting colloidal systems

Within the study, three types of conducting colloidal systems containing cellulose nanoparticles (CNC, CNF) and PANI were prepared, namely colloidal dispersions, Pickering emulsions, and thin films.

Colloidal dispersions

A pre-formulation study was carried out to find the optimal composition of stable colloidal dispersions. A series of samples with varying amounts of CNC or CNF particles and reactant concentrations were prepared (Tab. 4). The compositions giving samples with the best stability, PANI/CNC and PANI/CNF (marked in bold, Tab. 4) were then used in subsequent experiments.

The synthesis was carried out by the oxidation of aniline hydrochloride (AH) with ammonium persulfate (APS) in the presence of each type of cellulose nanoparticles. For PANI/CNF, aqueous CNF dispersion was kept at 55 °C overnight and sonicated for 10 min at 60% amplitude using a UP400S sonicator (Hielscher, Germany) before being used. The polymerization then proceeded in the same way for both types of dispersions. Specifically, AH was dissolved in 5 mL of aqueous CNC or CNF dispersion and the polymerization was started at room temperature by adding 5 mL of aqueous APS solution to the reaction mixture. The lower CNF concentration, compared to CNC, was chosen due to poor dispersibility of CNF caused by its longer and entangled fibres [292]. The polymerization was completed within 1 hour and the resulting colloidal dispersions were poured into dialysis tube Spectra Por 2 (MWCO 12,000–14,000; Spectrum Laboratories Inc., USA) to remove residual impurities. Dialysis was performed against 0.2M hydrochloric acid for 14 days.

Table 4 Compositions of the reaction mixtures of colloidal dispersions used in the preformulation study.

Nanocellulose type	Sample	CNC/CNF [wt.%]	AH [M]	APS [M]
CNC	PANI/CNC-A1	0.5	0.2	0.05
	PANI/CNC-A2	0.5	0.2	0.01
	PANI/CNC-B1 (PANI/CNC)*	**1.0**	**0.2**	**0.05**
	PANI/CNC-B2	1.0	0.2	0.01
	PANI/CNC-C1	2.0	0.2	0.05
	PANI/CNC-C2	2.0	0.2	0.01
CNF	PANI/CNF-D1	0.25	0.2	0.2
	PANI/CNF-D2	0.13	0.2	0.2
	PANI/CNF-D3 (PANI/CNF) *	**0.06**	**0.2**	**0.2**

* These stable samples will hereinafter be referred to as PANI/CNC or PANI/CNF and used in the follow up experiments.

Pickering emulsions

PANI/CNC and PANI/CNF particles in colloidal dispersions were used as Pickering stabilizers to prepare oil in water (O/W) emulsions with 20 % oil phase composed either of model oil undecane (U) or caprylic/capric triglyceride (T) which is a neutral high-purity oil used in cosmetics and pharmacy [293–295] (Tab. 5). To 8 g of colloidal PANI/CNC dispersion, 2 g of oil was added to form a Pickering emulsion. The sample was homogenized with UP400S sonicator (Hielscher, Germany) for 1 min at 30% amplitude on an ice bath. The preparation of Pickering emulsion with PANI/CNF proceeded in a slightly different way. At first, the PANI/CNF dispersion was diluted to either 30 or 50 % of initial concentration with demineralized water and then sonicated for 1 min at 30% amplitude. Then 2 g of oil were added to 8 g diluted PANI/CNF and the sample was sonicated again under the same conditions. A different approach based on dilution of CNF-based Pickering emulsions was used due to the mentioned poor dispersibility of CNF.

Table 5 Composition of Pickering emulsions (E) with O/W 20/80; oil phase: caprylic/capric triglyceride (T) or undecane (U) stabilized with PANI/CNC colloidal dispersion (non-diluted) or PANI/CNF diluted to 30 or 50 % of initial dispersion concentration.

Sample	Stabilizer type	Dilution [%][a]	Oil phase
E-PANI/CNC^T	PANI/CNC	None	Caprylic/capric triglyceride (T)
E-PANI/CNF^{T30}	PANI/CNF	30	
E-PANI/CNF^{T50}	PANI/CNF	50	
E-PANI/CNC^U	PANI/CNC	None	Undecane (U)
E-PANI/CNF^{U30}	PANI/CNF	30	
E-PANI/CNF^{U50}	PANI/CNF	50	

[a] Dilution relatively to initial 100% dispersion

Thin Films

Besides Pickering emulsions, PANI/CNC and PANI/CNF colloidal dispersions were used to synthetize composite films through *in situ* oxidative polymerization of aniline hydrochloride (AH) with ammonium peroxydisulfate (APS) in the presence of an aqueous nanocellulose suspension on the tissue polystyrene culture dishes (TPP; Switzerland) served as a substrate (Fig. 15).

For the synthesis of PANI/CNC composite films, APS (0.05 mol L^{-1}) was dissolved in water and AH (0.2 mol L^{-1}) was dissolved in an aqueous solution of CNC (1 wt%). Similarly, for the synthesis of PANI/CNF films, APS

(0.2 mol L^{-1}) was dissolved in water and AH (0.2 mol L^{-1}) was dissolved in an aqueous solution of CNF (0.06 wt%). A solution of stabilizing CNF (0.06 wt%) was prepared by the CNF overnight dissolution in stirred demineralized water at 55 °C followed by sonication for 10 min at 60% amplitude. The polymerization was then started by mixing the AH/CNC or AH/CNF solution and APS at room temperature. The polymerization of PANI/CNF, the composite film was completed in 1 h. Because the first layer of PANI/CNC film was too thin, the procedure was repeated and a second layer of the film was deposited on the top of the first layer. The polymerization of each layer was completed in 24 h. The resulting composite films were rinsed with 0.2M hydrochloric acid, followed by methanol, and allowed to dry in air. As a reference, standard PANI films were prepared and synthesized in a similar manner without the use a stabilizer.
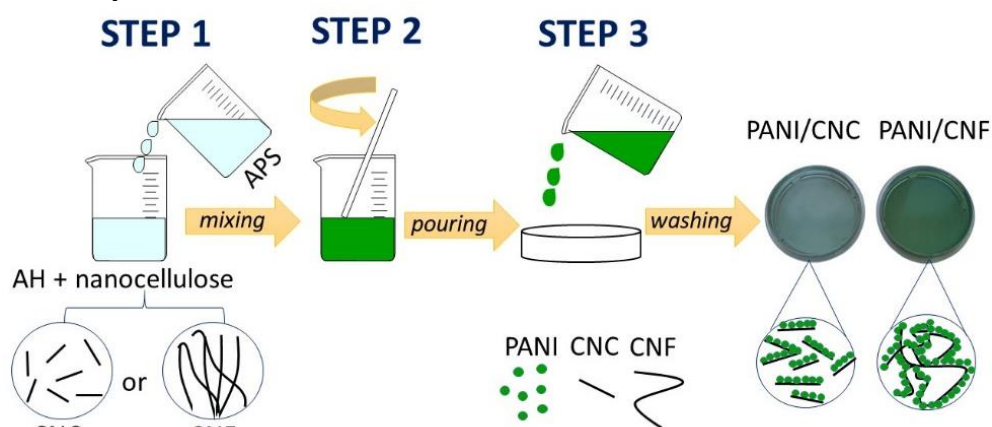

Figure 15 Schematic illustration of the synthesis of conducting thin films.

8.3 Methods

8.3.1 Study on TiO$_2$ particles

Physico-chemical characterization

Particle sizes and *particle size* distribution of TiO$_2$ particles were determined by dynamic light scattering (DLS) on a Zetasizer Nano ZS90 (Malvern Instruments, Malvern, Worcestershire, UK). Analyses were performed after dilution of the initial TiO$_2$ dispersions in the given media at a scattering angle of 90° and temperature of 25 °C. For measurements, 20 µL of dispersion was added to 1 mL of each medium. The time-dependent development of particle size was studied for 100 min at 20 min intervals and particle size was expressed as an average intensity-derived particle diameter (z-average diameter) calculated on the basis of at least three repeated measurements. In addition to particle size, the polydispersity index (PDI) was also obtained. The PDI is a measure of the distribution width spanning from 0 to 1, where ~0.1 would be achieved by a completely monodisperse system, while values greater than 0.7 indicate a sample with a very broad size distribution.

Zeta potential was measured using a Zetasizer Nano ZS90 (Malvern Instruments, Worcestershire, Malvern, UK). Measurements were performed in

Milli-Q water with pH varying within the pH range of 1 to 10. For analysis, 15 μL TiO$_2$ dispersion was mixed with 4 mL pH adjusted water to a final concentration of 3.75 μL mL^{-1}. Zeta potential measurements are calculated on the basis of at least three repeated measurements and expressed as means and standard deviations of respective values.

Morphology of TiO$_2$ particles was observed using a Nova NanoSEM 450 scanning electron microscope (SEM) (FEI, ThermoFischer Scientific, Waltham, MA, USA) at an accelerating voltage of 5 kV.

Biological characterization

Cytotoxicity. In order to evaluate the cytotoxic effect of TiO$_2$ particles, mouse embryonic fibroblast cell lines (ATCC CRL-1658 NIH/3T3) were used. ATCC–formulated Dulbecco's Modified Eagle's Medium (DMEM, PAA Laboratories GmbH, Pasching, Austria) containing 10% calf serum (Biosera, Nuaille, France) and 1% Penicillin/Streptomycin (GE Healthcare HyClone, Northumberland, UK) was used as the culture medium. Cytotoxicity evaluation was performed according to ISO 10 993-5:2009 protocol. Dispersions of TiO$_2$ were prepared by diluting the 5.0 mg mL^{-1} parent dispersion followed by homogenization in 10 mL culture medium for 30 min using a UP400S sonicator (Heielscher, Teltow, Germany). A series of concentrations (5.0, 4.0, 3.5, 3.0, 2.5, 2.0, 1.5, 1.0 mg mL^{-1}) was obtained. For the cytotoxicity assay, NIH/3T3 cells were pre-cultivated for 24 h and seeded at a concentration of 1×10^5 cells per well (96 well plates were used, TPP Trasadingen, Switzerland). The culture medium was subsequently replaced by TiO$_2$ dispersions with the above-given concentrations. The cytotoxicity was measured 24 h after exposure. As a reference, cells cultivated in pure medium without TiO$_2$ particles were used. Cytotoxic effects were evaluated using the ATP Determination Kit (A22066, Thermo Fisher Scientific, Waltham, MA, USA) and the luminescence was measured with an Infinite M200 PRO luminometer (Tecan, Männedorf, Switzerland). All tests were carried out in quadruplicates in two independent tests. Results are presented as the relative values of cell viability compared to cells cultivated in medium without the presence of the tested materials (reference with viability 1).

Cell morphology was observed using an inverted Olympus phase contrast microscope (Olympus IX81, Tokyo, Japan).

8.3.2 Study on cCNC/TiO$_2$-stabilized emulsions

Physico-chemical characterization

Size of emulsion droplets. The droplet size and distribution were measured using laser diffraction (Mastersizer 3000, Malvern Instruments, UK). For diffraction measurements, the emulsions were sampled and suspended in the instrument flow system containing milliQ-water at a pump velocity of 2220 rpm. The volume mean diameter D[4,3], corresponding to the mean diameter of spheres

with the same volume as the analysed droplets, was determined. Analyses were carried out on the day of preparation, as well as one and two weeks after preparation.

Zeta potential of emulsion droplets. Zeta potential was measured using a Zetasizer Nano ZS90 (Malvern Instruments, UK). Prior to measurements, 15 µL of emulsion was diluted with 4 mL of demineralized water adjusted to pH 3 or 5 and measured for the zeta-potential, which was reported as a mean and standard deviation of three measurements. The measurement took place at the same time intervals as the measurement of emulsion droplet size.

Phase studies. The stability of emulsions was evaluated visually on the day of preparation, the day after preparation, and one and two weeks after the preparation of the emulsions. The emulsions were stored at ambient temperature. The stability was assessed using emulsification index (EI), encapsulation efficiency (EE), and creaming index (CI). The emulsification index was calculated according to equation (2), where V_{emuls} is the volume of emulsion layer formed, and V_{total} is the total volume of the sample. The encapsulation efficacy was determined from a volume fraction of the encapsulated oil (V_{encaps}) and total volume of the oil phase (V_{total}) (equation 3). The creaming index was calculated as the height of the emulsion layer (H_{emuls}) relative to the total height of the emulsion (H_{total}) (equation 4).

$$EI = \frac{V_{emuls}}{V_{total}} \cdot 100\% \qquad (2)$$

$$EE = \frac{V_{encaps}}{V_{total}} \cdot 100\% \qquad (3)$$

$$CI = \frac{H_{emuls}}{H_{total}} \cdot 100\% \qquad (4)$$

Morphology. Atomic force microscopy (AFM) was used to examine the morphology of emulsion droplets. The analysis of emulsions was investigated using a Dimension ICON with ScanAsyst-AIR probe (Bruker Corporation; USA). The emulsions were diluted with demineralized water in a ratio of 1:9 and then 50 µL of the emulsion was placed on mica surface and allowed to dry at room temperature. The measurements were conducted at normal relative humidity and room temperature in ScanAsyst mode. The images were recorded at a scanning rate of 1 Hz. The dispersions prepared in the preformulation study were examined using an Olympus IX81 optical microscope (Tokyo, Japan) without dilution.

8.3.3 Study on conducting colloidal systems

Colloidal particles and Pickering emulsion: physico-chemical characterization

Particle sizes of colloidal particles and emulsion droplets were determined on freshly prepared samples by dynamic light scattering (DLS) using Zetasizer Nano ZS instrument (Malvern Instrument, UK). The sizes were expressed as an average intensity-derived diameter (z-average diameter) calculated on the basis of at least three repeated measurements. In addition to particle size, the polydispersity index (PDI) describing the distribution width was obtained. For analysis, 20 µL of freshly prepared sample was added to 3 mL 1M HCl twice filtered through a filter with a pore size of 0.22 µm (TPP Trasadingen, Switzerland). The measurements were performed at temperature of 25 °C in disposable cuvettes on the day of preparation. The particle sizes and distributions were confirmed on dialysed samples in the same manner.

Ultraviolet–visible (UV–vis) spectra of PANI/CNC and PANI/CNF dispersions were recorded for determining the concentration of PANI in the colloidal dispersions and verification of successful synthesis of the PANI-containing colloidal particles. The spectra were measured at the wavelength range of 200–800 nm using a Photo Lab 6600 UV-vis spectrometer (WTW, Germany). After dilution of the sample with twice filtered 1M HCl, the concentrations of PANI in PANI/CNC and PANI/CNF samples were calculated according to [296].

Morphology. The morphologies of nanocelluloses (CNC, CNF) and colloidal particles (PANI/CNC, PANI/CNF) were studied by transmission electron microscopy (TEM) using JEOL JEM 2000 FX (Japan). The emulsion droplets were investigated by confocal laser scanning microscopy in transmission mode, using Olympus model FV3000 microscope (Olympus, Tokyo, Japan).

Colloidal particles and Pickering emulsion: biological characterization

Biological testing of colloidal particles and emulsions was carried out in cooperation with the Institute of Biophysics of the Czech Academy of Sciences and the Faculty of Science at Masaryk University in Brno, and included testing of cytotoxicity, antioxidant activity, oxidative burst (ROS production), and nitric oxide (NO) and interleukin 6 (IL-6) production. Biological assays were performed on the murine peritoneal macrophage and isolated neutrophils.

Cell culture. The murine peritoneal macrophage RAW 264.7 (European Collection of Authenticated Cell Cultures, UK) were cultured in Dulbecco's Modified Eagle Medium (DMEM; Gibco), supplemented with 10% of heat-inactivated low endotoxin fetal bovine serum (FBS; PAN, Germany) and 1% combination penicillin-streptomycin. Cells were maintained at 37 °C in a humidified atmosphere containing 5 % CO_2 and 95 % air.

Neutrophils isolation. Blood samples were collected from the cubital vein of healthy individuals. The volunteers were aged 18–50, both female and male and they did not take any drugs and were free of any signs of cold or other diseases

for at least 3 weeks before blood sampling. The Ethics Committee for Research at Masaryk University, Brno, Czech Republic (number EKV-2018-083) approved the collection protocol. Sodium citrate (0.38% final concentration) was used as an anticoagulant. The whole blood was mixed with 3% dextran and left at room temperature for approx. 30 min. The resulting buffy coat was overlaid on Histopaque 1.077 and centrifuged at 390 g for 30 min without acceleration and brake. After centrifugation, the remaining erythrocytes were lysed by water hypotonic lysis for 30 sec. The neutrophils were washed in cold PBS, centrifuged at $190 \times g$ for 10 min, and finally re-suspended in cold PBS. The viability of neutrophils was verified by CASY cytometer (Roche, Switzerland) and only neutrophils with viability over 95 % were used for these experiments.

Cytotoxicity evaluation. Evaluation of RAW 264.7 cells cytotoxicity was based on the determination of the amount of metabolically active cells according to the analysis of the total amount of 3-(4,5-dimethylthiazol-2-yl)-2,5-diphenyltetrazolium bromide (MTT) in whole-cell lysates, which reflects the number of metabolically active viable cells in culture, as described in [297]. RAW264.7 cells were incubated in a 24-well plate with tested compounds and LPS (25 ng mL^{-1}) for 24 h at 37 °C in an atmosphere of 5% CO_2 and 95% air. At the end of the incubation period, the cultivation medium was collected for NO and IL-6 production detection and a new cell culture medium supplemented with MTT (final concentration 0.25 mg mL^{-1}) was added and incubated for another 1 h. The medium was removed and formazan from cells was extracted with 100 µl of 10% Triton X-100 in 0.1M HCl per well on a shaker for 15 minutes. The extracts were transferred into a 96-well plate and the absorbance was read at 570 nm on a SPECTRA Sunrise microplate reader (Tecan, Mannedorf, Switzerland).

Antioxidant activity. The luminol-HRP-H_2O_2 cell-free system was used to determine the antioxidant activity of colloidal particles and Pickering emulsions. The principle of the method was described previously in [298]. As a source of chemiluminescence signal, the H_2O_2 and horseradish peroxidase (HRP) were used. Aliquots of 50 µl of tested samples (diluted to 1 – 10 % of starting concentrations), HRP (final concentration 2 U mL^{-1}), and luminol (final concentration 10 µM) were mixed in a 96-well luminescence plate. The reaction was started by adding H_2O_2 to a final concentration of 100 µmol L^{-1}. Chemiluminescence signal was measured for 120 min at 37 °C by an LM-01 microplate luminometer (Immunotech, Czech Republic). Data were converted to a percentage of the control (HRP or luminol) and presented as mean (n=4) ± SEM.

The oxidative burst (ROS production) of isolated neutrophils. Kinetics of ROS formation by isolated neutrophils was determined by luminol-enhanced chemiluminescence for a period of 120 min at 37 °C, using 96-well white flat bottom culture plates on a luminometer (Immunotech, Czech Republic and Infinite M200, Tecan, Switzerland). The analysis was carried out according to [299]. Firstly, 25 µL of neutrophil suspension (2.5×10^5 cells/well) in Hank's

buffered salt solution (HBSS) were mixed with 25 μL of 10 mM luminol (in 0.2M borate buffer) and 25 μL of each of the tested samples (PANI/CNC, PANI/CNF, Pickering emulsions; diluted to $1 - 10$ % of starting concentrations with HBSS). The total volume was adjusted to 250 μL with HBSS and the samples were measured immediately. The response obtained was named spontaneous (non-stimulated with other activators) chemiluminescence. Secondly, 25 μL of neutrophil suspension (2.5×10^5 cells/well) mixed with 25 μL of 10 mM luminol and 25 μL each of the tested samples (diluted to $1 - 10$ % of starting concentrations). HBSS was also used to adjust the total reaction volume to 225 μL. Finally, neutrophils were activated with 25 μL of 62.5 μg mL^{-1} opsonized zymosan particles (OZP-activated chemiluminescence, Sigma-Aldrich). The data were based on integral values of chemiluminescence over 120 min and converted to a percentage of the respective control (without or with OZP) and presented as mean (n=4) ± standard error of the mean (SEM).

Nitric oxide (NO) and interleukin 6 (IL-6) production from murine macrophages. Changes in NO production were measured indirectly as the accumulation of nitrites (the end product of NO metabolism) in medium by using Griess reagent (Sigma-Aldrich), according to the method described previously in [300]. Murine macrophage cell line RAW 264.7 was cultured in 24-well flat bottom plates at 2.5×10^5 cells/well with tested samples (diluted to $1 - 10$ % of starting concentrations), dissolved in DMEM medium and 15 ng mL^{-1} lipopolysaccharide (LPS; E. coli/026:B6, Sigma-Aldrich) for 24 h. The total volume was 500 μL. At the end of the incubation, the supernatants were collected by centrifugation at $16000 \times$ g at 4 °C for 5 min and 80 μL of each sample was mixed with equal volume of the Griess reagent (Sigma-Aldrich) in a 96-well plate. The reaction mixtures were incubated at room temperature for 30 min in the dark and the absorbance was read at 540 nm. A calibration curve of 0.52 μM NaNO$_2$ was constructed and used for calculations. Data were converted to a percentage of the LPS control and presented as mean (n=4) ± SEM. The concentration of pro-inflammatory cytokine IL-6 produced by RAW264.7 cells in the cultivation medium was determined after 24 h of exposure to tested samples and LPS by commercially available immunoassays (Mouse IL-6 DuoSet, R&D Systems). The assays were carried out according to the manufacturer's instructions as described previously in [301]. Data were converted to a percentage of the LPS control and presented as mean (n=4) ± SEM.

Statistical analysis. Data related to biological properties are presented as mean ± SEM. All assays were performed in quadruplicates. The number of independent experiments (n) is stated in the figure legend. The data from some of the measurements were normalized to the reference in each experiment to account for the variability of individual cell passages. Statistical analysis was performed using GraphPad Prism version 6.01 for Windows, GraphPad Software, La Jolla California USA. Statistical differences were tested by one-way ANOVA, which was followed by Dunnett's multiple comparison test or by one-sample t-test to

compare values expressed as percentages. In the case of one sample t-test application, the Bonferroni correction of the p-value for multiple comparisons was performed. $P < 0.05$ was taken to indicate significant differences between data mean values.

Antibacterial properties. The testing of antibacterial properties of colloidal PANI/CNC and PANI/CNF dispersions was performed with two bacterial strains, gram positive *Staphylococcus aureus* CCM 4516 and gram negative *Escherichia coli* CCM 4517 (Czech Collection of Microorganisms). The density of bacterial suspensions was adjusted to obtain the starting inoculum concentration of 5×10^5 CFU mL^{-1} through diluting with Mueller-Hinton broth. Bacteria were grown on Plate Count-Agar (PCA, HiMedia laboratories, India) at 35 °C for 24 h. Antibacterial activity was determined as the minimum inhibitory concentration (MIC). The colloidal dispersions were diluted with distilled water to the concentrations corresponding to mg mL^{-1} PANI in dispersions ranging from 1.84 to 0.0009 mg mL^{-1} (PANI/CNC) and 2.88 to 0.0014 mg mL^{-1} (PANI/CNF), and inoculated with 2 mL of bacterial suspension. The samples were incubated at 35 °C for 24 h and then 100 μL of the samples were spread over agar plate surfaces. After 24 h of incubation at 37 °C, the MIC was determined. For antibacterial tests, each experiment was performed in duplicates.

Colloid-based thin films: physico-chemical characterization

Surface energy. Contact angle measurements and determination of surface energy were performed using a SEE System (Advex Instruments, Brno, Czech Republic) equipped with a CCD camera. For all tested films, deionized water, ethylene glycol, and diiodomethane (all from Sigma-Aldrich, Germany) were used as testing liquids and the droplet volume of the testing liquids was set to 5 μL. For each film, three replicate measurements were performed. The surface free energy was determined by the "acid–base" model.

Atomic force microscopy. The analysis of the surface topographies and electrical properties of the films was investigated by tunnelling AFM using the PeakForce TUNA module on a Dimension ICON instrument (Bruker Corporation; USA). Measurements were performed under laboratory temperature and atmosphere by using a PFTUNA probe (Bruker Corporation; USA) with a spring constant of 0.4 N m^{-1} covered on both sides with a conducting Pt/Ir layer. The scanning rate was 0.3 Hz and the TUNA current was measured by applying a bias voltage of 800 mV and the same peak force to all the studied samples. The resulting area roughness parameters and TUNA current signals were determined according to the protocol of ISO 25178-2 standard using NanoScope Analysis software v.1.5. The following parameters were determined: mean and maximum TUNA current, surface roughness (*Sa*) (arithmetical mean height), maximum surface height (*Sz*) (the sum of the largest peak and largest pit depth values on the surface), and surface area increase (*Rsa*).

51

Conductivity. The four-point van der Pauw method was used to determine the conductivity of the studied films. A programmable electrometer Keithley 6517B, a source meter Keithley 2410 and a switch Keithley 7002 (USA) were employed. Measurements were performed at ambient temperature.

Colloid-based thin films: biological characterization

Cell proliferation. Prior to testing, the samples of composite films were disinfected by 30 min of exposure to a UV-radiation source operating at a wavelength of 258 nm, emitted from a low-pressure mercury lamp. Investigation was performed into the compatibility of the PANI/CNC and PANI/CNF films with the mouse embryonic fibroblast NIH/3T3 cell line (ECACC 93061524, England). For this assay, ATCC–formulated Dulbecco's Modified Eagle's Medium (Biosera, France) containing 10% of calf serum (BioSera, France) and 100 U mL^{-1} Penicillin/Streptomycin (Biosera, France), was used as the culture medium. Cell proliferation was assessed on cells that had been seeded on the tested samples in the tissue polystyrene culture dishes (TPP, Switzerland) at an initial concentration of 1×10^5 cells mL^{-1} and cultivated. After 48 h of the proliferation, cells were observed by the confocal laser scanning microscopy, model FV3000 (Olympus, Tokyo, Japan) using ActinGreenTM 488 (Thermo Fisher Scientific, USA) and Hoechst 33258 (blue color, Thermo Fisher Scientific, USA).

Antioxidant activity. Antioxidant properties of PANI/CNC and PANI/CNF films was determined by a 1,1-diphenyl-2-picrylhydrazyl (DPPH) free-radical scavenging assay. Freshly prepared 1×10^{-4} M DPPH solution in ethanol (1 mL) was poured onto the petri dish (diameter of 3.5 cm) with *in situ* polymerized PANI/CNC or PANI/films and immediately placed in dark for 5 min. UV spectra of DPPH solution being in contact with studied films were recorded at 516 nm using Jasco V-750 Spectrophotometer (Jasco Inc, USA) and scavenging activity (SC) was calculated as $SC = [(A_0 - A_1)/A_0] \times 100$, where A_0 and A_1 are absorbance of DPPH solution prior to and after contact with tested samples, respectively.

Antibacterial properties. Antibacterial efficacy of the films was determined with gram-positive *Staphylococcus aureus* CCM 4516 and gram-negative *Escherichia coli* CCM 4517 purchased from the Czech Collection of Microorganisms (Czech Republic). The antibacterial activity was determined according to the protocol of EN ISO 22196:2011 (modified version). Prior to testing, the samples were disinfected by an exposure to an UV-radiation source (258 nm) at which PANI is stable [180]. Bacteria were grown on a plate count agar (PCA) (Sigma-Aldrich, USA) at 35 °C and a relative humidity of not less than 90 %. For antibacterial tests, bacteria were inoculated in tryptic soy broth (TSB) (HiMedia Laboratories, Mumbai, India) and then adjusted and diluted to obtain the starting inoculum concentration. The optical density (OD) measurement was used to determine the number of cells. The volume of bacterial suspension applied on the tested area was 300 µL. Incubation was carried out at

35 °C and a relative humidity of not less than 90 % for 24 h. After the incubation, the tested films were rinsed with 6.2 mL of soybean casein digest lecithin polysorbate (SCDLP) medium (HiMedia Laboratories, Mumbai, India) followed by determination of the viable bacteria number using a pour plate culture method. The standard PANI film was used as a reference surface.

8.4 Results and discussion

8.4.1 Study on TiO$_2$ particles

TiO$_2$ is interesting material with good biocompatibility, excellent stability, high refractive index, corrosion resistance, and low-cost production [302]. Due to the presence of TiO$_2$ in many dermal and cosmetic formulations such as sunscreens, creams, foundations or lip balms, the exposure of humans to TiO$_2$ *via* the dermal or oral route is inevitable [303], whereas a gap in knowledge about the possible adverse effects of TiO$_2$ still exists. As regards topical applications, according to most studies carried out on humans or animals, no penetration of TiO$_2$ beyond the outer layers of the *stratum corneum* to viable *epidermis* or *dermis* cells has been proven after dermal exposure [304,305]. Because of the accidental oral intake of some types of cosmetic products such as lip balms, it is also necessary to consider the possibility of TiO$_2$ NPs penetration into the oral and gastrointestinal mucosa [303]. Authors of publication [306] conducted a human *in vivo* study on the gastrointestinal absorption of TiO$_2$ NPs of different particle sizes and reported on the absence of significant TiO$_2$ absorption after oral exposure in humans, regardless of particle size [306]. Recently, Marucco et al. conducted a study using a simulated human digestive system to evaluate the biotransformation of food-grade and nanometric TiO$_2$ during the transit in the oral-gastro-intestinal tract. The results revealed particle aggregation as a result of the high ionic strength in the simulated gastric and intestinal fluids. The authors also observed the formation of a hard-biocorona, resulting in partial masking of the TiO$_2$ particles surface and reactivity [307]. In addition, Dudefoi et al. reported the formation of agglomerates mainly in the intestinal fluid as a result of α-amylase and divalent cation adsorption. Moreover, TiO$_2$ inhibited the enzymatic activity of α-amylase in saliva, while having no effect on pepsin activity in gastric fluid [308].

Generally, the penetration of TiO$_2$ NPs into the blood circulation system *via* the gastrointestinal tract (GIT) is affected by variety of factors. However, absorption from the GIT into blood and urine is rare, and recent studies suggest that most particles are discharged by the GIT after ingestion [309,310]. According to [311], TiO$_2$ nanoparticles could, however, accumulate in tissues and organs such as the liver, spleen, kidneys, and lungs after absorption by the GIT. If long-term exposure is considered, even minor penetration from the GIT, or skin, into blood could have a significant impact [311]. Several *in vivo* studies indicated that TiO$_2$ NPs can penetrate the intestinal mucosa after oral exposure [312]. All these

studies indicate a potential risk of the accumulation TiO_2 NPs in specific organs after repeated long-term oral exposure.

In the context of incidental oral exposure, this study was focused on the comparison of four different types of TiO_2 particles (rutile, anatase, and their mixture) with respect to their behaviour in simulated body fluids including saliva, simulated gastric and intestinal fluids appropriately supplemented with enzymes pepsin and pancreatin, as well as and human blood plasma. Correspondingly, behaviour of TiO_2 in media used in *in vitro* experiments (cell culture medium – DMEM and phosphate buffered saline – PBS) was investigated. The key contribution of the study is the following of the time-dependent agglomeration of TiO_2 particles under comparable conditions and the comparison of their cytotoxicity. This study serves as a basis for a follow-up study dealing with the formulation of Pickering emulsions stabilized by TiO_2 particles in combination with cellulose nanoparticles.

Characterization of TiO2 particles

The most commonly used TiO_2 forms include rutile and anatase. Although they have the same chemical composition, their structures differ [313]. In this study, the information on the structure and morphology of TiO_2 particles was investigated by SEM. The Fig. 16 demonstrates differences in shape and morphology among the studied particles. While Rutile 1 appears as clusters of elongated needle-like particles, sample of Rutile 5 is composed of spherical particles with a clear crystal contour and a smooth surface (Fig. 16A, B). In addition, the figures also display differences in the size of primary crystallites being 21 nm and 150 nm for Rutile 1 and Rutile 5, respectively. In contrast, commercial Anatase and Anatase/Rutile samples revealed similar morphology. The particles are spherical with an irregular shape and a rough surface (Fig. 16C, D).
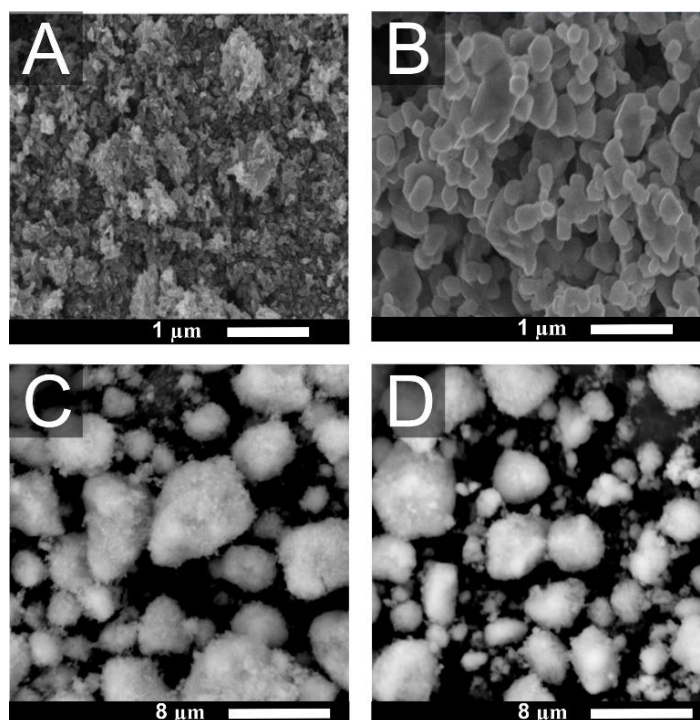
Figure 16 Scanning electron micrographs of (A) Rutile 1, (B) Rutile 5, (C) Anatase, and (D) Anatase/Rutile.

Particle size and polydispersity index (PDI) of TiO_2 particles were determined in Milli-Q water to acquire reference values. The results from DLS are shown in Tab. 6. The diameters of particles ranged from 142 ± 2 nm (Anatase/Rutile) to 553 ± 7 nm (Anatase) and PDI values ranged from 0.18 ± 0.01 (Rutile 5) to 0.35 ± 0.01 (Anatase/Rutile), which illustrated differences in studied particles.

Table 6 The diameter and PDI of TiO_2 dispersed in water together with zeta potentials determined in water with pH adjusted to 7 and isoelectric point (IEPs) of studied samples.

Sample	Z-average [nm]	PDI	Zeta potential [mV]	IEP
Rutile 1	215 ± 1	0.23 ± 0.01	-21.6 ± 1.0	4.4
Rutile 5	287 ± 8	0.18 ± 0.01	-35.5 ± 0.9	4.0
Anatase	553 ± 7	0.33 ± 0.02	-18.5 ± 0.4	5.5
Anatase/Rutile	142 ± 2	0.35 ± 0.01	-3.0 ± 0.6	6.0

Zeta potentials of TiO_2 were examined at different pH and the course of ζ *vs* pH dependencies revealed a similar trend (Fig. 17). However, the isoelectric point (IEP) varied within the pH range of ~4–6, and both Rutile samples displayed IEPs below pH 5. On the contrary, Anatase and Anatase/Rutile demonstrated IEPs of 5.5 and 6.0, respectively. Most commercial TiO_2 nano-powders exhibit IEPs ranging widely from pH 2–9 [314] and the differences can be attributed to several

factors, such as the insufficient surface purity of TiO_2 NPs [315] or the size and shape of NPs [316]. In addition, low IEP values may be due to the presence of phosphates or other anionic impurities in commercial TiO_2 [317].
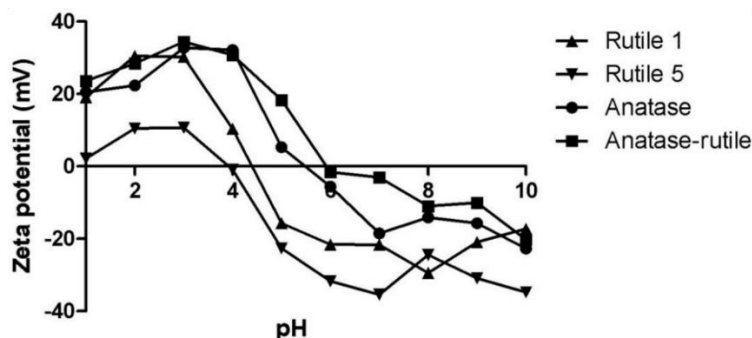
Figure 17 pH dependence of zeta potentials of the TiO_2 particles.

Behaviour of TiO_2 particles in cultivation media

Understanding of TiO_2 behaviour in a biological environment is essential for *in vitro* studies; therefore, TiO_2 particles were exposed to media commonly used for biological testing, namely PBS, serum-free DMEM, and DMEM supplemented with calf serum ($DMEM^{Serum}$) and their agglomeration was studied. As expected, immediately after the mixing the TiO_2 dispersion with PBS, the sizes of the particles increased, which was most significant for Rutile 1 (from 215 ± 1 nm to 3330 ± 190 nm), thus demonstrating rapid agglomeration in the samples (Fig. 18). Similar behaviour was observed with Anatase/Rutile and Anatase, but with different initial agglomeration levels. The decrease in size of Anatase particles after 80-min contact with PBS could be due to size-induced sedimentation of the formed agglomerates. On the other hand, Rutile 5 particles agglomerated least and their size grew gradually during the increasing time of contact. Also Teubl et al. observed a high level of TiO_2 NPs agglomeration in PBS due to the presence of ions [318]. In addition, Sager et al. stated that using PBS as a medium for preparing suspensions of nano-sized particles is unsuitable due to the formation of aggregates [319].

In serum free DMEM, TiO_2 samples agglomerated as well, which was due to the presence of electrolytes screening the particle surface charge; however, the behaviour of individual samples varied (Fig. 18). The Rutile 5 in DMEM, like in PBS, showed the smallest initial agglomeration and lower rate of agglomeration over time. The colloidal stability of TiO_2 NPs in cell culture medium was investigated by Allouni et al. who observed growing agglomeration of NPs with increasing particle concentrations. The authors explained this effect by the increasing frequency of direct particle-to-particle interactions caused by the ionic strength of the medium [315].

In contrast, the supplementation of DMEM with calf serum significantly reduced agglomeration in all studied samples. Rutile 1 and 5 increased their sizes the least and behaved almost the same during the entire measurement period, and

agglomeration of the Rutile/Anatase mixture and Anatase was significantly reduced in the presence of serum (Fig. 18). Thus, it is clear that the calf serum hindered interactions of TiO_2 particles through the formation of a protective protein layer, a corona, on the surface of the particles. This is consistent with the study of Ji et al. who investigated the effect of calf serum on the size and stability of TiO_2 NPs in different culture media and concluded that even 1% serum effectively stabilized dispersions and prevented NPs agglomerating due to the content of specific proteins forming a corona [320]. The protein corona consists of two layers, soft and hard. The former contains proteins with high affinity and direct interaction with the NP surface, while the latter contains low-affinity proteins. Biological fluids contains a variety of molecules that compete for adsorption on the NP surface, such as proteins, enzymes, lipids, etc.; however, proteins are primarily involved in corona formation [321].
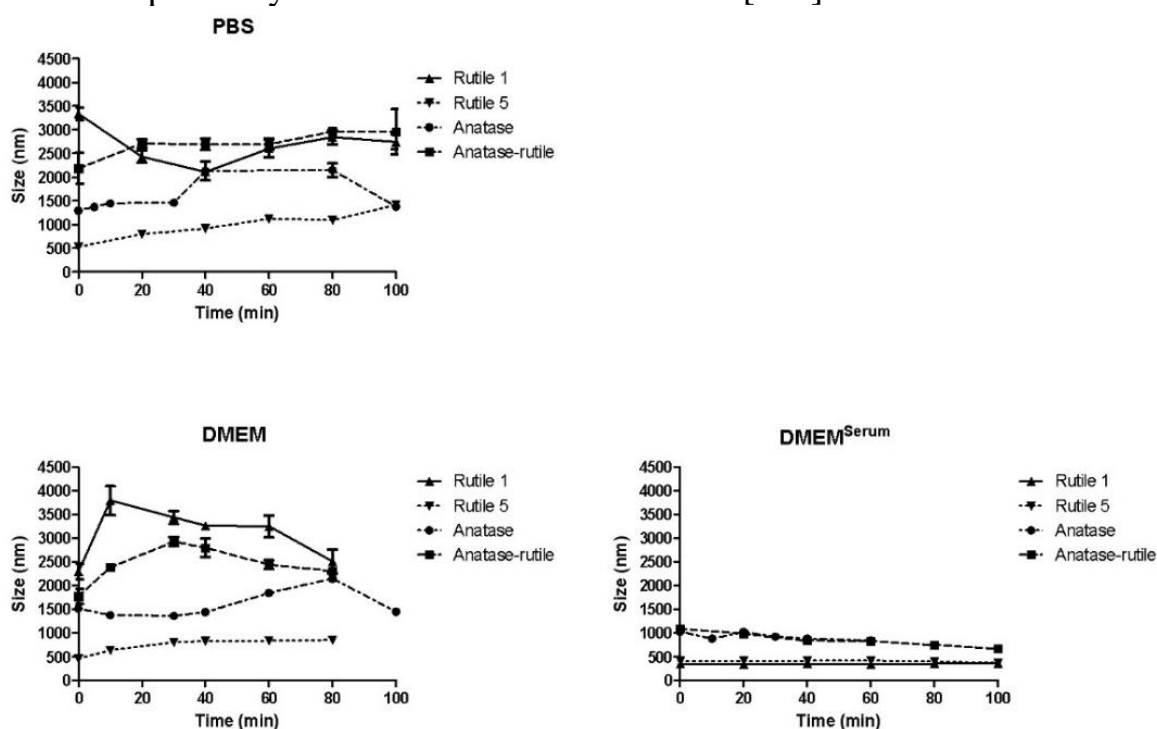
Figure 18 The time-dependent changes in size of TiO_2 particles in media used for in vitro experiments. The starting concentration of the TiO_2 particles in dispersion media was 0.5 mg mL^{-1}.

Behaviour of TiO_2 particles in simulated body fluids and human blood plasma

The simulated gastrointestinal fluids were used to describe fate of TiO_2 particles with respect to their agglomeration after ingestion. The study is further enriched with a description of the agglomeration behaviour of TiO_2 by observing the direct contact of particles with blood plasma, which can occur when epithelium or skin are injured.

In the case of oral exposure, saliva is the first part of the digestive system coming into contact with particles. In this environment (pH 6.8), TiO_2 particles behaved similarly as in PBS and DMEM, as it is seen in Fig. 19), and Rutile 5

exhibited the smallest agglomeration. After an initial increase from 287 ± 8 nm (water) to 392 ± 13 nm (saliva), the particle diameter remained almost unchanged. In contrast, the maximum size of agglomerates/particles in saliva was recorded for Rutile 1 immediately after mixing with saliva (2908 ± 854 nm). In Anatase/Rutile and Anatase, significant agglomeration was observed, though it was minor in comparison with Rutile 1. The observed agglomeration is consistent with findings of the study [318]. The authors reported a significant agglomeration of TiO_2 NPs in simulated saliva independent of the surface properties (hydrophilicity/hydrophobicity) of the NPs [318]. In addition, our results also show that agglomerates form rapidly and immediately after mixing with saliva. On the other hand, these agglomerates may disintegrate and equilibrium may be established between agglomerated and non-agglomerated particles.
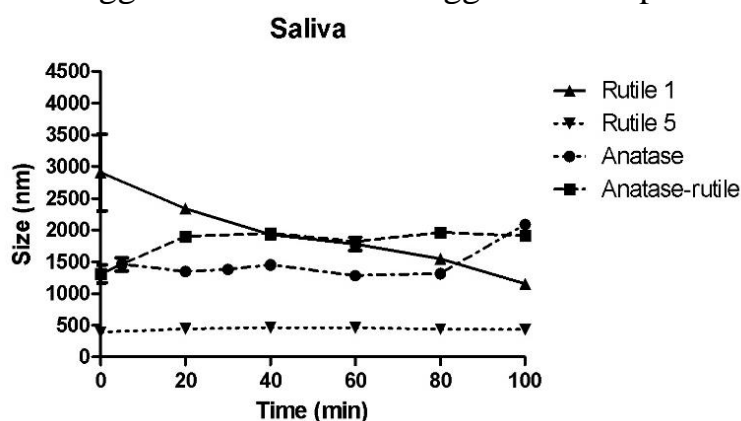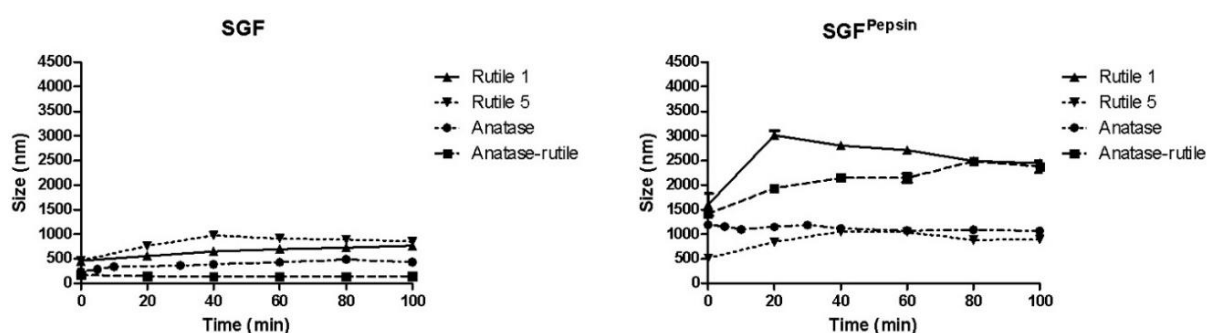

Figure 19 Time-dependent change in particle size of TiO_2 particles in simulated saliva. The starting concentration of the TiO_2 particles was 0.5 mg mL^{-1}.

The behaviour of the TiO_2 particles in simulated gastric fluid (SGF, pH 1.2) was fundamentally different from that observed in other simulated body fluids (Fig. 20). Anatase/Rutile particles were the most stable in the SGF environment, with their size increasing only slightly with measurement time to a maximum value of 169 ± 10 nm from a reference value of 142 ± 2 nm in Milli-Q water. On the other hand, particles of Rutile 1 and Rutile 5 increased their size approximately three times in size from the value determined in Milli-Q water. Anatase particles dispersed in SGF were smaller than those in water, reaching a size of 241 ± 9 nm after mixing and gradually increasing to a maximum value of 478 ± 17 nm during the measurement time. Thus, the low pH of SGF (1.2) appears to contribute to lower particle agglomeration when compared to other simulated body fluids, despite the fact that the charge and agglomeration of TiO_2 NPs are strongly affected by pH [322]. On the contrary, the particles of all samples strongly agglomerated in SGF^{Pepsin}, despite the low pH of this body fluid (Fig. 20). A particle size of 1605 ± 320 nm was measured in Rutile 1 immediately after mixing with SGF, which grew sharply to 3014 ± 124 nm, and then gradually decreased to a final size of 2444 ± 76 nm after 100 min. The particles of Rutile 5 showed an initial size of 512 ± 52 nm, which increased to around 1000 nm during

the measurement. Anatase/Rutile particles grew from an initial size of 1417 ± 313 nm to a maximum value of 2485 ± 95 nm, and the particles of Anatase grew immediately after mixing with the SGF^{Pepsin} to a value of 1189 ± 134 nm, which did not change further during the analysis. In this context, Sun et al. reported on the formation of a soft corona with the low affinity between TiO_2 NPs and pepsin and, correspondingly to our study, corona formation on the TiO_2 NPs surface did not reduce NP aggregation. The difference in charges of TiO_2 NPs and pepsin could explain this effect; specifically, at acidic pH, TiO_2 NPs in the presence of SGF without pepsin displayed a positive charge, while pepsin in SGF showed a minor negative charge. As a result of the weak electrostatic interactions between NP and pepsin, the protein corona formed may not sufficiently separate NPs, allowing their agglomeration [323].

Figure 20 Time-dependent changes in size of TiO₂ particles in simulated gastric fluids. The starting concentration of the TiO₂ particles in dispersion media was 0.5 mg mL⁻¹.

The agglomeration of TiO_2 particles was also recorded in simulated intestinal fluid (SIF, pH 6.8) (Fig. 21). Particles of Rutile 1 changed their size the most, correspondingly to the situation in simulated saliva. At the start of analysis, a size of 2226 ± 79 nm was detected, which remained nearly constant throughout the measurement. In contrast, Rutile 5 showed significantly less agglomeration, with an initial increase in particle size to 520 ± 58 nm followed by further growth to a maximum value of 797 ± 79 nm, and then a decrease to 650 ± 27 nm at the end of the measurement, indicating agglomerate sedimentation. A progressive agglomeration of particles was observed in Anatase/Rutile, reaching a maximum size of 1998 ± 40 nm. The particle sizes of Anatase fluctuated during the analysis, with values below 1000 nm. Similarly to presence of pepsin in SGF, pancreatin in SIF triggered a significant agglomeration of TiO_2 particles (Fig. 21). The greatest changes were recorded for Anatase/Rutile, where the particle/agglomerate size increased dramatically up to a maximum value of 4286 ± 41 nm measured after 20 min, and then decreased slightly, indicating the sedimentation of agglomerated particles. Significant agglomeration also occurred in both Rutile samples. Authors of publication [324] reported a steady increase in the concentration of TiO_2 (Anatase) nanoparticles in simulated intestinal fluid, as well as a notable increase in agglomerate size over time.
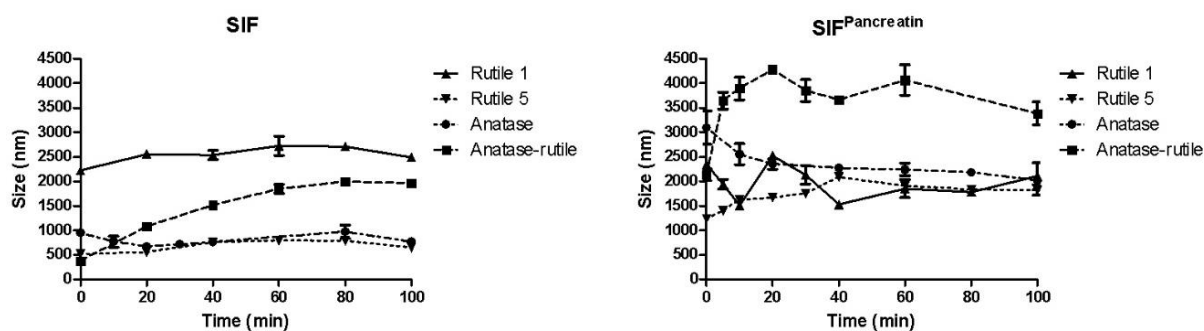
Figure 21 Time-dependent change in particle size of TiO$_2$ particles in simulated intestinal fluid. The starting concentration of the TiO$_2$ particles in dispersion media was 0.5 mg mL^{-1}.

In contrast to the gastrointestinal fluids, TiO$_2$ agglomeration was significantly reduced in the blood plasma (Fig. 22). The smallest change in particle size after mixing with plasma was observed with Rutile 1, with only a slight increase in size from 215 ± 1 nm (MilliQ water) to 318 ± 11 nm. Conversely, the particle size increased most for Rutile 5, from the reference value of 287 ± 8 nm to 607 ± 22 nm. Particles of Anatase/Rutile and Anatase in plasma were even smaller than those in water. Blood plasma reduced agglomeration of TiO$_2$ particles compared to other fluids because of the rapid interactions of TiO$_2$ particles with plasma proteins and the formation of the protein corona mentioned above. Deng et al. investigated the binding of human plasma proteins to commercially available TiO$_2$ NPs and observed equilibrium during the first five minutes of incubation [325], which could account for the constant particle size observed during the measurement period in our study. Additionally, according to a study by [326], fibrinogen showed the strongest affinity for all tested NPs, including TiO$_2$, which could inhibit the adsorption of other proteins. The authors further observed that the crystal structure of TiO$_2$ NPs may affect protein adsorption, and they stated that, in contrast to expectations, particles with a higher specific surface area do not bind more protein than larger ones [326]. According to [325], the degree of agglomeration has a significant influence on the binding of plasma proteins. As a result, the biodistribution of particles may be, to a certain extent, dictated by the degree of agglomeration of nanoparticles, with this affecting cell surface protein binding [325].
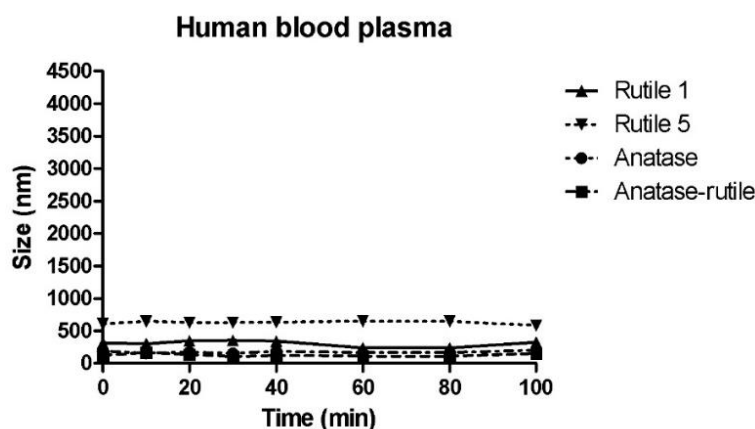
Figure 22 Time-dependent change in particle size of TiO$_2$ particles in human blood plasma. The starting concentration of the TiO$_2$ particles in dispersion media was 0.5 mg mL^{-1}.

Biological properties

Cytotoxicity is the most important test for determining primary indication of particles behaviour in contact with living systems. The experiment was designed to determine the toxic dose of TiO$_2$ particles for NIH/3T3 cells. The results of the experiment presented in Fig. 23 show that the cytotoxicity levels for each of the TiO$_2$ sample were different. Rutile 1 was cytotoxic at 4000 μg mL^{-1} dispersion concentration of, whereas Rutile 5 was cytotoxic at a dispersion concentration of 1500 μg mL^{-1} and, thus more cytotoxic than Rutile 1. Anatase exhibited cytotoxicity at concentration of 1500 μg mL^{-1}, similarly to Rutile 5. These differences could be attributed to the different physicochemical properties of the tested samples, such as particle size or surface chemistry. Although many cytotoxicity studies of commercial TiO$_2$ NPs on different cell types were performed, results are inconsistent. This can be caused by a variety of factors, such as the type of TiO$_2$ particles, the type of cells used, the concentration range tested, etc. For testing, some studies used mouse fibroblasts. Pittol et al., for example, observed no significant reduction in viability after the exposing mouse fibroblast cells (L929) to TiO$_2$ particles at concentrations as high as of 10,000 μg g^{-1}. The authors attributed the non-toxic effect of the particles to their agglomeration tendency, composition, and crystalline form, as well as their interaction in culture media [327]. Similarly, Rosłon et al. observed only a minor effect of TiO$_2$ NPs on the viability of mouse fibroblasts (L929), however, at significantly lower concentrations (10–200 μg mL^{-1}) [328].
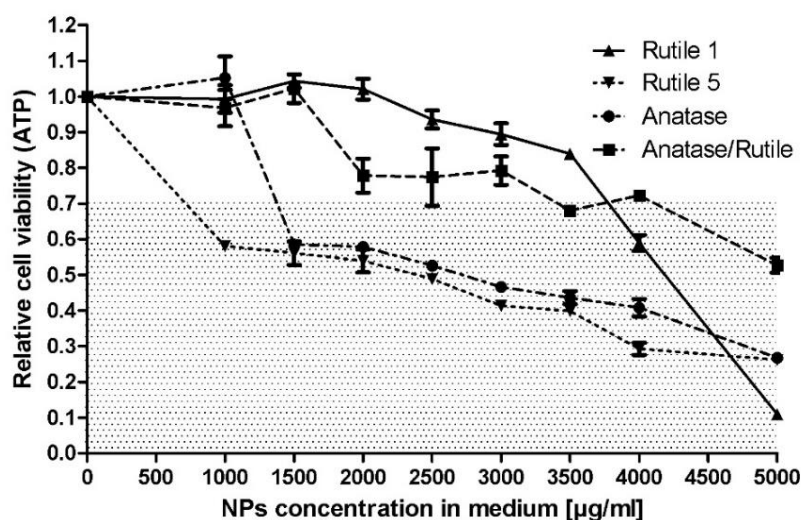
Figure 23 Cytotoxicity of TiO₂ particles after 24 h of exposure to NIH/3T3 mouse embryonic fibroblast cells. The patterned area shows concentrations with cytotoxic effects, as defined by EN ISO 10993-5, where a viability > 0.7 corresponds to an absence of cytotoxicity.

Summary of the study

The growing application of materials containing TiO_2 particles necessitates a thorough understanding of their impact on human health. The aim of this experiment was to investigate the behaviour of different forms of TiO_2 particles (rutile, anatase, and their commercial mixture) in media used for biocompatibility testing, simulated body fluids, and human blood plasma. Simulated body fluids of different compositions, ionic strengths, and pH were used, and the impact of the absence or presence of chosen enzymes was investigated as well. Under comparable conditions, the physicochemical properties and time-dependent agglomeration of TiO_2 particles in these media were determined. The time-dependent agglomeration of TiO_2 was related to the type of TiO_2, and more specifically to the type and composition of the environment investigated. The results showed that, due to the presence of electrolytes that screen particle surface charge, all tested forms of TiO_2 particles agglomerated immediately after contact with PBS and serum-free DMEM. The presence of calf serum in DMEM, on the other hand, significantly reduced agglomeration due to the formation of a protective protein corona around the particle surface. To mimic the digestive process, TiO_2 particles were exposed to simulated saliva, gastric and intestinal fluid, suitably supplemented with the digestive enzymes, pepsin or pancreatin. The TiO_2 samples behaved similarly as in PBS and DMEM after being mixed particles with saliva. Contrary to the protective effect of calf serum in DMEM, pepsin and pancreatin triggered the significant agglomeration of TiO_2 particles in SGF and SIF. Here the formation of agglomerates was notably higher in comparison with the situation when the enzymes were absent. TiO_2 agglomeration, on the other hand, was significantly reduced in human blood

plasma due to the protective protein corona hindering interactions between TiO_2 particles. In summary, the crystalline form of TiO_2 particles, the ionic strength of the surrounding media, and the presence of proteins were the key factors that influenced their behaviour in different environments. Cytotoxicity data determined with NIH/3T3 cells demonstrated that the cytotoxicity depends on the type of tested TiO_2 particles. The lowest cytotoxic effects were recorded for Rutile 1 and the Anatase/Rutile mixture, which were cytotoxic at TiO_2 concentrations of 4000 and 3500 µg mL^{-1}, respectively. Anatase and Rutile 5, which were cytotoxic at 1500 µg mL^{-1}, exhibited higher cytotoxicity. This understanding of TiO_2 behaviour in all the abovementioned environments is critical when considering TiO_2 safety, particularly in light of the significant impact of protein presence and size-related cytotoxicity.

Results of the study were summarized and published in *"Behaviour of Titanium Dioxide Particles in Artificial Body Fluids and Human Blood Plasma"* by *Korábková E., et al. International Journal of Molecular Sciences 2021, 22(19), 10614; https://doi.org/10.3390/ijms221910614.*

8.4.2 Study on cCNC/TiO$_2$-stabilized emulsions

Over the last century, there has been growing awareness of the risks associated with excessive exposure to UV radiation. This increases the use of sunscreens (also known as sunprotectants), which provide protection against sunburn, skin aging, and melanoma due to their ability to absorb, reflect, and scatter UV radiation [329,330].

Currently, commercial products are manufactured in the form of emulsions, gels, aerosols and sticks using conventional organic and inorganic UV filters or hybrid and botanical ingredients. However, the use of sunscreens has faced many challenges, such as the occurrence of photoallergic dermatitis or environmental pollution [330]. As a result, there is an increasing effort to develop sunscreens with a favorable composition in terms of effectiveness, safety, and aesthetic appeal [329]. Compared to organic UV filters, inorganic filters such as TiO_2 a ZnO have significantly lower risk for developing photoallergic and allergic reaction. For these reasons, TiO_2 and ZnO have been widely recommended as safe and effective UV filters in sunscreens [331].

The current trend in this field is to reduce the number of ingredients in sunscreens, which can be accomplished by using compounds that can perform more than one function. Pickering emulsions may be of particular interest in this regard. Because these emulsions are stabilized with solid particles instead of traditional surfactants; particles can simultaneously function as both a stabilizer and a functional component. The surfactant-free nature of Pickering emulsions, therefore, reduces irritation potential of the product, and simultaneously increases its environmental friendliness. However, only a few studies have focused on the development sunscreen emulsions free of surfactants [99]. Moreover, due to hydrophilic nature of TiO_2 particles, it is difficult to prepare commercially usable

emulsions for cosmetic applications stabilized only by unmodified TiO_2 [109]. Since anatase is more photoactive than the rutile, [332], rutile or a mixture of rutile and anatase is commonly used in cosmetic sunscreens [333]. In connection with the use of TiO_2 for emulsion stabilization, scientific studies freequently use hydrophobically modified TiO_2 nanoparticles or particles in combination with the addition of another emulsion-forming substance.

Based on findings of the previous study (8.4.1), the goal of the second study was to develop a surfactant-free sunscreen emulsion stabilized with nanocrystals of pH-responsive carboxylated cellulose (cCNC) in combination with TiO_2 particles (a mixture of Rutile/Anatase), which could provide an effective and safe alternative to conventional sunscreens. The particle size, zeta potential, and phase studies were used to investigate the effect of different emulsion composition, preparation method, and pH on the stability of these O/W Pickering emulsions.

cCNC/TiO₂ dispersions

In order to investigate the behaviour of the combination of cCNC and TiO_2 particles at different pH values, a preformulation study with cCNC and TiO_2 dispersions was first performed according to the procedure described in 8.2.2. The cCNC obtained by oxidation with a strong oxidizing agent bears carboxyl groups on the surface, which provide to particles a certain pH responsiveness. Specifically, a high dispersion stability was observed at pH 6–10, however, the stability with decreasing pH gradually decreased to a value of zeta potential close to zero at pH 2 [83].

The principle of the combination of cCNC and TiO_2 for the successful stabilization of emulsions using layer-by-layer (LbL) method was the use of the opposite charge of cCNC and TiO_2 at a certain pH value. Therefore, based on the pH dependence of the zeta potential of cCNC and TiO_2 particles and the assumption of topical applications of the resulting product, the pH values of 3; 4; 4,5 and 5 were chosen for the preformulation study. The prepared dispersions were visually observed after 24 hours of equilibration and the results demonstrated formation of complex between cCNC and TiO_2 particles in dispersions prepared at pH 3 (Fig. 24A). On the contrary, in all dispersions that were not adjusted to pH 3, sedimentation of TiO_2 particles occurred without major differences between cCNC:TiO_2 ratios (Fig. 24B-D). Based on the obtained results, the next part of the study was focused on the preparation of Pickering emulsions at pH 3 with LbL method.
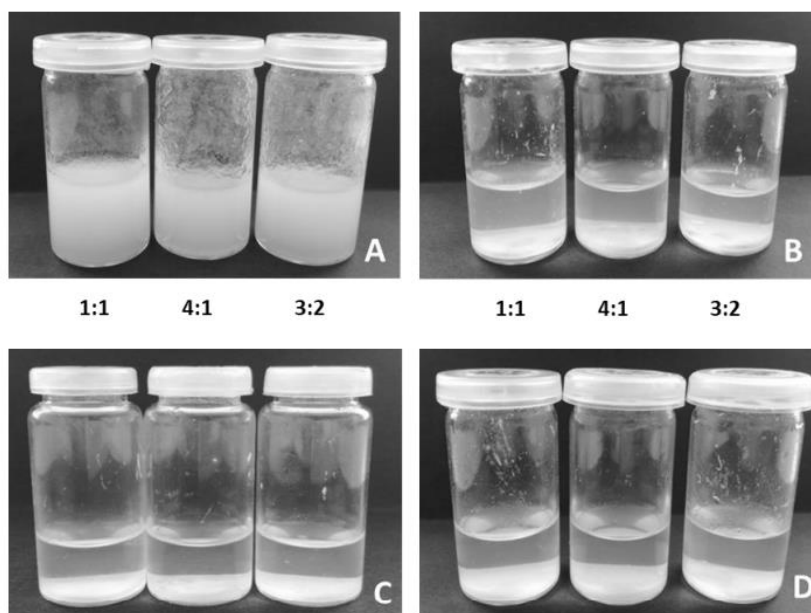
Figure 24 Dispersion of TiO₂ and cCNC complexes 24 hours after preparation, A = pH 3, B = pH 4, C = pH 4.5, D = pH 5.

Emulsions prepared at pH 3

- *Effect of O/W and cCNC:TiO₂ ratio*

In the next part of the study, the LbL method was used to prepare emulsions with different O/W and cCNC:TiO$_2$ ratios at pH 3 (Tab. 7). The influence of the O/W and the cCNC:TiO$_2$ ratios on the properties of emulsions was investigated and composition resulting in the most stable emulsions was identified.

Table 7 Formulation of emulsions prepared by LbL method at pH = 3.

Total stabilizer content [%]	O/W ratio	cCNC:TiO₂
0.3	10/90	1:1; 3:2; 4:1
	20/80	1:1; 3:2; 4:1
	30/70	1:1; 3:2; 4:1

Droplet size of emulsions revealed differences between individual samples (Fig. 25). The main factor influencing the size of the emulsion droplets was the ratio of oil and water phase. On the day of preparation, the sizes of the droplets in the emulsions with an O/W ratio of 10/90 and 20/80 were comparable for all cCNC:TiO$_2$ ratios. The droplet size was always the largest for the O/W ratio 30/70 regardless of the cCNC:TiO$_2$ ratio. The droplet size increased with time for most emulsions, with the biggest increase occurring one week after emulsion preparation. On the other hand, the droplet sizes did not grow further after two weeks for any of the emulsion samples. It is known that with insufficient concentration of stabilizing particles, Pickering emulsions undergo limited

65

coalescence and the droplets merge until their surface is sufficiently covered by stabilizing particles. Above a certain threshold, however, the droplet size remains nearly constant and the coalescence process is stopped [72,334]. Furthermore, the size measurement of the emulsion droplets revealed that after two weeks of preparation, the emulsion droplet size at the same O/W ratio reached a maximum at cCNC:TiO_2 ratio of 1:1 and minimum at 4:1 ratio. This suggests that with increasing amounts of cCNC in the emulsion, the size of the emulsion droplets decreases, confirming that cCNCs have better stabilization capabilities than TiO_2 particles.
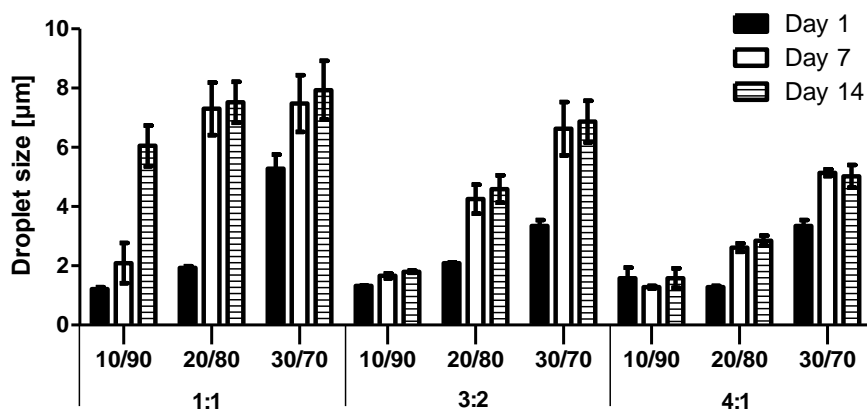
Figure 25 Size of emulsion droplets D[4,3]; dependence on the O/W ratio (10/90, 20/80, 30/70) and the cCNC:TiO_2 ratio (1:1, 3:2, 4:1).

Zeta potential measurements revealed the highest absolute zeta potential recorded on the day of preparation for emulsions with an O/W ratio of 30/70 for all cCNC:TiO_2 ratios, (Fig. 26).
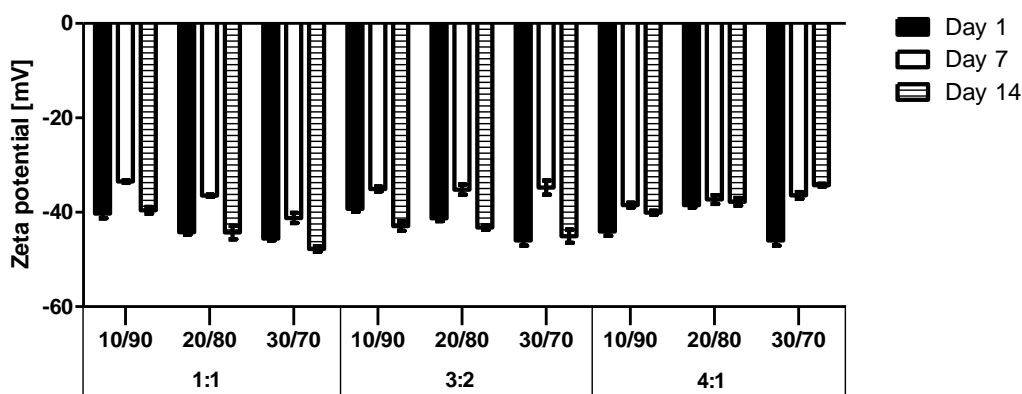
Figure 26 Zeta potential of emulsions; dependence on the O/W ratio (10/90, 20/80, 30/70) and cCNC:TiO_2 ratio (1:1, 3:2, 4:1).

As regards phase studies, the most important indicator of the emulsion stability is their encapsulation efficiency (EE). The phase behaviour of emulsions showed that the greatest release of oil occurred for emulsions with all O/W ratios at a cCNC:TiO_2 ratio of 1:1 (EE values: 72-94 %) (Fig. 27A). The phase studies also showed that creaming occurred for all emulsions (Fig. 27A, B), which was due to

66

the density of used oil ($\rho = 0.947$ g/cm^3). However, creaming did not always result in emulsion breakdown.

Overall, the emulsion with the stabilizer content of 0.3 %, cCNC:TiO$_2$ ratio of 4:1 and O/W 30/70 demonstrated good stability without any break-down process observed.

| 10/90 | 20/80 | 30/70 | | 10/90 | 20/80 | 30/70 |

1:1 **4:1**
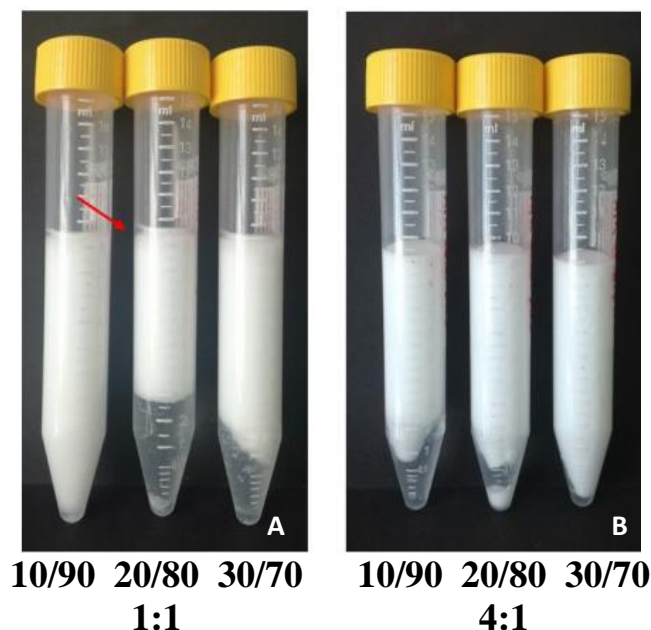
Figure 27 Emulsions after two weeks of preparation. Red arrow indicates a visible oil layer.

The experiments carried out in this part of the study confirmed the ability of cCNC and TiO$_2$ particles to stabilize emulsions at a pH of 3. Considering the results discussed above, emulsions prepared with cCNC:TiO$_2$ ratios of 3:2 and 4:1 showed both good ability to encapsulate oil and favorable stability over time.

Emulsions with the cCNC:TiO$_2$ ratio of 1:1 and emulsions with the O/W ratio of 10/90 were excluded from further testing. The reason was their low encapsulation potential and stability.

- *Effect of the total content of stabilizers*

Based on the observation of a limited coalescence for emulsions prepared with 0.3 % stabilizers, their two higher total amounts, namely 0.5 and 0.7 %, were chosen for further experiments. The O/W and cCNC:TiO$_2$ ratios were same as in previous study (O/W 20/80; 30/70 and cCNC:TiO$_2$ 3:2; 4:1). The goal was to investigate the effect of the total content of stabilizers at the selected O/W and cCNC:TiO$_2$ ratios on the properties and behaviour of emulsions prepared by the LbL method.

When increasing the total amount of stabilizer (0.5 and 0.7 %), the limited coalescence was restricted and the concentration of particles was sufficient to stabilize emulsions. Correlation between droplet size and increasing content of

particles was not, however, unambiguous (Fig. 28) and depended on several variables. Emulsions with an O/W ratio of 20/80 prepared with 0.5 and 0.7 % stabilizer and cCNC:TiO$_2$ 4:1 proved that the higher cCNC content in mixture led to smaller droplets compared to emulsions with a cCNC:TiO$_2$ ratio of 3:2. However, at O/W 30/70 this trend was not preeserved.
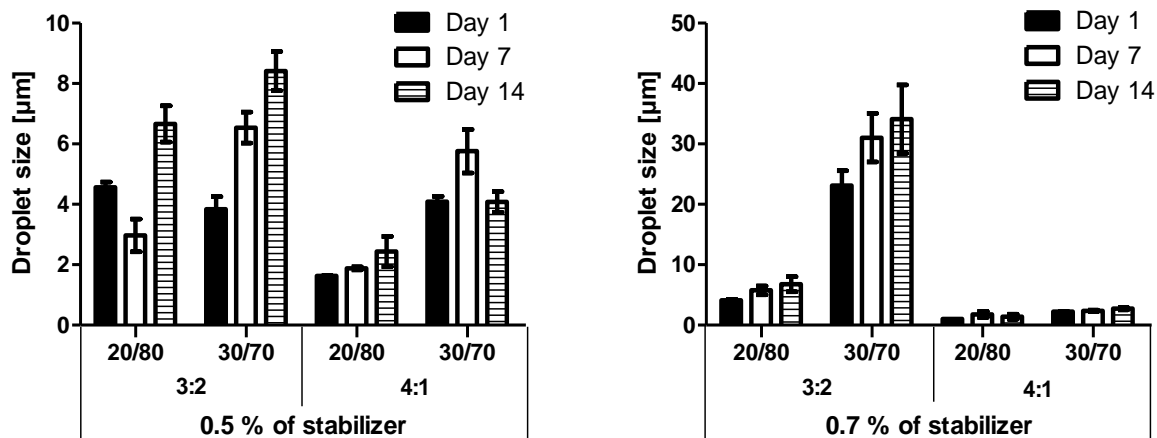
Figure 28 Size of emulsion droplets D[4,3]; dependence on the total stabilizer content (0.5; 0.7), cCNC:TiO$_2$ ratio (3:2, 4:1), and O/W ratio (20/80, 30/70).

Zeta potential measurements of emulsions containing 0.5 and 0.7 % of stabilizer are given in Fig. 29. On the day of preparation, emulsions with an O/W ratio 30/70 showed a more negative zeta potential at both cCNC:TiO$_2$ ratios than 20/80 emulsions. However, this effect was not observed with emulsions containing 0.7 % of stabilizer.
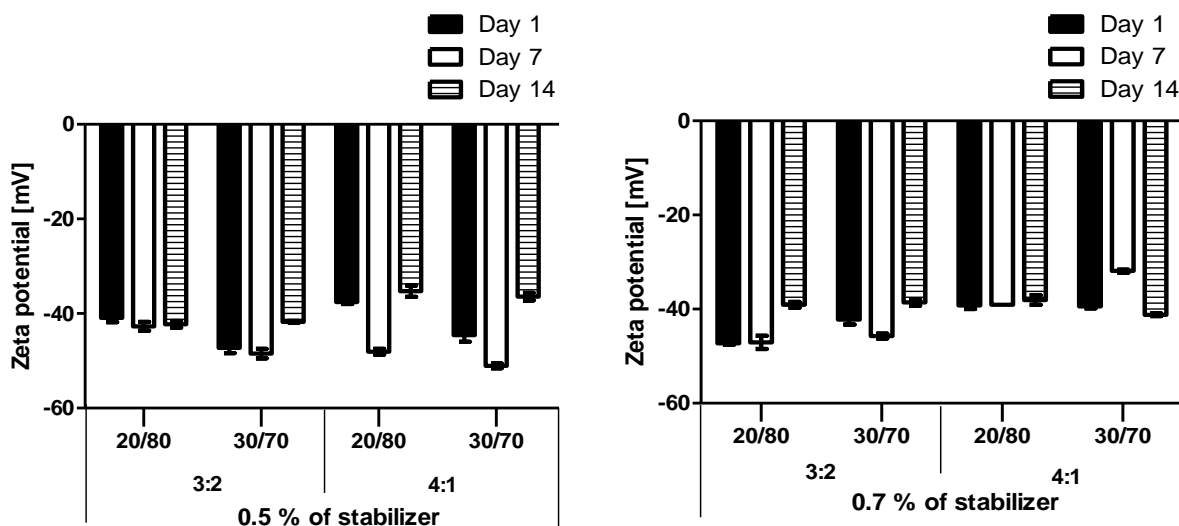
Figure 29 Zeta potential of emulsions; dependence on the total stabilizer content (0.5; 0.7), cCNC:TiO$_2$ ratio (3:2, 4:1), and O/W ratio (20/80, 30/70).

Although it would seem that the higher the particle concentration, the better is the stability of the emulsion, the phase behaviour revealed the opposite. The

greatest oil release was observed in emulsions with the highest stabilizer content of 0.7 % regardless of the cCNC:TiO$_2$ ratio (Fig. 30A), whereas the oil was released less or not at all at stabilizer contents of 0.5 % (Fig. 30B). Within two weeks, a creaming process was observed for all emulsions except the emulsion with a 0.5 % stabilizer, a cCNC:TiO$_2$ ratio of 4:1 and an O/W ratio of 20/80, which also showed no oil release and the EI of 100 %. As a result, this formulation has the potential to be used in practice.

	0.7 %					0.5 %		
20/80	30/70	20/80	30/70		20/80	30/70	20/80	30/70
3:2	3:2	4:1	4:1		3:2	3:2	4:1	4:1
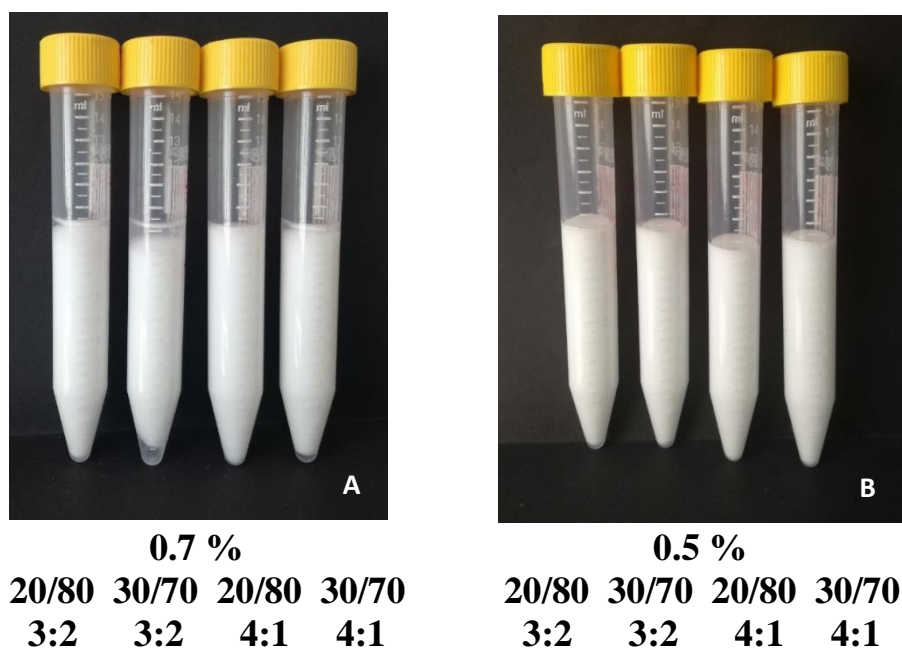
Figure 30 Emulsions with the total amount of cCNC/TiO$_2$ 0.5 and 0.7 % after a day of preparation.

The results of this part of the study revealed that increasing the total amount of stabilizer to 0.7 % did not contribute to greater emulsion stability, but on the contrary increased oil release. However, stable emulsions were prepared with a 0.5 % of stabilizer.

- *The influence of the preparation method*

The next step in the research was to determine whether another emulsification method could be used for the preparation of emulsions and how the method affected the properties of Pickering emulsions. The conventional emulsification (CE) method described in 8.2.2 was chosen in this study and compared with LbL method. Based on the previous results, emulsions prepared by LbL and CE with composition listed in the Tab. 8 were selected for this purpose.

Table 8 Formulation of emulsions prepared by the conventional emulsification and the layer-by-layer method.

Total stabilizer content [%]	O/W ratio	cCNC:TiO$_2$ ratio
0.5	20/80 30/70	3:2; 4:1

Measurement of the emulsion droplet size showed that, when compared to the LbL method, the CE method produced larger droplets regardless of O/W ratio and cCNC:TiO$_2$ (Fig. 31), which was likely due to the shorter sonication time used (8.2.2). Interestingly, regardless of the preparation method used, the ratio of cCNC:TiO$_2$ of 4:1 resulted in smaller emulsion droplets compared to samples prepared with the 3:2 ratio at both studied O/W ratios of 20/80 and 30/70.
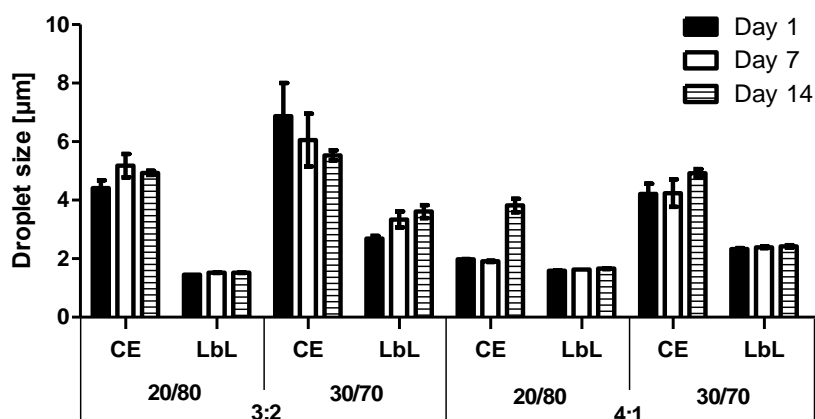
Figure 31 Size of emulsion droplets D[4,3]; dependence on the preparation method (CE, LbL), cCNC:TiO$_2$ ratio (3:2, 4:1), and O/W ratio (20/80, 30/70).

The study of the effect of emulsification method on the zeta potential did not find any significant differences between the CE and LbL methods (Fig. 32). However, it is worth noting that the zeta potential of the emulsions was close to −30 mV on the day of preparation, at pH 3. As previously stated, the zeta potential of TiO$_2$ particles at pH 3 was higher than +30 mV, while the potential of the cCNC dispersion at pH 3 was around −20 mV. This implies that the overall charge of the emulsion droplets is primarily determined by the cCNC particles.
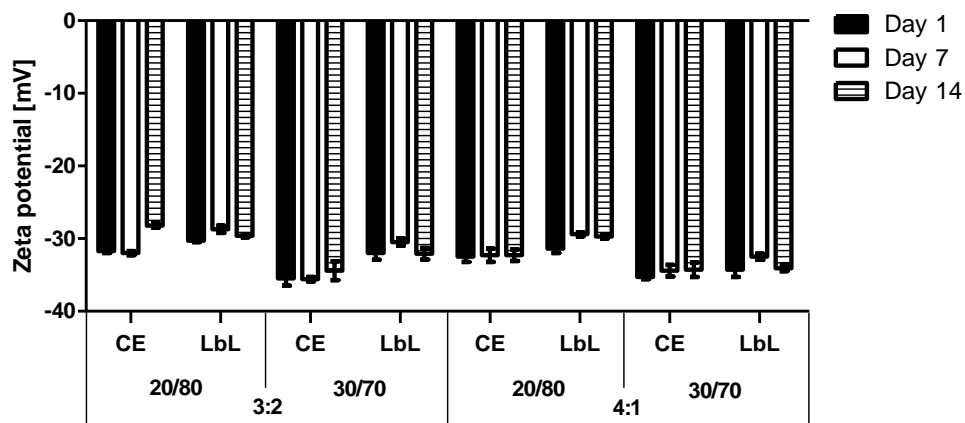
Figure 32 Influence of the preparation method (CE, LbL) on zeta potential of emulsions, cCNC:TiO₂ ratio (3:2, 4:1) and O/W ratio (20/80, 30/70).

The conventional emulsification was shown to be effective for the preparation of emulsions stabilized by combinations of cCNC and TiO_2 particles, with the encapsulation efficiency of all emulsions prepared by this method being 100 % for over a two-week period. Furthermore, greater creaming was observed in CE samples than in the case of emulsions prepared by the LbL method, depending on the formulation of individual emulsions.

The AFM method was used to investigate the morphology of emulsion droplets prepared by CE and LbL. For this imaging, stable emulsions with a total stabilizer content of 0.5 %, cCNC:TiO_2 ratio of 4:1 and O/W ratio of 20/80 were selected. An image of the emulsion prepared by the CE method (Fig. 33A) showed the presence of a steric barrier formed by a complex of cCNC/TiO_2 particles, whereas the emulsion droplet prepared by the LbL method is covered by a much smaller amount of cCNC particles, despite the fact that the total cCNC concentration was the same in both cases (Fig. 33B).

A)   B)
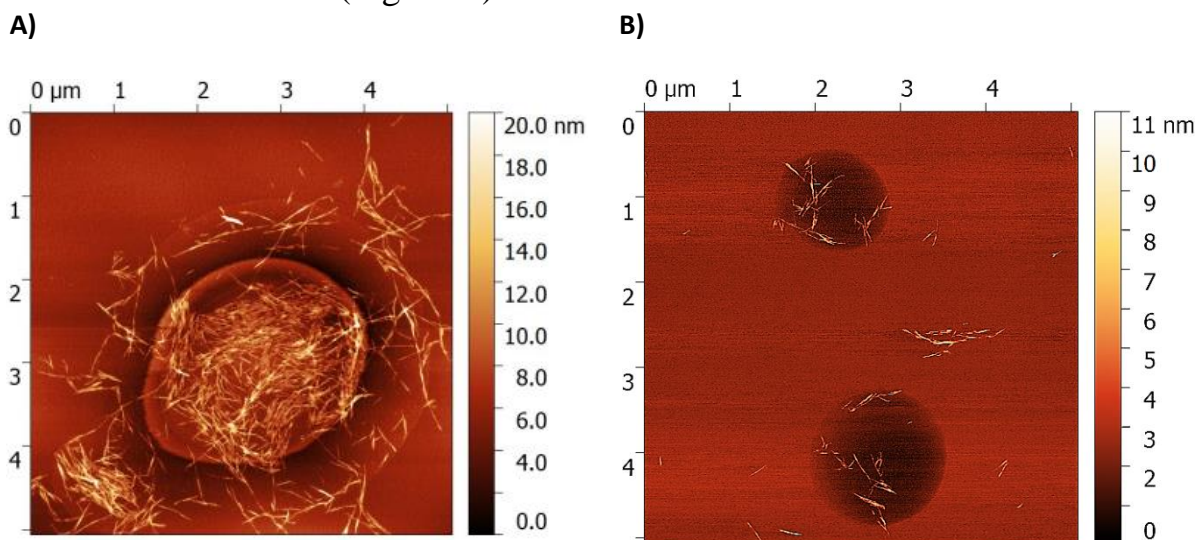
Figure 33 AFM image of emulsion droplet with cCNC:TiO₂ ratio of 4:1 and O/W ratio of 20/80 prepared by the CE method (A); and by the LbL method (B).

71

The feasibility of preparing emulsions stabilized by cCNC and TiO_2 particles using the conventional emulsification method was successfully demonstrated in this part of study. Despite the larger size of the emulsion droplets, the CE method produced emulsions with good stability. This suggests that emulsion stability and droplet size may not be directly correlated.

Emulsions prepared at pH 5

The aim of the study on cCNC/TiO_2-stabilized emulsions was to prepare Pickering emulsions suitable for topical use. Therefore, the emulsions prepared at pH 3 were not suitable for this purpose. The reason is the pH value of the skin, which on average reaches a value of 4.7 [335]. As a result, the research further focused on finding optimal conditions for the preparing Pickering emulsions stabilized by cCNC and TiO_2 particles at pH 5. As already mentioned, complexes between cCNC and TiO_2 particles did not form at pH between 4-5 (Fig. 24). However, according to studies published in [83,89], the addition of inorganic salts increases the stability of Pickering emulsions. Therefore, the next step was to look into the effect of added NaCl ($CaCl_2$) on the formation of Pickering emulsions stabilized by a combination of cCNC and TiO_2 at pH 5. The emulsions were supplemented either with NaCl (27 mmol L^{-1}) or $CaCl_2$ (3 mmol L^{-1}) as given in 8.2.2. The emulsions with stabilizer content of 0.5 %, the cCNC:TiO_2 ratio of 4:1 and the O/W ratios of 20/80 and 30/70 were prepared by both CE and LbL methods.

Although a complex of cCNC and TiO_2 in the presence of each of the salts in dispersions was formed, it was not possible to prepare the emulsion with NaCl using CE. However, the addition of $CaCl_2$ allowed preparing the emulsion at pH 5 with this method. Difference in NaCl and $CaCl_2$ efficacy can be caused either by different valence (divalent *vs.* monovalent cations) or by greater affinity of cCNC carboxyl groups to calcium cations [83].

As for the LbL method, in case of electrolyte addition after the second sonication, sedimentation of TiO_2 particles occurred, regardless of the type of salt used. Therefore, adding electrolyte at this stage of emulsion preparation was unsatisfactory. Addition of electrolyte both before and after the first sonication, however, led to the formation of relatively stable LbL emulsions, even in the presence of NaCl. The addition of salts also acted as a modifier of viscosity, which could contribute to increasing the stability of prepared emulsions.

The presence of electrolytes, whether NaCl or $CaCl_2$, increased droplet sizes in emulsions regardless of the preparation method. Moreover, irrespective of the preparation method or electrolyte used, an O/W ratio of 30/70 always produced larger droplets than O/W 20/80 (Fig. 34). Emulsions prepared by the LbL method with $CaCl_2$ added before the first sonication showed larger droplets than emulsions prepared with $CaCl_2$ added after the first sonication. This effect was

not, however, observed in emulsions containing NaCl. Based on the data acquiered, it is not possible to unequivocally say if the time of adding salt to the emulsion affected the emulsion droplet sizes. The preparation method, on the other hand, had a considerable impact on the size of the emulsion droplets. When employing the CE approach, bigger emulsions droplets were formed, likely due to the shorter sonication time or different mechanism of stabilization (Fig. 34).
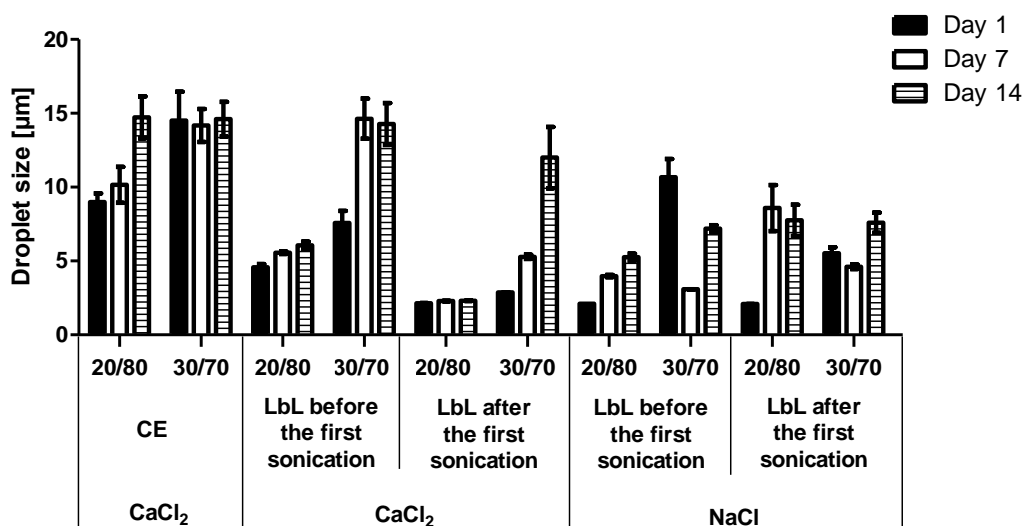

Figure 34 Size of emulsion droplets D[4,3]; dependence of preparation method (CE, LbL), O/W ratio (20/80 and 30/70) and the type of electrolyte used. Ratio cCNC:TiO₂ was 4:1.

Zeta potential of all emulsions prepared at pH 5 was significantly lower (Fig. 35) than that of emulsions prepared at pH 3 (Fig. 32), which is related to the lower potential values of the cCNC and TiO_2 particles at pH 5. The zeta potential was also influenced by the content of the oil in the emulsions. When the same preparation method and electrolyte were employed, a higher amount of oil (O/W 30/70) resulted in a higher zeta potential at all emulsions compared to samples with O/W 20/80.
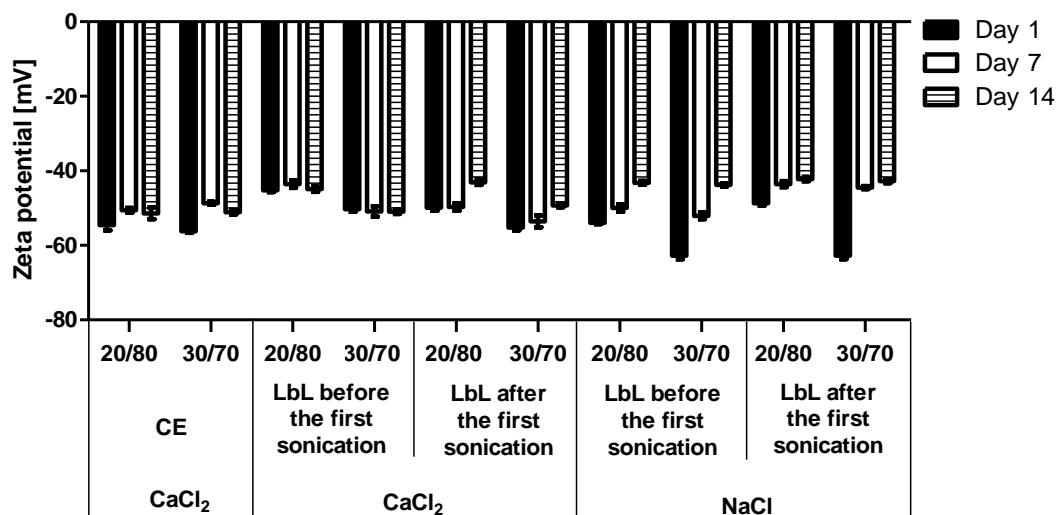
Figure 35 Zeta potential of the emulsions prepared with cCNC:TiO₂ ratio of 4:1 and 0,5 % stabilizer. Dependence on the preparation method (CE, LbL), O/W ratio of 20/80 and 30/70, and type of electrolyte used.

In a phase study, it was shown that the addition of electrolyte to the emulsions significantly increased their stability at pH 5. Although for the monitored period of two weeks there was no breakdown of the emulsions into the original phases, oil release was observed for all prepared samples. However, the encapsulation efficiency was of about 95 % in most emulsions (Fig. 36). The time of electrolyte addition in the the LbL method is not essential for emulsion stability if it takes place before the second sonication, because there was no significant difference between the encapsulation efficiencies of the studied samples (Fig. 36).
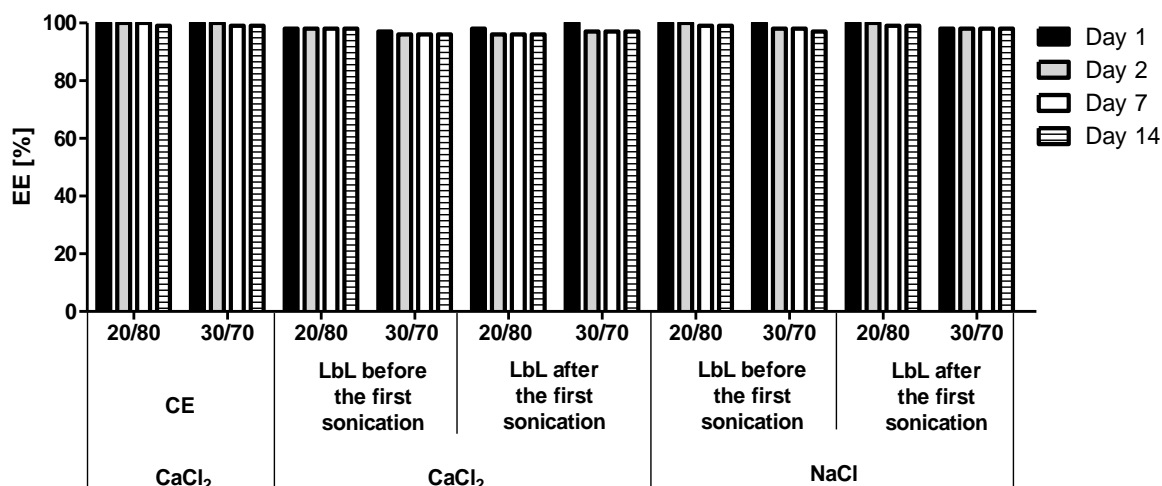
Figure 36 Comparison of encapsulation efficiency (EE) values for emulsions prepared with cCNC:TiO₂ ratio of 4:1. Dependence on the preparation method (CE, LbL), O/W ratio of 20/80 and 30/70, and type of electrolyte used.

When observing the creaming process, the differences between individual emulsions were greater (Fig. 37). Creaming was more apparent in emulsions containing $CaCl_2$ than in emulsions containing NaCl. Moreover, adding NaCl before the first sonication inhibited creaming in the emulsion for two weeks. In the emulsions prepared with CE method, the creaming started already on the day of preparation, while in the same emulsion prepared by the LbL method creaming occurred a day after their preparing.
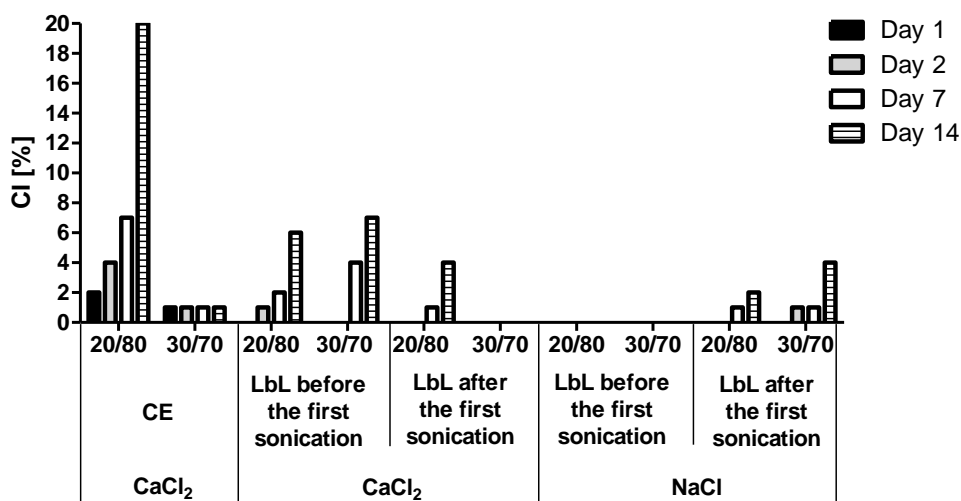
Figure 37 Comparison of creaming index (CI) of emulsions prepared with cCNC:TiO₂ ratio of 4:1; dependenceof preparation method (CE, LbL), O/W ratio (20/80 and 30/70), and type of electrolyte used.

This part of the study confirmed that emulsions stabilized by combination of cCNC and TiO_2 particles can be prepared at pH 5 with the support of electrolytes that promote complex formation between cCNC and TiO_2. Using the CE method, formation of emulsion was possible only with $CaCl_2$. LbL method, on the other hand, produced emulsions with both $CaCl_2$ and NaCl. The presence of electrolyte was a decisive factor in the emulsification process. Stable emulsions were obtained if the electrolyte was added before the second sonication. Regardless of the preparation method, the presence of electrolyte in the emulsions resulted in a size increase of the emulsion droplets and a reduction of the zeta potential.

Summary of the study

The study focuses on emulsions stabilized by carboxylated cellulose nanocrystals (cCNC) in combination with titanium dioxide (TiO_2) particles that could be applied in UV protection.

The preformulation study confirmed the formation of complexes between cCNC and TiO_2 particles at pH 3, which was a prerequisite for successful preparation of emulsions using the layer by layer (LbL) method.

The effect of different cCNC:TiO_2 and O/W ratios on emulsion properties revealed that with the increasing amount of cCNC in the emulsions, their stability

improved. This suggests that cCNC particles were primarily involved in the stabilization of the emulsions. The emulsions with the cCNC:TiO$_2$ ratio of 1:1 and emulsions with the O/W ratio of 10/90 had the lowest encapsulation potential and stability. As for the total stabilizer content, the results showed that limited coalescence occurred at its 0.3 % content. When the amount of stabilizers increased (0.5 and 0.7 %) and the concentrations of particles were sufficient for emulsion stabilization. The release of oil, on the other hand, demonstrated that the highest concentration of stabilizing particles (0.7 %) did not result in the emulsions with best stability. The most stable and the most promising formulation for potential use in practice was an emulsion with the 0.5 % stabilizer, cCNC:TiO$_2$ ratio of 4:1 and the O/W ratio of 20/80. It was also demonstrated that, in addition to the layer by layer (LbL) method, the conventional emulsification (CE) method can be used for the preparation of stable emulsions under mentioned conditions.

The final goal of the study was to prepare emulsions at pH 5, which is favorable for the topical applications. The results confirmed that at pH 5, emulsions stabilized by cCNC and TiO$_2$ particles can be prepared only with the aid of electrolytes. Although emulsions with the addition of CaCl$_2$ and NaCl could be prepared using the LbL method, the CE method provided emulsions only with CaCl$_2$. The explanation may be the affinity of cCNC particles to calcium cations and the effect of cation valence on the formation of effective stabilizing system. The study thus resulted in the preparation of an effective and ecological emulsions with possible uses in UV protection.

8.4.3   Study on conducting colloidal systems

Colloidal particles and Pickering emulsions

Polyaniline (PANI) is one of the most investigated members of the conducting polymer (CP) family. Unfortunately, due to its stiff polymer backbone, PANI has poor processability and lacks solubility in aqueous environments [251]. These two shortcomings can be overcome by PANI synthesis in the presence of water-soluble steric stabilizers, yielding colloidal PANI [131]. Many scientific studies report on the synthesis of colloidal PANI in the presence of nanocellulose, specifically CNC or CNF. A typical process for the synthesis of materials combining PANI and nanocellulose includes the oxidative polymerization of aniline *in situ* in the presence of CNC or CNF as stabilizers. For example, PANI/CNC nanocomposites were prepared in two studies that both confirmed the homogeneous polymerization of the monomer on the CNC surface [216,219]. A variety of studies have shown that CNF in combination with PANI can be used to increase the stability of conducting nanocolloids [227,228,231,336]. Although many studies on the synthesis of colloidal PANI in the presence of CNC or CNF have been conducted, the composite particles based on these polymers have not been used to prepare Pickering emulsions (PE). PE have have attracted attention

due to their ability to improve immune response [337], which is associated with their morphology providing a large specific surface area for cell interactions [338]. Several studies have also focused on the preparation of PE for wound healing applications [339,340]. In this process, free radicals and their scavenging systems play an important role in the immune response [341]. In addition, it has been found that electrical stimulation of the wound area can accelerate its healing [342], which can be facilitated using CPs [343]. Thus, the use of substances with free radical scavenging activity in combination with CPs in one systems, such as PE, could enhance these applications.

The aim of this study was to investigate whether stable, bioactive PE could be made of colloidal particles composed of conducting polymer PANI and biocompatible cellulose nanoparticles (CNC or CNF). PE bioactivity was assumed to be derived from these composite particles used for PE stabilization and the encapsulated oil. Therefore, the PANI/CNC (or PANI/CNF) particles were first prepared and characterized. The next step was to prepare PE from these particles and an oil phase of undecane or caprylic/capric triacylglyceride. Finally, extensive characterization of their biological properties were conducted, primarily focusing on antioxidant activity in terms of immune response studies and scavenging ROS. This work, therefore, fills a knowledge gap and adds novelty to the field of PE.

- **Colloidal particles**

Particle size and morphology
The size distribution of PANI/CNC and PANI/CNF particles was measured by DLS. In fact, DLS is not the best technique for determining the particle size distribution of the samples investigated here, which contain rod-shaped CNC (or fibre-like CNF) and PANI. This is due to the fact that DLS technique determines particle diameters by considering all irregular or anisotropic shapes to be spheres [344]. As a result, PANI/CNC and PANI/CNF sizes reported here are only indicative and are supported by microscopy analyses.

DLS analysis revealed that the studied samples had large particle sizes (Tab. 9). Considering the morphology of the CNC and CNF particles (Fig. 38), a larger particle size was surprisingly measured for PANI/CNC both before and after dialysis. Although the particles of the non-dialyzed PANI/CNF were also relatively big, their sizes decreased after dialysis and were of approximately half the size compared to dialysed PANI/CNC. This decrease in the size of PANI/CNF colloidal particles after dialysis could be attributed to size changes in CNF fibres under dialysis due to the removal of residual low-molecular weight salts and reactants. The larger particle sizes of nanocellulose-based PANI colloids, compared to other polysaccharide PANI colloids (hyaluronate or chitosan) [345], are due to their more complex morphology and the formation of clusters, in which the cellulose nanoparticles are interconnected PANI (Fig. 38).

Table 9 Z-average particle diameter (z-average ± SD) of PANI/CNC and PANI/CNF colloidal particles.

	Z-average [nm]	
	Before dialysis	**After dialysis**
PANI/CNC	2983 ± 43	3163 ± 26
PANI/CNF	2200 ± 33	1214 ± 18

Microscopic images of colloidal dispersions were captured using TEM (Fig. 38). Images confirmed that after polymerization, clusters of CNC particles interconnected by PANI chains formed, mainly in PANI/CNC colloidal particles (Fig. 38). In the PANI/CNF sample, spherical PANI particles covering the CNF fibers are visible (Fig. 38), whereas PANI/CNC displays mesh-like structure with CNC clusters interconnected with PANI. As a result, the fibrous morphology of CNF seems to offer a better substrate for the polymerization of polyaniline.
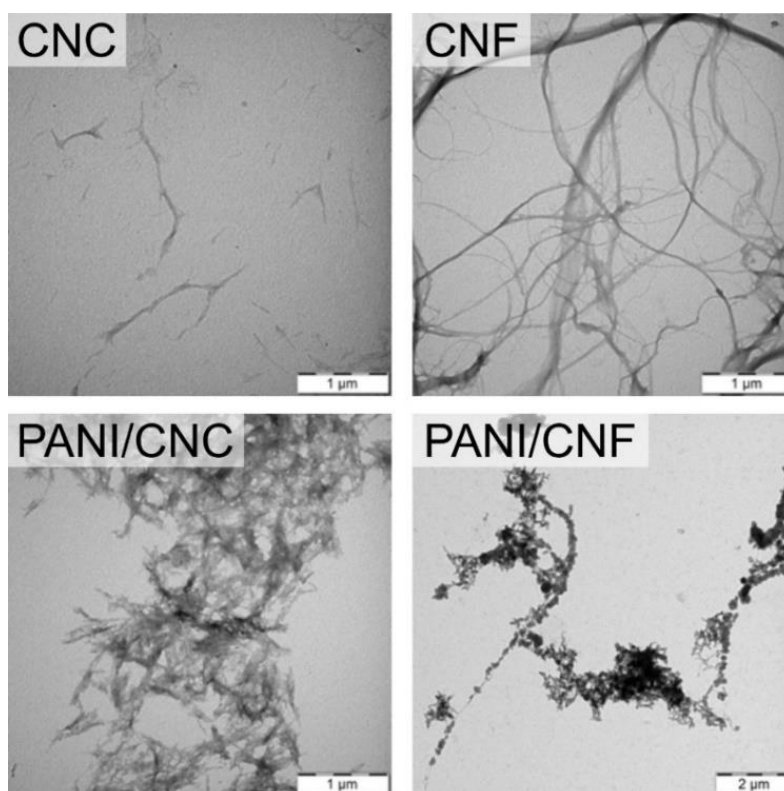
Figure 38 TEM images of CNC, CNF, PANI/CNC and PANI/CNF particles.

UV-vis analysis

The presence of PANI polymer in particles was confirmed by UV-vis spectra (Fig. 39). The UV–vis absorption spectra of PANI/CNC and PANI/CNF showed typical maxima at λ ~361 and ~768 nm for PANI/CNC, and λ ~390 and ~794 nm for PANI/CNF. Stejskal and Sapurina [172] reported absorption maxima of colloidal PANI stabilized with poly(N-vinylpyrrolidone) at $\lambda = 392$ and $\lambda = 854$ nm, which slightly differ from the maxima of the here-tested samples.

The first absorption band is assigned a π–π* transition of benzenoid ring, whereas the second absorption band belongs to the π−polaron and polaron−π transitions [133]. The above characteristics of PANI/CNC and PANI/CNF hence confirm the formation of PANI in the dispersions. The concentrations of PANI in colloids were calculated using the procedure reported in [296]. Overall, a higher concentration of PANI was present in PANI/CNF (5762 μg mL^{-1}), compared to PANI/CNC (3676 μg mL^{-1}).
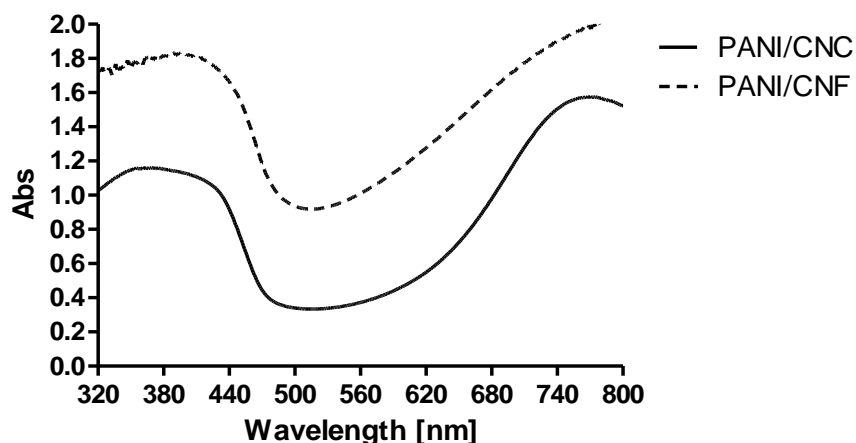
Figure 39 UV–vis spectra of PANI/CNC and PANI/CNF colloids.

Cytotoxicity

In order to investigate the cytotoxic effect of colloidal dispersions, murine peritoneal macrophage RAW 264.7 cell lines were used. Cytotoxicity testing revealed that PANI/CNC had no cytotoxic effects on macrophages (Fig. 40) even at the lowest used 10% dilution, which corresponds to 368 μg PANI/mL. The increased viability of cells on PANI/CNC is due to interference of the absorbance of the released PANI into the culture medium. However, on the basis of microscopic observation, no morphological differences from untreated cells were observed. Thus, the PANI/CNC does not affect the viability of the used cells. On the other hand, PANI/CNF was not toxic at 1% dilution, but at 2.5% (144 μg PANI/mL) showed weak toxicity (viability of 66 %). The other dilutions corresponding to a PANI concentration higher than 288 μg PANI/mL were toxic (viability under 50 % compared to the reference) (Fig. 40).
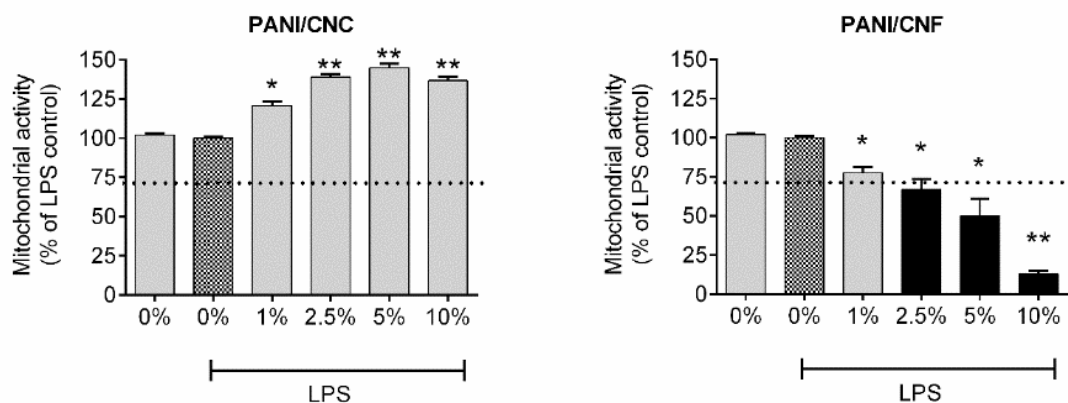
Figure 40 Cytotoxicity of PANI/CNC and PANI/CNF colloidal dispersions. Dashed line corresponds to cytotoxicity limit (70% viability relativelly to reference).

Antioxidant activity

The antioxidant activity of a sample plays an important role in reducing immune response and the chemiluminescence signal. To exclude the direct scavenging effects of the colloidal dispersions, their antioxidant properties were measured in a luminol-HRP-H_2O_2 cell-free system. Tests demonstated strong antioxidant activity of both PANI/CNC and PANI/CNF, which were both able to reduce the chemiluminescence signal below 5 % of the total signal produced by the system itself (Fig. 41).
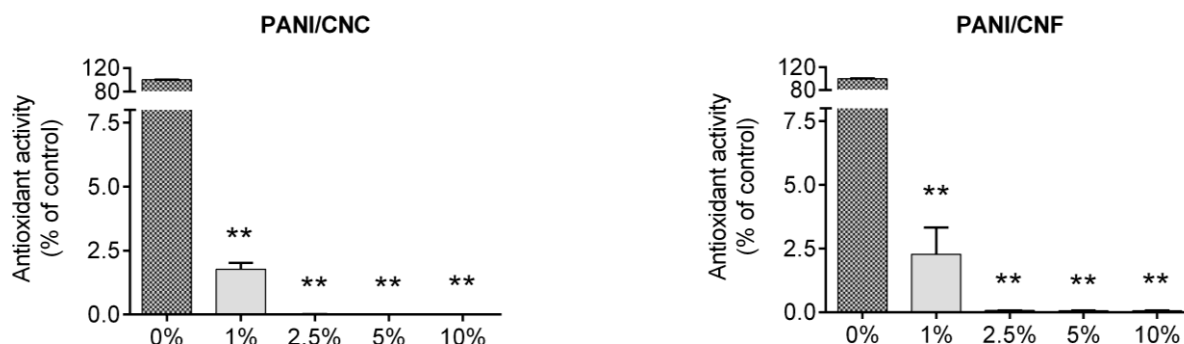
Figure 41 The antioxidant activity of colloidal dispersions.

The oxidative burst (ROS production) of isolated neutrophils

In the next step, the effect of colloidal particles on the detectable amount of ROS produced by neutrophils spontaneously and after their activation was tested. The oxidative burst of neutrophils is primarily characterized by the production of the superoxide anion radical, the first ROS produced by neutrophils upon their contact with a variety of stimuli (e.g., opsonins, cytokines, fragments of bacterial membranes, and others). Activation by yeast cell walls in the form of OZP is evident in Fig. 42 (lower panel). OZP-activated neutrophils showed a dramatic increase in ROS production compared to non-activated neutrophils.

80

Data shown in Fig. 42 confirmed the ability of PANI/CNC to strongly reduce ROS production in a concentration-dependent manner in both spontaneous and OZP-stimulated neutrophils. The PANI/CNC dispersion diluted to 1 % (37 µg PANI/mL) was able to decrease the signal below 50 % of control. Dispersions diluted to 2.5 % (92 µg PANI/mL) then reduced the chemiluminescence signal below 15 % of the control, while other dilutions reduced the chemiluminescence signal to zero. As regards OZP-stimulated ROS, the effect of PANI/CNC on their production was even stronger. At 1% dilution the dispersions reduced the chemiluminescence signal to below 15 % of control, while other tested dilutions decreased the signal to zero. Compared to PANI/CNC, PANI/CNF reduced ROS production even strongly and again in a concentration-dependent manner. Specifically, dilution of PANI/CNF to 1 % (corresponding to 58 µg PANI/mL) was able to reduce the signal below 15 % of the control, while the other concentrations lowered the chemiluminescence signal to zero. In addition, PANI/CNF showed an even stronger effect in the scavenging of ROS stimulated by OZP activated neutrophils, with all dilutions tested reducing the signal to zero or close to zero. Given the antioxidant activity of the tested colloidal dispersions (Fig. 41), the reduction of ROS production is probably related to ROS scavenging activity.
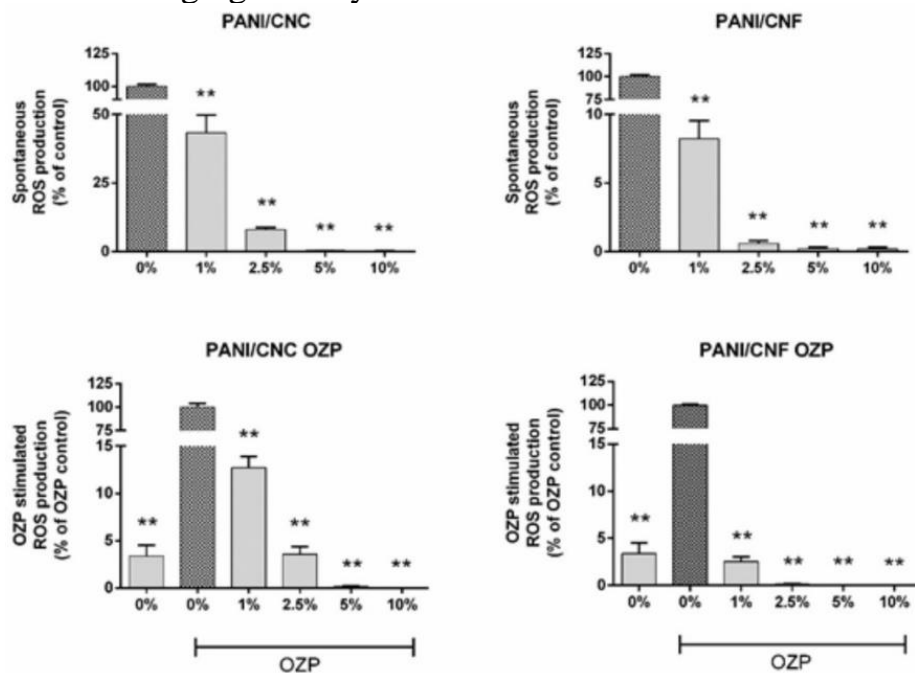
Figure 42 The effect of colloidal dispersions on spontaneous ROS production and on OZP-activated ROS production by neutrophils.

Nitric oxide (NO) and interleukin 6 (IL-6) production from murine macrophages
The activation of macrophages, for example by bacteria or their parts, such as LPS, triggers the production of pro-inflammatory compounds including, for example, cytokines, chemokines, and NO. These experiments focused on NO and

IL-6 production, two important pro-inflammatory signaling molecules of macrophages.

The results demonstrate that NO production (level nitrite in medium) was significantly decreased in a concentration-dependent manner by both PANI/CNC and PANI/CNF. On the basis of the results of PANI/CNF cytotoxicity testing, it can be assumed that lower concentrations of this sample reduce NO production directly. A higher cytotoxic effect was involved in this reduction at higher concentrations of the dispersions. (Fig. 43). Similarly to the reduction of NO, both PANI/CNC and PANI/CNF decreased IL-6 production. The reduction was also dependent on the dispersion concentration/dilution.
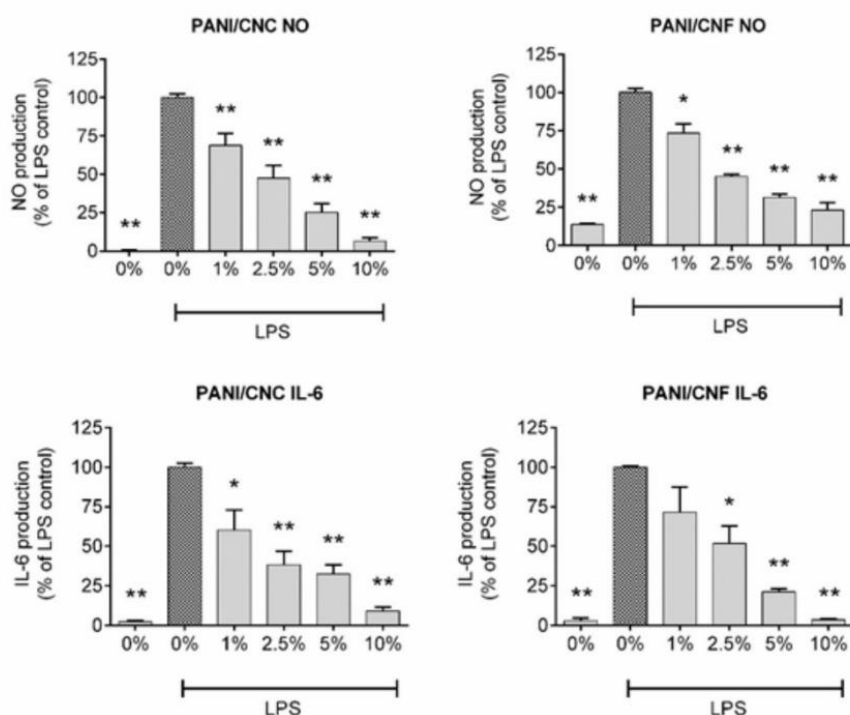
Figure 43 The effect of colloidal dispersions on NO and IL-6 production of RAW264.7 macrophages.

Antibacterial activity

The results showed that the PANI-containing dispersion were able to inhibit growth of both gram positive and gram negative bacteria. Despite having a lower concentration of PANI polymer (3676 µg/mL), PANI/CNC had higher activity against both strains than PANI/CNF with a PANI concentration of 5762 µg/mL. Here, it can be speculated that PANI polymer is more accesible for antibacterial action in PANI/CNC particles than in PANI/CNF, where it can be hidden in the entangled CNF fibres. PANI/CNC had a lower MIC value against gram negative *E. coli* (1.7 µg/mL PANI in dispersion) than against gram positive *S. aureus* (3.4 µg/mL PANI in dispersion), which was also observed for colloidal PANI particles stabilized with chitosan and sodium hyaluronate [345]. In the PANI/CNF sample, the effects against both strains were similar with MIC detected at a PANI concentration of 8.3 µg/mL. Given the low antibacterial activity of colloidal

PANI containing poly(*N*-vinnylpyrrolidone) reported by [191], the incorporation of cellulose nanoparticles, whether CNC or CNF, significantly altered the antibacterial efficacy of the here-examined samples.

- **Pickering emulsions**

Particle size, morphology and stability

PANI/CNC or PANI/CNF particles were used to stabilize Pickering emulsions with 20 % undecane (U) or caprylic/capric triglyceride (T). The size of E-PANI/CNC^T droplets was 2985 ± 6 nm (PDI of 0.15 ± 0.05). Thus, there was only a minimum increase in the size of emulsion droplets in comparison with the PANI/CNC particles. This is likely caused by the effect of sonication, which destroys the mesh-like structure of the PANI/CNC particles used to stabilize emulsions, reducing their size and allowing them to form emulsion droplets. Emulsions stabilized with the same particle type containing undecane (E-PANI/CNC^U) revealed droplets larger than 3000 nm (3399 ± 51, PDI $= 0.15 \pm 0.11$). Because the emulsion droplets were too large for DLS measurements and unsuitable for measurements by laser diffraction (PANI in emulsions could cover the measuring cell of the instrument with a green film), the droplet sizes of emulsions stabilized with PANI/CNF were determined using microscopy combinrd with image analysis. Average size of E-PANI/CNF^U droplets was of 33 μm, with range from 6.5 to 81 μm, and E-PANI/CNF^T droplets were smaller, with an average size of 19 μm ranging from 4.7 to 30 μm.

All prepared Pickering emulsions demonstrated excellent encapsulation efficiency, with no evidence of oiling-off in the samples after storage at room temperature. However, creaming, a process caused by the different densities of the oil and water phases, was clearly demonstrated (Fig. 44). This figure also shows how the concentration of stabilizing particles affected creaming in PANI/CNF-based emulsions. Creaming was lower in emulsions stabilized with PANI/CNF at 50 % initial concentration than in emulsions prepared with dispersions diluted to 30 %. Nevertheless, all emulsions could easily be re-dispersed by soft shaking, showing that creaming in the studied emulsions did not indicate a loss of their stability [61]. However, dilution of the initial PANI/CNF dispersion was critical because emulsions prepared with undiluted dispersion were unstable. PANI/CNC-based emulsions were stable in terms of encapsulation efficiency and creaming even after two years of storage at room temperature.

Figure 44 Creaming of Pickering emulsions with undecane (U) and caprylic/capric triglyceride (T) oils stabilized with PANI/CNF: E-PANI/CNF^{T50}; E-PANI/CNF^{T30}; E-PANI/CNF^{U50}; E-PANI/CNF^{U30} after preparation.

The appearance and morphology of emulsion droplets were investigated using confocal laser scanning microscopy (CLSM), (Fig. 45). Undecane produced emulsions with larger droplets than caprylic/capric triglyceride oil, regardless of the type of PANI/cellulose stabilizer used. These variances may be due to differences in physicochemical properties of the oils, such as density, polarity, or viscosity. Furthermore, images of PANI/CNF-stabilized emulsions revealed the presence of residual CNF fibers adsorbed around the emulsion droplets, providing additional stabilization.
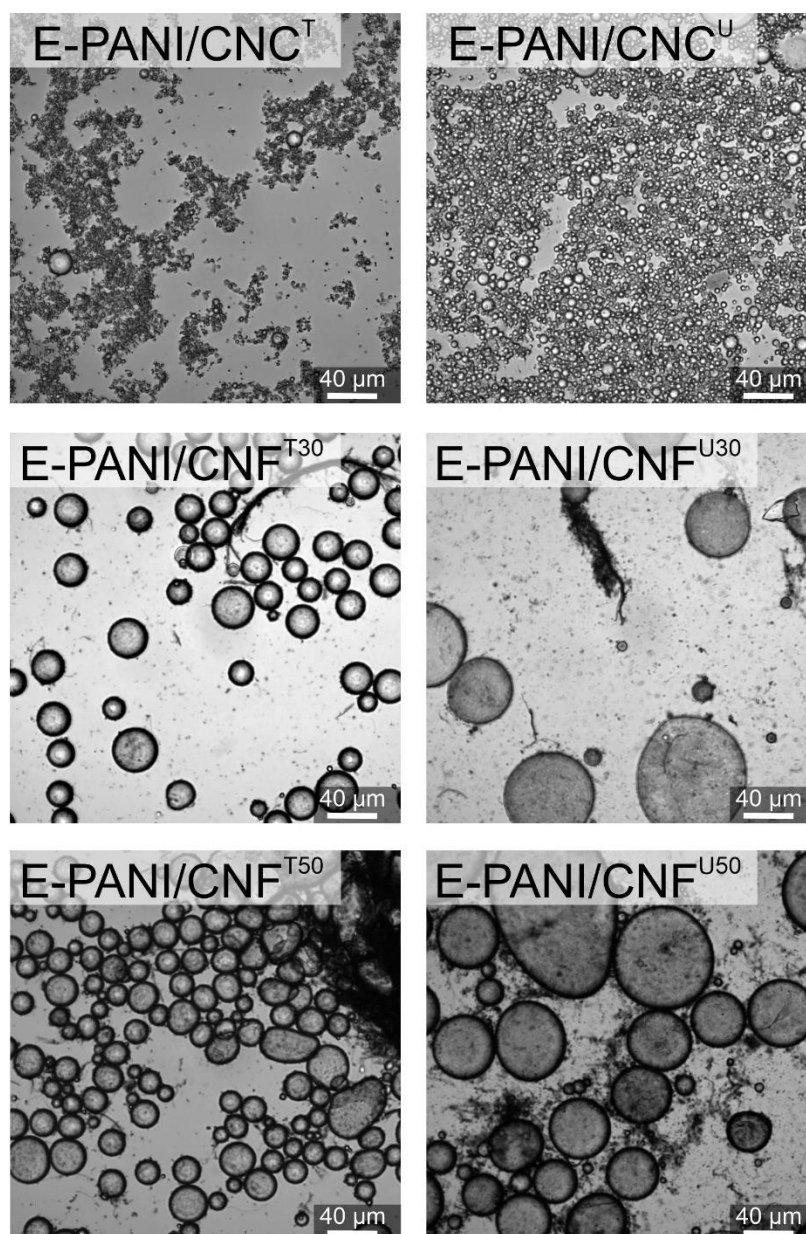
Figure 45 CLSM images of O/W Pickering emulsions with 20 % caprylic/capric triglyceride (T) and undecane (U).

Cytotoxicity

As mentioned previously, PANI/CNC dispersions were not cytotoxic, whereas PANI/CNF showed significant toxicity at dilutions higher than 2.5 % (Fig. 40). According to [346], undecane was among the major hydrocarbons associated with high cytotoxicity in human epidermal keratinocytes. Triglycerides, on the other hand, show very low levels of toxicity in laboratory animals and humans after oral, parenteral or dermal administration [347]. These differences in oil cytotoxicities are reflected by the results presented in Fig. 46, revealing that triglyceride-based E-PANI/CNC^T had no cytotoxic effects on macrophages, whilst E-PANI/CNC^U with undecane showed strong cytotoxicity at all concentrations tested. The results also show that cytotoxicity was higher in

undecane-containing emulsions stabilized with PANI/CNC than in emulsions stabilized with PANI/CNF. This could be due to the formation of a thicker, more impermeable PANI/CNF layer protecting the oil droplets from undecane leakage. Nevertheless, the cytotoxicity of PANI/CNF-stabilized emulsions with triclyceride was higher than that of PANI/CNC emulsions and was dependent on the sample concentration used for testing.

The cytotoxicity of the PANI/CNC dispersion (Fig. 40) and corresponding emulsions (Fig. 46) revealed that the triglyceride oil had no cytotoxic effects on macrophages, but undecane significantly reduced their viability, and the samples were cytotoxic at all tested concentrations. As a result, PANI/CNC colloids retained their properties when used as emulsion stabilizers. Similar conclusions can be drawn for PANI/CNF dispersions and their emulsions. Dispersions were cytotoxic at 2.5 % dilution (144 µg/mL PANI) and emulsions prepared with non-harmful triglyceride oil exhibited cytotoxicity at a dilution of 5% corresponding to 115 µg/mL PANI. However, emulsions with undecane prepared with the same concentration of PANI/CNF showed severe cytotoxicity with a cell viability of only 5 %.
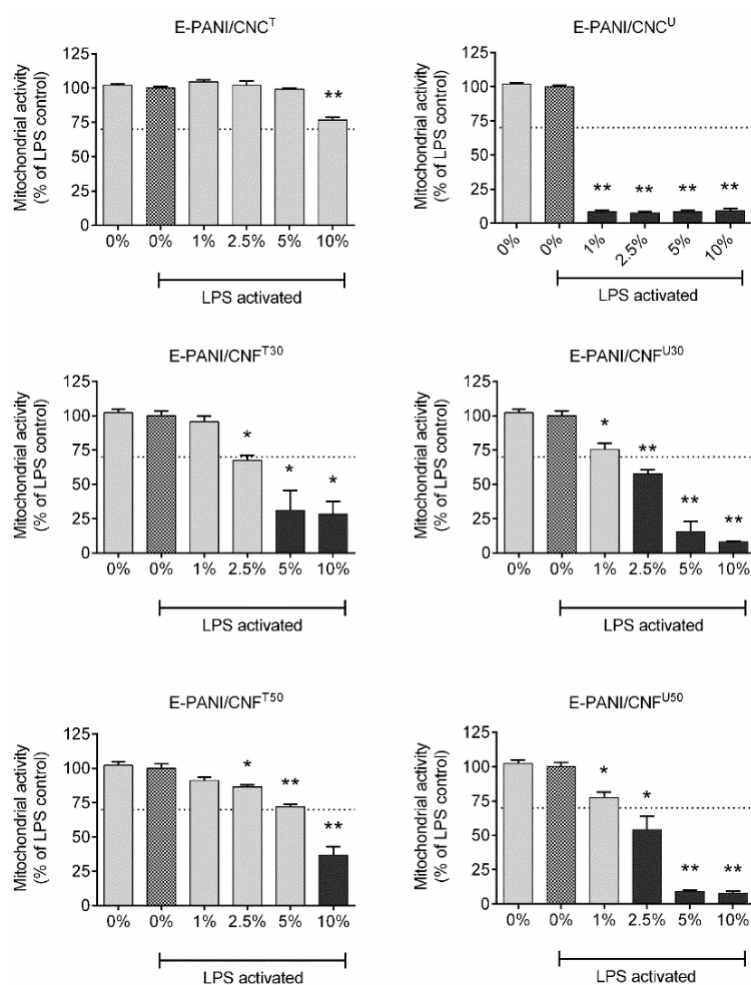
Figure 46 Cytotoxicity of Pickering emulsions expressed as cell viability of murine macrophage RAW 264.7 cells. Dashed line corresponds to cytotoxicity limit (70% viability relativelly to reference).

Antioxidant activity

Correspondingly to the strong antioxidation activity of PANI/CNC dispersions, the results demonstrated the strong antioxidation activity of emulsions prepared with these particles – specifically, E-PANI/CNC^T and E-PANI/CNC^U (Fig. 47). All tested concentrations were able to reduce the chemiluminescence signal to below 5 % of the total signal produced by the system itself. As regards PANI/CNF-based emulsions, at 1% dilution, E-PANI/CNF^{T50} and E-PANI/CNF^{U50} reduced the chemiluminescence signal to approximately 10 to 15 % of control. The other concentrations reduced the chemiluminescence signal to below 5% of control.
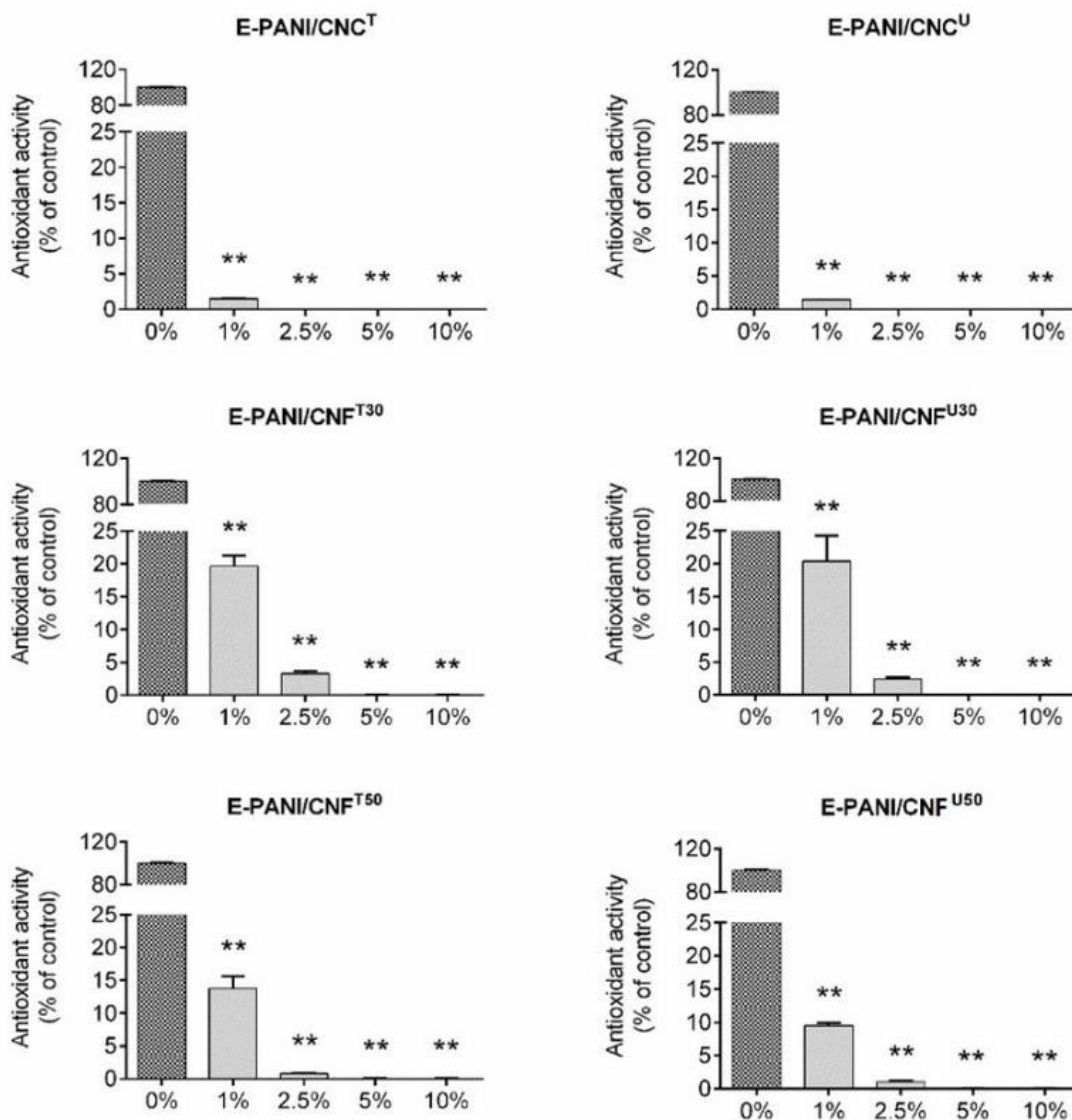
Figure 47 The antioxidant activity of Pickering emulsions.

The oxidative burst (ROS production) of isolated neutrophils

As can be seen in Fig. 48, E-PANI/CNC^T and E-PANI/CNC^U in 1% dilution were able to reduce the chemiluminescence signal to below 50 % of control, while the 2.5% dilution reduced the chemiluminescence signal to below 15 % of control (without emulsions), and other samples reduced the chemiluminescence signal to

zero, evidencing thus the ability of both emulsions to reduce spontaneously produced ROS. The efficacy of both samples was even higher as regards their ability to scavenge OZP-stimulated ROS production. Specifically, emulsions at 1% dilution reduced the chemiluminescence signal to below 15 % of control, while other tested concentrations reduced the signal to zero (Fig. 48). The chemiluminescence signal was reduced more by the PE stabilized with PANI/CNF at 50 % dilution (E-PANI/CNF^{T50} and E-PANI/CNF^{U50}) than by the emulsions prepared with PANI/CNF diluted to 30 % (E-PANI/CNF^{T30} and E-PANI/CNF^{U30}), most likely because the former two samples contained a higher concentration of PANI polymer (Fig. 48). For OZP-stimulated ROS production, a stronger effect for samples with undecane was observed (Fig. 48). Given the antioxidant activity of all the tested samples (Fig. 47), this effect is apparently related to ROS scavenging activity.
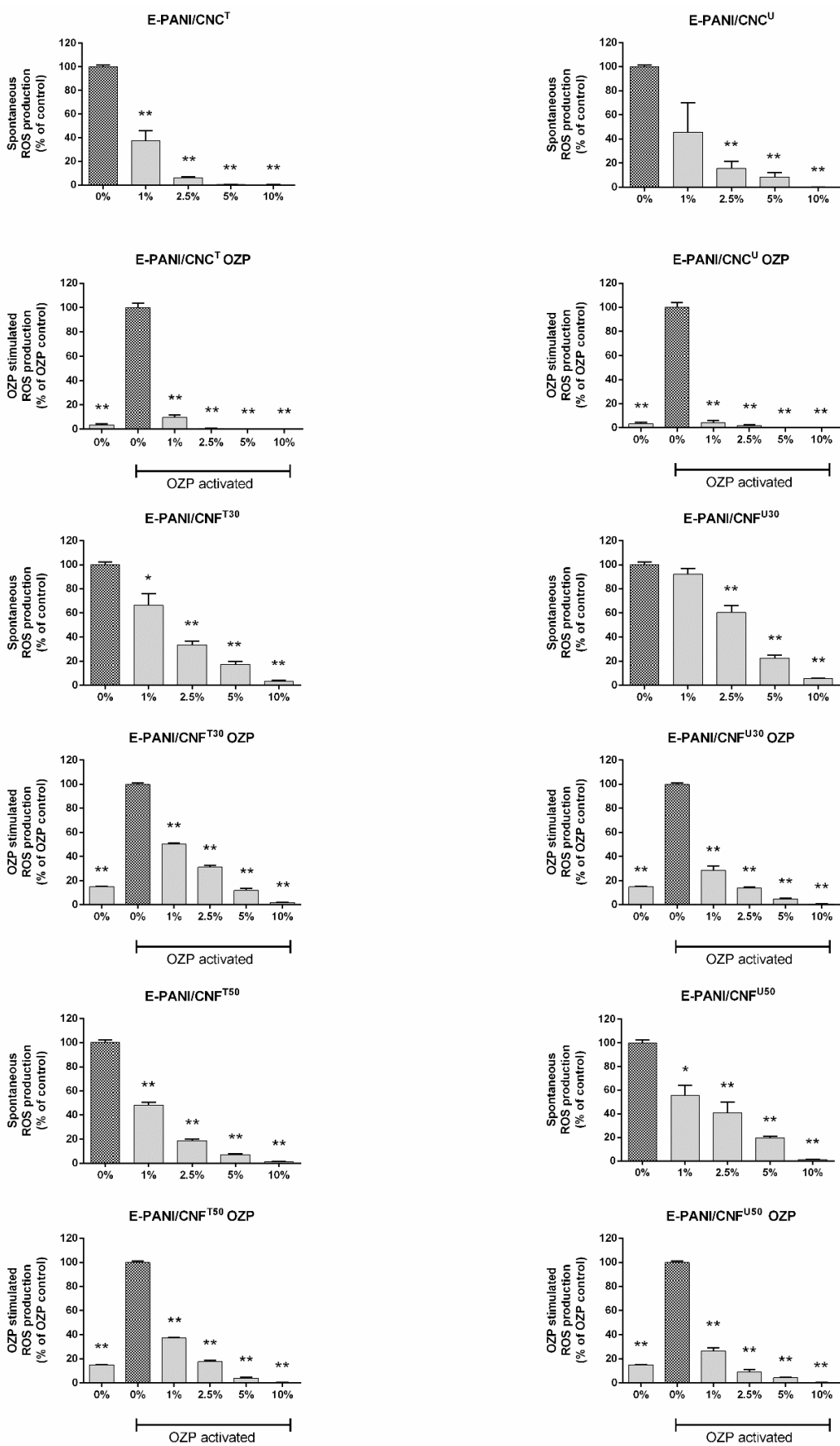
Figure 48 The effect of Pickering emulsions on spontaneous ROS production and on OZP-activated ROS production by neutrophils.

89

Nitric oxide (NO) and interleukin 6 (IL-6) production from murine macrophages

The ability of PE to influence IL-6 production differed and depended on emulsion composition, mainly on the type of oil. Whilst triglyceride-based E-PANI/CNC^T did not appear to decrease IL-6 production, the effect of emulsions prepared with PANI/CNF particles (E-PANI/CNF) was opposite and a concentration-dependent decrease in IL-6 generation was observed, as seen in Fig. 49 and 50. Pickering emulsions prepared with undecane, however, behaved differently and all tested samples of E-PANI/CNC^U reduced IL-6 production to below 5 % of control, which is associated with their cytotoxicity (Fig. 46). On the other hand, undecane emulsions with CNF (E-PANI/CNF^{U50}) decreased the production of IL-6 in concentration-dependent manner. Correspondingly, the studied emulsions were able to reduce the production of NO in a dose-dependent manner, as can be seen in Fig. 49 and 50.
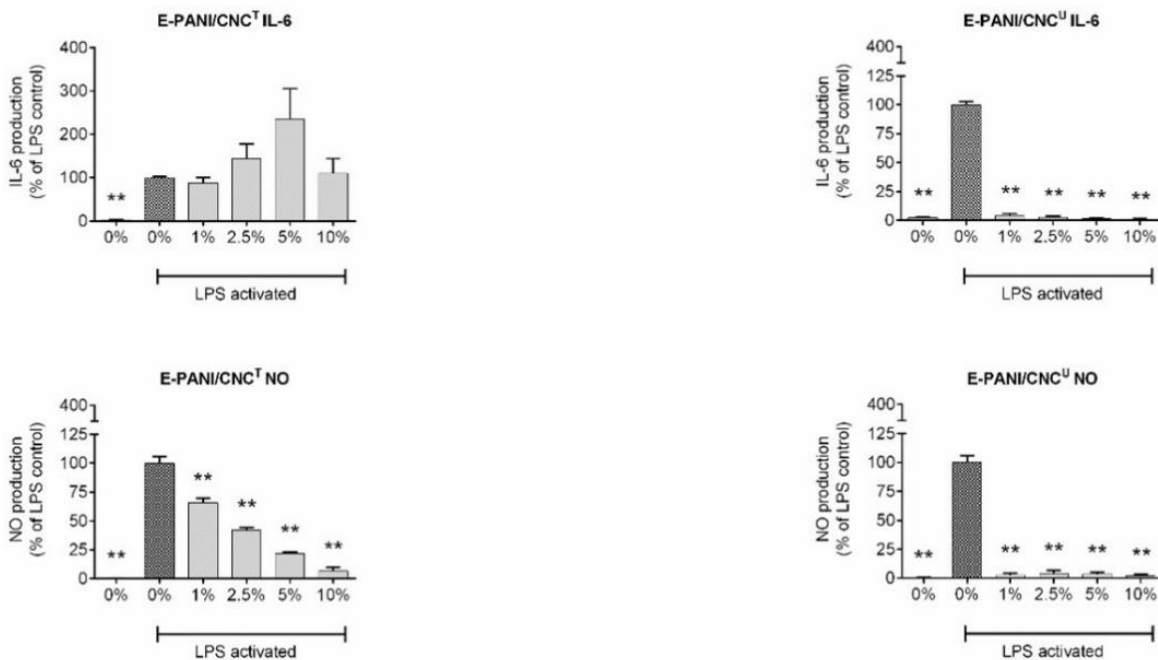
Figure 49 The effect of Pickering emulsions with PANI/CNC particles on NO production of RAW264.7 macrophages.
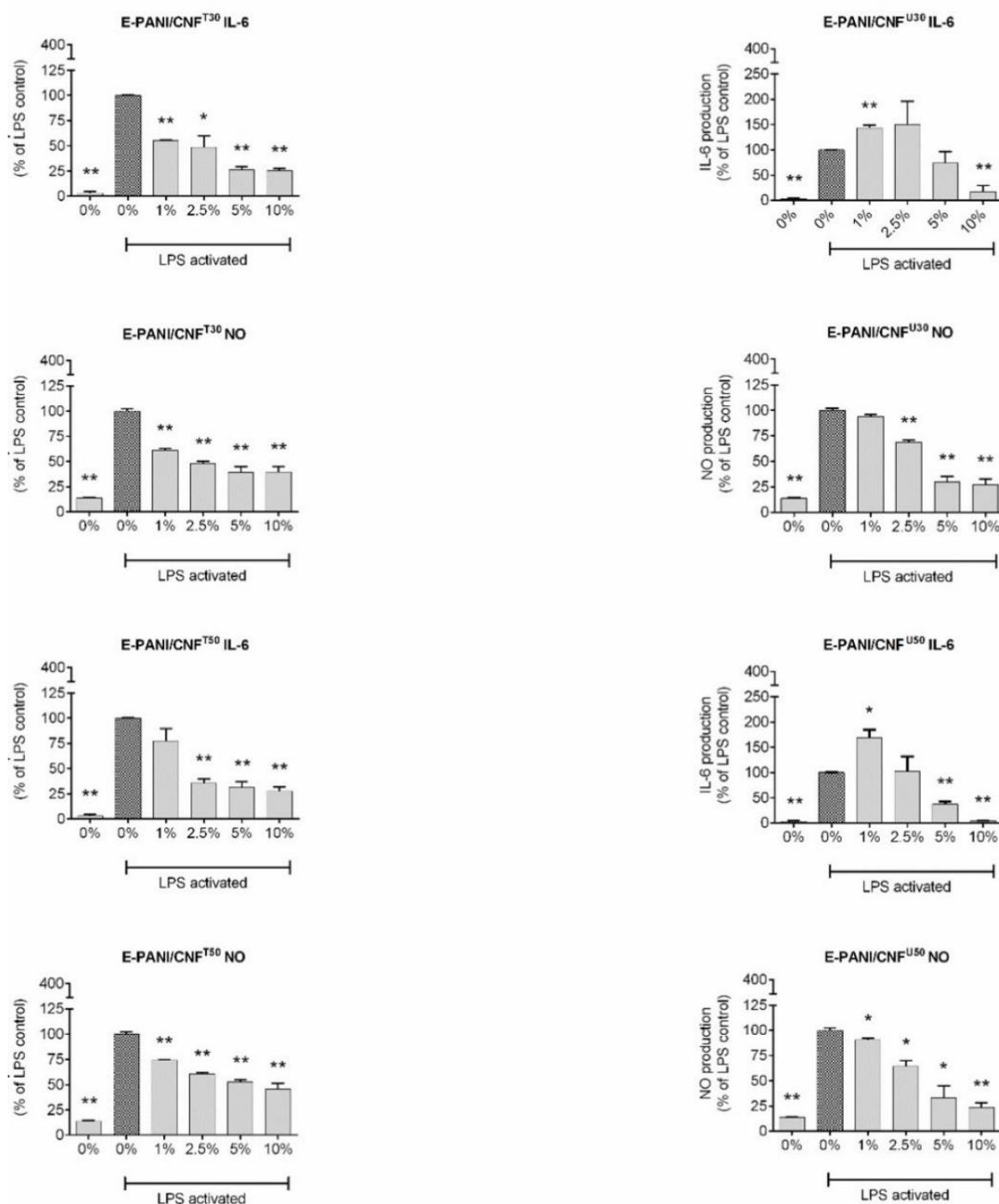
Figure 50 The effect of Pickering emulsions with PANI/CNF particles on NO production of RAW264.7 macrophages.

Summary of the study

The oxidative polymerization of aniline with ammonium persulfate in the presence of each of the mentioned cellulose particles resulted in composite particles (PANI/CNC and PANI/CNF) containing conducting polyaniline (PANI) and cellulose nanocrystals (CNC) or nanofibers (CNF). Testing of the biological properties of the particles provided information on their cytotoxicity and antioxidation activity, and demonstrated their immunomodulatory effect on

91

macrophages. The detection of anti-inflammatory activity was crucial in this case. The study further revealed that PANI/CNC composite had better antibacterial activity against the two most common model microorganisms *S. aureus* and *E. coli*.

In the next step, Pickering emulsions containing 20 % undecane or an equal amount of capric/caprylic triglyceride oil were successfully formulated using PANI/CNC or PANI/CNF. The biological activity of the particles used to stabilize the emulsions was preserved in these systems, whereas the physico-chemical and biological properties of the emulsions were determined by the properties of the particles used for stabilization and the type of oil in emulsions.

In conclusion, these systems demonstrated strong antioxidant and ROS scavenging activity, indicating their potential use in biomedical applications, particularly wound healing.

Thin PANI/celulose films

One of the unique properties of colloidal PANI dispersions is their ability to form thin films and coatings on all surfaces that are immersed in the reaction mixture. In this regard, PANI/CNC and PANI/CNF dispersions are not exceptions.

Several papers deal with the preparation of cellulose-PANI conducting materials using *in situ* chemical polymerization [238,348–355] or interfacial polymerization [356]. Liu et al. created thin CNC-PANI composite films by polymerizing aniline hydrochloride (AH) with ammonium peroxydisulfate (APS) in aqueous nanocellulose suspension. The reaction resulted in PANI particles formed on the surface of cellulose. The composite films displayed good flexibility and conductivity, the latter growing with increasing PANI content [357]. Similarly, Nepomuceno et al. [358] prepared flexible nanostructured materials based on CNC-PANI. The study [359] confirmed the homogenous polymerization of aniline on the surface of CNC, and formation of CNC-PANI nanocomposites have been also reported by [360–366]. Also coating of cellulose nanofibers (CNF) with PANI has been conducted with the aid of different procedures including *in situ* oxidative polymerization [230,367–373].

Despite the recent advances mentioned above, the biological properties of nanocellulose-PANI composites have received little attention. Therefore, the aim of this study was to investigate whether two different types of thin conducting composite films based on PANI and cellulose nanocrystals (CNC) or cellulose nanofibers (CNF) could serve as a suitable substrate for cells. The novelty of the study stems not only from a unique comparison of two types of nanocelluloses used in the preparation of composite films under the same conditions using *in situ* oxidative polymerization method, but also in the thorough physicochemical and

biological characterization that contributes to a deeper understanding of cell behaviour on these surfaces.

Morphology

When considering materials suitable for biomedical applications, the surface morphology of the material is an important characteristic influencing cellular behaviour. Therefore, the surface topography and surface electrical properties of the films were determined using AFM. The topography of the PANI/CNC and PANI/CNF films was significantly different compared to the pristine PANI (Fig. 51). The PANI film without cellulose nanoparticles showed a typical granular surface and a noticeably higher surface roughness ($Sa \sim 100$ nm). Despite having comparable thicknesses (21 and 25 nm), the two composite films showed different properties. The film of PANI/CNC exhibited rough structure with needle-like structures of celluloses visible on the surface. These structures are typical for cellulose nanocrystals, and the image thus confirms that the CNC was incorporated into the PANI composite film. Moreover, the structures are well connected to one another, which indicate the existence of strong hydrogen bonding [357]. On the other hand, the PANI/CNF film contained fibre aggregates rather than the long nanofibers typical of CNFs without PANI. Regarding the electrical properties of the composites, the results from AFM showed that PANI/CNF exhibited considerably higher surface conductivity than PANI/CNC, which is in good agreement with the conductivities obtained with the van der Pauw method.
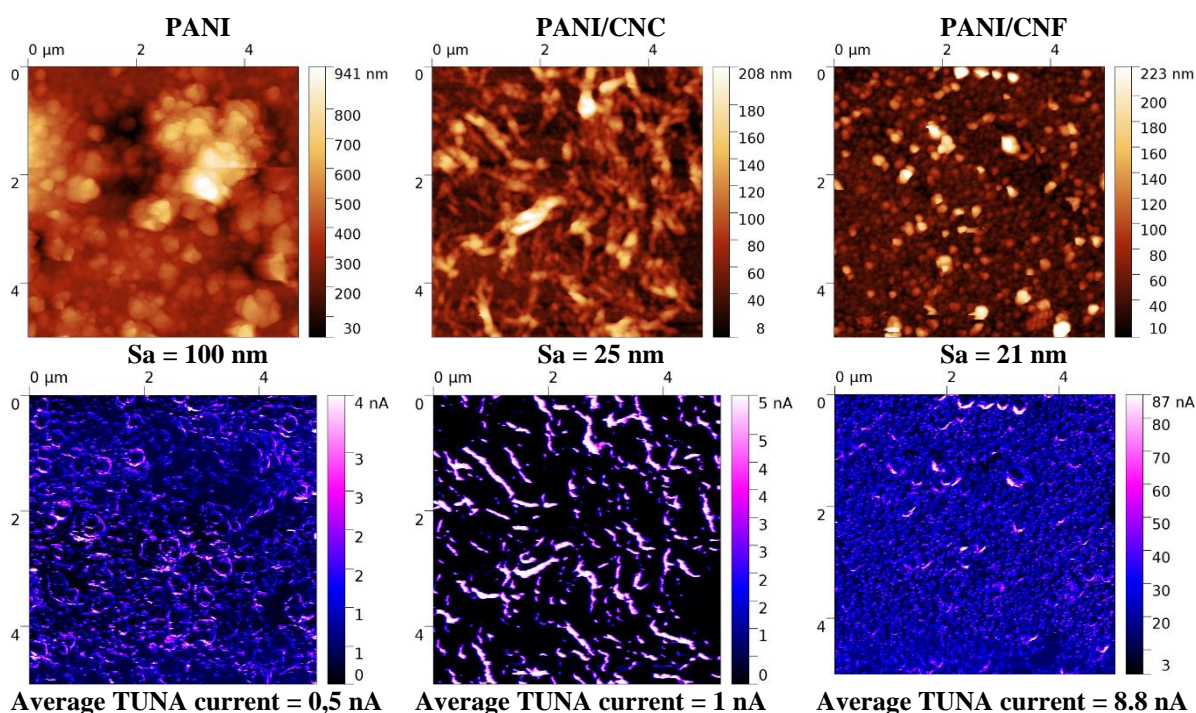

Figure 51 AFM images of PANI reference film and composite films of PANI/CNC and PANI/CNF. Top images show height changes, below TUNA current maps.

Surface energy

The measurement of surface energy revealed that the values of the total surface energy (γ^{tot}) of PANI/CNC corresponded to that of PANI film determined earlier [374] (Tab. 10). In addition, the PANI/CNC sample showed almost the same values of the surface energy components representing both disperse (γ^{LW}) and polar (γ^{AB}) parts as reference PANI without cellulose nanoparticles. This may indicate that the properties of PANI predominated and affected the surface characteristics of PANI/CNC composite film. Compared to these two samples, the total surface energy (γ^{tot}) and disperse (γ^{LW}) part of PANI/CNF were slightly higher. In contrast, polar (γ^{AB}) part of PANI/CNF was the lowest of all surfaces. Interestingly, surface energy values γ^{tot} obtained for the cell monolayer of NIH/3T3 cells [286] were close to the reported PANI/CNC and PANI/CNF values, which could indicate suitable biological properties of such surfaces.

Table 10 Contact angles together with total surface energy (γ^{tot}) and it's disperse (γ^{LW}) and polar (γ^{AB}) parts determined on tested PANI, PANI/CNC, and PANI/CNF surfaces.

Sample	Contact angles (°)			Free surface energy (mN m^{-1})		
	Water	**Ethylene glycol**	**Diiodomethane**	γ^{TOT}	γ^{LW}	γ^{AB}
PANI*	n.r.	n.r.	n.r.	52.5	46.1	6.5
PANI/CNC	51.3 ± 2.0	30.1 ± 0.9	20.5 ± 0.8	52.7	47.6	5.1
PANI/CNF	40.8 ± 1.2	9.5 ± 1.3	4.3 ± 3.0	54.8	50.7	4.2

* The values adopted from [374]; n.r. not reported

Conductivity

The conductivity is considered as important cell-instructive characteristic in biomedical applications. The virgin PANI films commonly show conductivity values within units of S cm^{-1} [172] depending on the conditions of polymer synthesis and dopant used. In here presented study, the conductivities of PANI/CNC and PANI/CNF composite films differed from each other with the higher PANI/CNF conductivity of 4.7 S cm^{-1}, close to of the virgin PANI film (5.5 ± 0.7 S cm^{-1}) [288]. In contrast, the PANI/CNC film displayed a significantly lower conductivity of 0.1 S cm^{-1}. Assuming almost identical thicknesses of PANI/CNC and PANI/CNF films determined by AFM (S_a values in Fig. 51), the differences in the conductivity of PANI/CNF and PANI/CNC films can be attributed mainly to the different morphology of the CNC and CNF particles. In comparison to small needle-like CNC, long CNF fibres can provide superior support for growth of conducting PANI. In addition, the concentrations of CNC (1 %) and CNF (0.06 %) used in the samples can explain this difference. Despite the presence of nanocellulose, the results demonstrated that the composite films retained good electrical conductivity.

Antioxidant activity

The DPPH assay was used to determine the *in vitro* antioxidant activity of the films. The ability of polyaniline and its composites to act as antioxidants has previously been confirmed by published studies [375–378]. Also this work showed that PANI/CNC and PANI/CNF films are effective scavengers of DPPH radicals. Moreover, the analyses revealed that the activity of the samples did not differ significantly, with both samples demonstrating similar scavenging activity of about 50 % in 10 min.

Cell proliferation

The cell proliferation on tested surfaces is crucial for their use in biomedical materials. The results of cell proliferation on the composite films are presented in Fig. 52. The micrographs clearly show that the cells reached semi-confluence on the tissue polystyrene culture dishes used as a reference (Fig. 52a). Interestingly, the proliferation of NIH/3T3 cell line on the composite films was fully comparable to the reference (Fig. 52b, c), which indicates properties favourable for cell growth. Also proliferation of cells on virgin PANI film reported in [286] was comparable to that on the tissue polystyrene culture dishes. Therefore, the presence of CNC or CNF in the composite films does not affect the cell proliferation, confirming absence of their *in vitro* cytotoxicity.
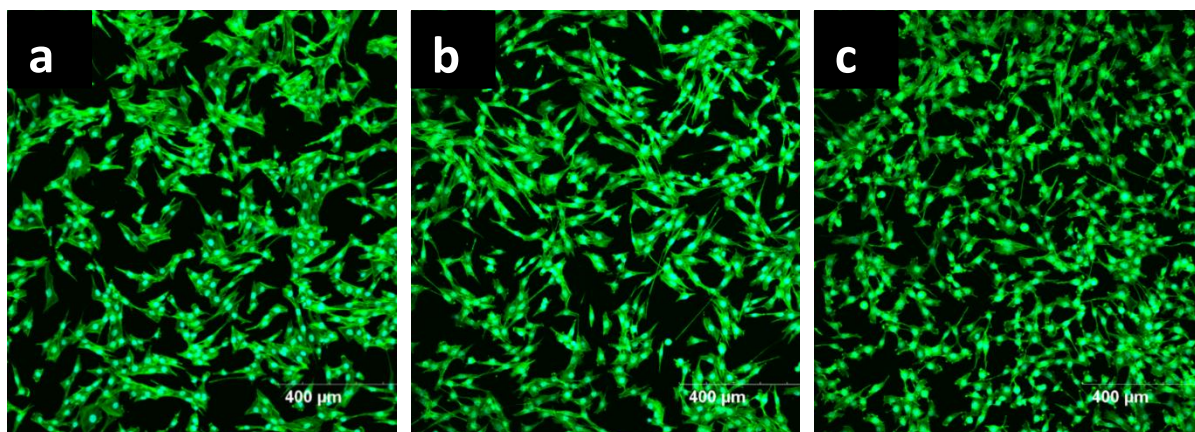
Figure 52 Proliferation of NIH/3T3 cells on studied films recorded after 48 h cultivation: a) Reference – tissue polystyrene culture dishes; b) PANI/CNC; c) PANI/CNF.

Antibacterial activity

It is well known that nanocellulose itself has no antimicrobial properties [379]. To achieve antimicrobial activity, surface functionalization of nanocellulose with suitable antibacterial agent is required, which allows a wide application rage of such composites as an antimicrobial materials [380]. On the other hand, the antibacterial activity of PANI has already been demonstrated both in films [381]

and colloidal particles [345]. It is therefore expected that the antibacterial effect of the composites will be caused primarily by PANI present in the composite film.

According to the protocol used for antibacterial testing, an antibacterial agent is considered effective if its antimicrobial activity R > 1. The antibacterial properties were assesed using EN ISO 20743:2021. The criteria for antibacterial efficacy (R) given at the standard are following: R < 2 corresponds to a low level of efficacy, 2< R <3 a significant level of efficacy, and R > 3 a strong level of efficacy. Results in Tab. 11 reveal that both PANI/CNC and PANI/CNF have low antibacterial activity against both gram positive *Staphylococcus aureus* and gram negative *Escherichia coli* bacterial strains. The results further demonstrate somewhat higher efficacy of both composites against *E. coli*.

Table 11 Number of viable bacteria N and antibacterial activity R of PANI/CNC and PANI/CNF composite films.

Sample	Antimicrobial activity *R*	
	S. aureus	*E. Coli*
PANI/CNC	1.26	1.30
PANI/CNF	1.26	1.30

Summary of the study

Electrically conducting nanocellulose-based polyaniline (PANI) composite films were prepared by *in-situ* oxidative polymerization of aniline hydrochloride in aqueous nanocellulose suspension (CNC or CNF) by using APS as oxidant. The PANI/CNC and PANI/CNF composite films displayed good conductivity, which was higher for the PANI/CNF (4.7 S cm^{-1}). The surface topography of the films was controlled by the type of cellulose nanoparticles present in the sample, and the thicknesses of both films were comparable. The surface energy values were not significantly different and were similar to the surface energy od cell monolayer of NIH/3T3 cells, indicating that both films had favourable biological properties. The composites also demonstrated *in vitro* antioxidation activity as determined *via* scavenging of DPPH radicals and mild antibacterial efficiency against gram positive *Staphylococcus aureus* and gramnegative *Escherichia coli.* Biological testing demonstrated that both PANI/CNC and PANI/CNF have exellent cytocompatibility, comparable to tissue polystyren. The presence of cellulose in the films have no effect on cell proliferation. As a result, the biocompatible nanocellulose-based composites formed may be promising materials for use in biomedicine.

9. CONCLUDING SUMMARY

Nanocellulose is a well-known material used, among others, as a stabilizer in a variety of colloidal dispersions. The use of nano-structured cellulose to stabilize colloids is a promising concept providing more minimalist and environmentally friendly formulations in a wide range of indistrial applications.

The thesis is focused on the investigation of colloidal dispersions based on cellulose nanoparticles. This includes research into classical dispersions based on cellulose nanoparticles and TiO_2 for cosmetic applications, as well as conducting polyaniline-nanocellulose systems for biomedical applications. Based on the defined objectives of the thesis, the results can be divided into three areas: 1) investigate and description of the behaviour of TiO_2 particles under simulated and *in vitro* conditions before incorporating them into Pickering emulsions; 2) development Pickering emulsions stabilized by a combination of TiO_2 and cellulose nanoparticles for skin photoprotection applications; and 3) confirmation of the ability of various cellulose nanoparticles to stabilize conducting PANI in colloidal form and use these dispersions to prepare thin films and Pickering emulsions for potential biomedical applications.

The first part of the thesis was a preliminary investigations into the behaviour of various forms of TiO_2 particles (rutile, anatase, and their commercial mixture) prior to their incorporation into Pickering emulsions. The behaviour of the particles was studied in media used for biocompatibility testing (PBS and DMEM), simulated body fluids (saliva, gastric and intestinal fluids) and human blood plasma. These media mimicked the *in vivo* conditions that occur after oral and dermal exposure of TiO_2. Monitoring the time-dependent agglomeration of TiO_2 particles in the aforementioned media revealed a strong dependence of crystalline form of TiO_2, ionic strength of the media, and presence of proteins on the TiO_2 behavior. The electrolytes present in PBS, serum-free DMEM and saliva caused TiO_2 agglomeration, which is related to the screening of the surface charge of the particles. On the contrary, the presence of calf serum in DMEM as well as presence of proteins in blood plasma significantly reduced agglomeration due to the formation of a protective protein corona around the particles. Unlike the previously mentiond protective effect of protein corona, the enzymes pepsin and pancreatin triggered considerable agglomeration of TiO_2 particles in SGF and SIF. Cytotoxicity of TiO_2 was found to depend on the crystalline type of TiO_2 particles tested. The findings contributed to a better understanding of the behaviour of TiO_2-based composites under simulated *in vivo* conditions.

The second follow-up study focused on the formulation and characterization of Pickering oil-in-water emulsions stabilized with pH-responsive carboxylated cellulose nanocrystals (cCNC) in combination with TiO_2 particles, which could serve as platforms for skin photoprotection. The study revealed that Pickering emulsions stabilized by the combination of cCNC and TiO_2 particles can be prepared at pH 3 due to the formation of cCNC-TiO_2 complexes at this pH.

Moreover, it was also demonstrated that, in addition to the layer by layer (LbL) method, the conventional emulsification (CE) method can also be used for the preparation of stable emulsions. Furthermore, emulsions with these particles can be formed at pH 5 when electrolytes ($CaCl_2$ and NaCl) are added. Although LbL method could produce emulsions with $CaCl_2$ and NaCl, the CE method only produced emulsions with $CaCl_2$. The study resulted in the preparation of an effective and ecological product with possible application in UV protection.

The last part of this thesis concentrated on the development of three polyaniline conducting systems based on cellulose nanoparticles, nanocrystals (CNC) and nanofibers (CNF). The initial step involved synthesis and characterization of PANI colloidal particles *via* oxidative polymerization of aniline hydrochloride in the presence of CNC or CNF. The created composite particles (PANI/CNC and PANI/CNF) showed interesting biological properties in terms of immunomodulatory effect on macrophages, opening up new avenues for their potential biomedical applications. The prepared composite particles (PANI/CNC or PANI/CNF) were then used to formulate novel Pickering emulsions containing 20 % undecane or an equal amount of capric/caprylic triglyceride oil. The results demonstrated that the biological activity of the composite particles was maintained even in emulsions containing mentioned oils. The physico-chemical properties of the emulsions were influenced by the stabilizing particles (PANI/CNC or PANI/CNF) and the type of oil. The samples also demonstrated high antioxidant activity, implying their potential applications in wound healing. Finaly, conducting thin composite films based on PAN/CNC and PANI/CNF colloidal particles were prepared via the in-situ dispersion polymerization. The conductivity of the resulting eco-friendly composite films was 0.1 and 4.7 S cm^{-1} for PANI/CNC and PANI/CNF films, respectively. The surface properties revealed indicated suitable biological properties of both composites. The composite films demonstrated low antibacterial efficacy against both gram positive and gram negative bacteria, as well as in vitro antioxidation activity. The testing of biological properties demonstarted that the presence of CNC or CNF in the films has no effect on cell proliferation, making them suitable candidates for biomedical fields, particularly in tissue engineering.

10. CONTRIBUTION TO SCIENCE AND PRACTICE

The stability of colloidal systems is a fundamental prerequisite for their use. In this context, one of the key areas of colloid research is the development of new colloid stabilizers. The increasing application of renewable, biodegradable, green materials, which is in the focus of this thesis, has attracted global interest in the drive towards sustainable development. As a result, the thesis deals with the particle-based stabilizers obtained from celluose (CNC and CNF) and their ability to stabilize different types of dispersions and systems derived from them. The most important contributions of the doctoral thesis to science and practice are outlined in the following points:

A novel eco-friendly system for UV protection with potential applications in cosmetic practice has been created. Surfactant-free emulsions with sunscreen properties were prepared by combining pH-responsive carboxylated cellulose nanocrystals (cCNC) with TiO_2 particles. The study demonstrated that Pickering emulsions stabilized by cCNC and TiO_2 particles can be prepared in two ways: layer by layer and conventional emulsification. The study contributed to better understanding of of the factors that influence emulsion formation and stability, which is crucial for their practical applications.

The formulation of these emulsions was only possible thanks to a thorough understanding of the TiO_2 properties gained within the thesis. The study of TiO_2 behaviour in media used for biocopmatibility testing, simulated body fluids, and human blood plasma revealed a significant impact of the media, mainly the presence of proteins on particle agglometarion. Here, the crystalline form of TiO_2 particles, in combination with composition of media, play important role. The form of TiO_2 particles also had significant impact on cytotoxicity. The findings of this study are decisive when considering the safety of TiO_2 in connection with oral and dermal exposure, which is freequent in cosmetics.

The next study included in the thesis significantly contributed to existing knowledge on systems that utilize cellulose combined with conducting polyaniline (PANI). Colloidal PANI dispersions prepared by dispersion polymerization in the presence of cellulose nanocrystals (CNC) or nanofibers (CNF) yielded PANI/CNC and PANI/CNF composites with promising biological properties, including antibacterial and antioxidation activity, as well as immunomodulatory effect on macrophages.

Novel Pickering emulsions containing undecane or capric/caprylic triglyceride oil were successfully formulated using the composite particles synthetized in the previous step. The work confirmed that the biological activity of the particles that stabilized the emulsions was preserved, and that the used oil (capric/caprylic triglyceride) introduced additional benefits to these systems. This approach is interesting for the application of such systems in biomedicine, particularly in the area of wound healing.

Finally, PANI/CNC and PANI/CNF colloids were used to fabricate conducting composite films *via* the *in-situ* dispersion polymerization. The films exhibited conductivity and antioxidation activity, both of which are essential for tissue engineering of electrically conducting tissues (cardiac, nerve). The biological tests showed that the films were not cytotoxic, and allowed cell proliferation comparable to the reference. Overall, this research provided a deeper understanding of the various conducting cellulose-based systems of new generation with interesting tunable properties that can be used in a variety of applications.

REFERENCES

[1] I. Khan, K. Saeed, I. Khan, Nanoparticles: Properties, applications and toxicities, Arab. J. Chem. 12 (2019) 908–931. https://doi.org/10.1016/j.arabjc.2017.05.011.

[2] P.V. Khandve, Nanotechnology for Building Material, Int. J. Basic Appl. Res. 4 (2014) 146–151.

[3] M. Nasrollahzadeh, S.M. Sajadi, M. Sajjadi, Z. Issaabadi, Applications of Nanotechnology in Daily Life, in: Interface Sci. Technol., Elsevier, 2019: pp. 113–143. https://doi.org/10.1016/B978-0-12-813586-0.00004-3.

[4] S. Horikoshi, N. Serpone, Introduction to Nanoparticles, in: S. Horikoshi, N. Serpone (Eds.), Microw. Nanoparticle Synth., Wiley-VCH Verlag GmbH & Co. KGaA, Weinheim, Germany, 2013: pp. 1–24. https://doi.org/10.1002/9783527648122.ch1.

[5] D.R. Boverhof, C.M. Bramante, J.H. Butala, S.F. Clancy, M. Lafranconi, J. West, S.C. Gordon, Comparative assessment of nanomaterial definitions and safety evaluation considerations, Regul. Toxicol. Pharmacol. 73 (2015) 137–150. https://doi.org/10.1016/j.yrtph.2015.06.001.

[6] J. Jeevanandam, A. Barhoum, Y.S. Chan, A. Dufresne, M.K. Danquah, Review on nanoparticles and nanostructured materials: history, sources, toxicity and regulations, Beilstein J. Nanotechnol. 9 (2018) 1050–1074. https://doi.org/10.3762/bjnano.9.98.

[7] J. Catalán, H. Norppa, Safety Aspects of Bio-Based Nanomaterials, Bioengineering. 4 (2017) 94. https://doi.org/10.3390/bioengineering4040094.

[8] K. Heise, E. Kontturi, Y. Allahverdiyeva, T. Tammelin, M.B. Linder, Nonappa, O. Ikkala, Nanocellulose: Recent Fundamental Advances and Emerging Biological and Biomimicking Applications, Adv. Mater. 33 (2021) 2004349. https://doi.org/10.1002/adma.202004349.

[9] D. Trache, A.F. Tarchoun, M. Derradji, T.S. Hamidon, N. Masruchin, N. Brosse, M.H. Hussin, Nanocellulose: From Fundamentals to Advanced Applications, Front. Chem. 8 (2020) 392. https://doi.org/10.3389/fchem.2020.00392.

[10] H. Seddiqi, E. Oliaei, H. Honarkar, J. Jin, L.C. Geonzon, R.G. Bacabac, J. Klein-Nulend, Cellulose and its derivatives: towards biomedical applications, Cellulose. 28 (2021) 1893–1931. https://doi.org/10.1007/s10570-020-03674-w.

[11] R. Zhang, T. Belwal, L. Li, X. Lin, Y. Xu, Z. Luo, Recent advances in polysaccharides stabilized emulsions for encapsulation and delivery of bioactive food ingredients: A review, Carbohydr. Polym. 242 (2020) 116388. https://doi.org/10.1016/j.carbpol.2020.116388.

[12] J. Credou, T. Berthelot, Cellulose: from biocompatible to bioactive material, J. Mater. Chem. B. 2 (2014) 4767–4788. https://doi.org/10.1039/C4TB00431K.

[13] N. Halib, F. Perrone, M. Cemazar, B. Dapas, R. Farra, M. Abrami, G. Chiarappa, G. Forte, F. Zanconati, G. Pozzato, L. Murena, N. Fiotti, R. Lapasin, L. Cansolino, G. Grassi, M. Grassi, Potential Applications of Nanocellulose-Containing Materials in the Biomedical Field, Materials. 10 (2017) 977. https://doi.org/10.3390/ma10080977.

[14] O. Hajlaoui, R. Khiari, L. Ajili, N. Batis, L. Bergaoui, Design and Characterization of Type I Cellulose-Polyaniline Composites from Various Cellulose Sources: A Comparative Study, Chem. Afr. 3 (2020) 783–792. https://doi.org/10.1007/s42250-020-00148-1.

[15] J. Henschen, M. Ek, J. Illergård, D. Li, E. Cranston, Wood Chemistry and Pulp Technology, KTH, bioteknologi och hälsa (CBH) Skolan för kemi, Bio-based preparation of nanocellulose and functionalization using polyelectrolytes, 2019. http://urn.kb.se/resolve?urn=urn:nbn:se:kth:diva-252580 (accessed June 28, 2021).

[16] V.A. Barbash, O.V. Yaschenko, S.V. Alushkin, A.S. Kondratyuk, O.Y. Posudievsky, V.G. Koshechko, The Effect of Mechanochemical Treatment of the Cellulose on Characteristics of Nanocellulose Films, Nanoscale Res. Lett. 11 (2016) 410. https://doi.org/10.1186/s11671-016-1632-1.

[17] N. Lin, A. Dufresne, Nanocellulose in biomedicine: Current status and future prospect, Eur. Polym. J. 59 (2014) 302–325. https://doi.org/10.1016/j.eurpolymj.2014.07.025.

[18] M.P. Illa, S. Adepu, M. Khandelwal, CHAPTER 2 - Industrial-scale fabrication and functionalization of nanocellulose, in: R. Oraon, D. Rawtani, P. Singh, Dr.C.M. Hussain (Eds.), Nanocellulose Mater., Elsevier, 2022: pp. 21–42. https://doi.org/10.1016/B978-0-12-823963-6.00006-5.

[19] V. Thakur, A. Guleria, S. Kumar, S. Sharma, K. Singh, Recent advances in nanocellulose processing, functionalization and applications: a review, Mater. Adv. 2 (2021) 1872–1895. https://doi.org/10.1039/D1MA00049G.

[20] T. Abitbol, A. Rivkin, Y. Cao, Y. Nevo, E. Abraham, T. Ben-Shalom, S. Lapidot, O. Shoseyov, Nanocellulose, a tiny fiber with huge applications, Curr. Opin. Biotechnol. 39 (2016) 76–88. https://doi.org/10.1016/j.copbio.2016.01.002.

[21] N.K. Guimard, N. Gomez, C.E. Schmidt, Conducting polymers in biomedical engineering, Prog. Polym. Sci. 32 (2007) 876–921. https://doi.org/10.1016/j.progpolymsci.2007.05.012.

[22] A. Meftahi, P. Samyn, S.A. Geravand, R. Khajavi, S. Alibkhshi, M. Bechelany, A. Barhoum, Nanocelluloses as skin biocompatible materials for skincare, cosmetics, and healthcare: Formulations, regulations, and emerging applications, Carbohydr. Polym. 278 (2022) 118956. https://doi.org/10.1016/j.carbpol.2021.118956.

[23] Cellulose Lab | Nanocellulose, Cellulose NanoCrystal (CNC or NCC), Cellulose Nanofibrils (CNF) and Bacterial Cellulose (BC) Supplier - Provide the most diversified nanocellulose products / cellulose nanomaterials in the market, Cellul. Lab Nanocellulose Cellul. NanoCrystal CNC NCC Cellul. Nanofibrils CNF Bact. Cellul. BC Supplier. (n.d.). https://www.celluloselab.com/ (accessed October 2, 2021).

[24] S. Hashmi, I.A. Choudhury, eds., Encyclopedia of renewable and sustainable materials, Elsevier, Amsterdam Boston Heidelberg London New York Oxford Paris San Diego San Francisco Singapore Sydney Tokyo, 2020.

[25] T. Abitbol, E. Kloser, D. Gray, Estimation of the surface sulfur content of cellulose nanocrystals prepared by sulfuric acid hydrolysis, Cellulose. 20 (2013). https://doi.org/10.1007/s10570-013-9871-0.

[26] D. Saidane, E. Perrin, F. Cherhal, F. Guellec, I. Capron, Some modification of cellulose nanocrystals for functional Pickering emulsions, Philos. Trans. R. Soc. Math. Phys. Eng. Sci. 374 (2016) 20150139. https://doi.org/10.1098/rsta.2015.0139.

[27] T. Saito, Y. Okita, T.T. Nge, J. Sugiyama, A. Isogai, TEMPO-mediated oxidation of native cellulose: Microscopic analysis of fibrous fractions in the oxidized products, Carbohydr. Polym. 65 (2006) 435–440. https://doi.org/10.1016/j.carbpol.2006.01.034.

[28] L. Zhou, N. Li, J. Shu, Y. Liu, K. Wang, X. Cui, Y. Yuan, B. Ding, Y. Geng, Z. Wang, Y. Duan, J. Zhang, One-Pot Preparation of Carboxylated Cellulose Nanocrystals and Their Liquid Crystalline Behaviors, ACS Sustain. Chem. Eng. 6 (2018) 12403–12410. https://doi.org/10.1021/acssuschemeng.8b02926.

[29] P. Jutakridsada, S. Theerakulpisut, M. Sillanpää, K. Kamwilaisak, Characterisation of carboxylate nanocrystal cellulose /silver nanoparticles from eucalyptus pulp and its antitumour activity, In Review, 2021. https://doi.org/10.21203/rs.3.rs-331735/v1.

[30] A.C.W. Leung, S. Hrapovic, E. Lam, Y. Liu, K.B. Male, K.A. Mahmoud, J.H.T. Luong, Characteristics and Properties of Carboxylated Cellulose Nanocrystals Prepared from a Novel One-Step Procedure, Small. 7 (2011) 302–305. https://doi.org/10.1002/smll.201001715.

[31] M. Marwanto, M.I. Maulana, F. Febrianto, N.J. Wistara, S. Nikmatin, N. Masruchin, L.H. Zaini, S.-H. Lee, N.-H. Kim, Effect of Oxidation Time on the Properties of Cellulose Nanocrystals Prepared from Balsa and Kapok Fibers Using Ammonium Persulfate, Polymers. 13 (2021) 1894. https://doi.org/10.3390/polym13111894.

[32] H.P.S. Abdul Khalil, Y. Davoudpour, Md.N. Islam, A. Mustapha, K. Sudesh, R. Dungani, M. Jawaid, Production and modification of nanofibrillated cellulose using various mechanical processes: A review,

Carbohydr. Polym. 99 (2014) 649–665. https://doi.org/10.1016/j.carbpol.2013.08.069.

[33] P. Chawla, I. Bajaj, S. Survase, R. Singhal, Microbial Cellulose: Fermentative Production and Applications, Food Technol. Biotechnol. 47 (2009) 107–124.

[34] M. Nasir, R. Hashim, O. Sulaiman, M. Asim, 11 - Nanocellulose: Preparation methods and applications, in: M. Jawaid, S. Boufi, A.K. H.p.s. (Eds.), Cellul.-Reinf. Nanofibre Compos., Woodhead Publishing, 2017: pp. 261–276. https://doi.org/10.1016/B978-0-08-100957-4.00011-5.

[35] M.M. Amiji, T.J. Cook, W.C. Mobley, McGraw-Hill Companies, AccessPharmacy (Online service), Applied physical pharmacy, 2014. http://www.vlebooks.com/vleweb/product/openreader?id=EdgeHill&isbn= 9780071804424 (accessed May 15, 2021).

[36] T.F. Tadros, Rheology of Dispersions: Principles and Applications, Wiley-VCH Verlag GmbH & Co. KGaA, Weinheim, Germany, 2010. https://doi.org/10.1002/9783527631568.

[37] C. Manoharan, A. Basarkar, J. Singh, Various Pharmaceutical Disperse Systems, in: A.K. Kulshreshtha, O.N. Singh, G.M. Wall (Eds.), Pharm. Suspens., Springer New York, New York, NY, 2010: pp. 1–37. https://doi.org/10.1007/978-1-4419-1087-5_1.

[38] M.E. Aulton, ed., Pharmaceutics: the science of dosage form design, 2nd ed, Churchill Livingstone, Edinburgh [u.a.l], 2002.

[39] L.L. Schramm, Emulsions, foams, and suspensions: fundamentals and applications, Wiley-VCH, Weinheim, 2005.

[40] T.F. Tadros, Surfactants, Industrial Applications, in: Encycl. Phys. Sci. Technol., Elsevier, 2003: pp. 423–438. https://doi.org/10.1016/B0-12-227410-5/00758-4.

[41] Y. Yang, Z. Fang, X. Chen, W. Zhang, Y. Xie, Y. Chen, Z. Liu, W. Yuan, An Overview of Pickering Emulsions: Solid-Particle Materials, Classification, Morphology, and Applications, Front. Pharmacol. 8 (2017) 287. https://doi.org/10.3389/fphar.2017.00287.

[42] B. Liu, X. Hu, Hollow Micro- and Nanomaterials: Synthesis and Applications, in: Adv. Nanomater. Pollut. Sens. Environ. Catal., Elsevier, 2020: pp. 1–38. https://doi.org/10.1016/B978-0-12-814796-2.00001-0.

[43] S. Akbari, Emulsion types, stability mechanisms and rheology: A review, (2018).

[44] D.J. McClements, E.A. Decker, J. Weiss, Emulsion-Based Delivery Systems for Lipophilic Bioactive Components, J. Food Sci. 72 (2007) R109–R124. https://doi.org/10.1111/j.1750-3841.2007.00507.x.

[45] Barkat Ali Khan, Basics of pharmaceutical emulsions: A review, Afr. J. Pharm. Pharmacol. 5 (2011). https://doi.org/10.5897/AJPP11.698.

[46] C.P. Whitby, Nanoparticles at Fluid Interfaces: From Surface Properties to Biomedical Applications, in: Compr. Nanosci. Nanotechnol., Elsevier, 2019: pp. 127–146. https://doi.org/10.1016/B978-0-12-803581-8.10459-X.

[47] J. Bergfreund, S. Siegenthaler, V. Lutz-Bueno, P. Bertsch, P. Fischer, Surfactant Adsorption to Different Fluid Interfaces, Langmuir. 37 (2021) 6722–6727. https://doi.org/10.1021/acs.langmuir.1c00668.

[48] I. Nursakinah, A.R. Ismail, M.Y. Rahimi, A.B. Idris, Evaluation of HLB values of mixed non-ionic surfactants on the stability of oil-in-water emulsion system, in: Selangor, Malaysia, 2013: pp. 850–856. https://doi.org/10.1063/1.4858761.

[49] C. Li, Y. Li, P. Sun, C. Yang, Pickering emulsions stabilized by native starch granules, Colloids Surf. Physicochem. Eng. Asp. 431 (2013) 142–149. https://doi.org/10.1016/j.colsurfa.2013.04.025.

[50] D. Marku, M. Wahlgren, M. Rayner, M. Sjöö, A. Timgren, Characterization of starch Pickering emulsions for potential applications in topical formulations, Int. J. Pharm. 428 (2012) 1–7. https://doi.org/10.1016/j.ijpharm.2012.01.031.

[51] B. Horváth, S. Pál, A. Széchenyi, Preparation and in vitro diffusion study of essential oil Pickering emulsions stabilized by silica nanoparticles, Flavour Fragr. J. 33 (2018) 385–396. https://doi.org/10.1002/ffj.3463.

[52] P.E. Ruiz-Rodriguez, D. Meshulam, U. Lesmes, Characterization of Pickering O/W Emulsions Stabilized by Silica Nanoparticles and Their Responsiveness to In vitro Digestion Conditions, Food Biophys. 9 (2014) 406–415. https://doi.org/10.1007/s11483-014-9346-3.

[53] F. Huang, Y. Liang, Y. He, On the Pickering emulsions stabilized by calcium carbonate particles with various morphologies, Colloids Surf. Physicochem. Eng. Asp. 580 (2019) 123722. https://doi.org/10.1016/j.colsurfa.2019.123722.

[54] J. Marto, A. Nunes, A.M. Martins, J. Carvalheira, P. Prazeres, L. Gonçalves, A. Marques, A. Lucas, H.M. Ribeiro, Pickering Emulsions Stabilized by Calcium Carbonate Particles: A New Topical Formulation, Cosmetics. 7 (2020) 62. https://doi.org/10.3390/cosmetics7030062.

[55] P.A. Demina, T.V. Bukreeva, Pickering Emulsion Stabilized by Commercial Titanium Dioxide Nanoparticles in the Form of Rutile and Anatase, Nanotechnologies Russ. 13 (2018) 425–429. https://doi.org/10.1134/S1995078018040043.

[56] M. Nawaz, W. Miran, J. Jang, D.S. Lee, Stabilization of Pickering emulsion with surface-modified titanium dioxide for enhanced photocatalytic degradation of Direct Red 80, Catal. Today. 282 (2017) 38–47. https://doi.org/10.1016/j.cattod.2016.02.017.

[57] S. Stiller, H. Gers-Barlag, M. Lergenmueller, F. Pflücker, J. Schulz, K.P. Wittern, R. Daniels, Investigation of the stability in emulsions stabilized with different surface modified titanium dioxides, Colloids Surf.

Physicochem. Eng. Asp. 232 (2004) 261–267. https://doi.org/10.1016/j.colsurfa.2003.11.003.

[58] S. Fujisawa, E. Togawa, K. Kuroda, Nanocellulose-stabilized Pickering emulsions and their applications, Sci. Technol. Adv. Mater. 18 (2017) 959–971. https://doi.org/10.1080/14686996.2017.1401423.

[59] M. Rayner, P. Dejmek, Engineering aspects of food emulsification and homogenization, 2015. http://www.crcnetbase.com/isbn/9781466580442 (accessed July 20, 2021).

[60] E. Dickinson, Use of nanoparticles and microparticles in the formation and stabilization of food emulsions, Trends Food Sci. Technol. 24 (2012) 4–12. https://doi.org/10.1016/j.tifs.2011.09.006.

[61] Y. Chevalier, M.-A. Bolzinger, Emulsions stabilized with solid nanoparticles: Pickering emulsions, Colloids Surf. Physicochem. Eng. Asp. 439 (2013) 23–34. https://doi.org/10.1016/j.colsurfa.2013.02.054.

[62] J. Tang, P.J. Quinlan, K.C. Tam, Stimuli-responsive Pickering emulsions: recent advances and potential applications, Soft Matter. 11 (2015) 3512–3529. https://doi.org/10.1039/C5SM00247H.

[63] J. Wu, G.-H. Ma, Recent Studies of Pickering Emulsions: Particles Make the Difference, Small. 12 (2016) 4633–4648. https://doi.org/10.1002/smll.201600877.

[64] M. Zembyla, B.S. Murray, A. Sarkar, Water-in-oil emulsions stabilized by surfactants, biopolymers and/or particles: a review, Trends Food Sci. Technol. 104 (2020) 49–59. https://doi.org/10.1016/j.tifs.2020.07.028.

[65] M. Rayner, D. Marku, M. Eriksson, M. Sjöö, P. Dejmek, M. Wahlgren, Biomass-based particles for the formulation of Pickering type emulsions in food and topical applications, Colloids Surf. Physicochem. Eng. Asp. 458 (2014) 48–62. https://doi.org/10.1016/j.colsurfa.2014.03.053.

[66] D. Guzey, D.J. McClements, Formation, stability and properties of multilayer emulsions for application in the food industry, Adv. Colloid Interface Sci. 128–130 (2006) 227–248. https://doi.org/10.1016/j.cis.2006.11.021.

[67] D.J. McClements, C.E. Gumus, Natural emulsifiers — Biosurfactants, phospholipids, biopolymers, and colloidal particles: Molecular and physicochemical basis of functional performance, Adv. Colloid Interface Sci. 234 (2016) 3–26. https://doi.org/10.1016/j.cis.2016.03.002.

[68] E.M. Shchukina, D.G. Shchukin, Layer-by-layer coated emulsion microparticles as storage and delivery tool, Curr. Opin. Colloid Interface Sci. 17 (2012) 281–289. https://doi.org/10.1016/j.cocis.2012.06.003.

[69] L. Fu, Q. Ma, K. Liao, J. An, J. Bai, Y. He, Application of Pickering emulsion in oil drilling and production, Nanotechnol. Rev. 11 (2021) 26–39. https://doi.org/10.1515/ntrev-2022-0003.

[70] D. Gonzalez Ortiz, C. Pochat-Bohatier, J. Cambedouzou, M. Bechelany, P. Miele, Current Trends in Pickering Emulsions: Particle Morphology and

Applications, Engineering. 6 (2020) 468–482. https://doi.org/10.1016/j.eng.2019.08.017.

[71] M. Xiao, A. Xu, T. Zhang, L. Hong, Tailoring the Wettability of Colloidal Particles for Pickering Emulsions via Surface Modification and Roughness, Front. Chem. 6 (2018) 225. https://doi.org/10.3389/fchem.2018.00225.

[72] C. Albert, M. Beladjine, N. Tsapis, E. Fattal, F. Agnely, N. Huang, Pickering emulsions: Preparation processes, key parameters governing their properties and potential for pharmaceutical applications, J. Controlled Release. 309 (2019) 302–332. https://doi.org/10.1016/j.jconrel.2019.07.003.

[73] Q. Guo, Progress in the preparation, stability and functional applications of Pickering emulsion, IOP Conf. Ser. Earth Environ. Sci. 639 (2021) 012028. https://doi.org/10.1088/1755-1315/639/1/012028.

[74] Z. Sun, X. Yan, Y. Xiao, L. Hu, M. Eggersdorfer, D. Chen, Z. Yang, D.A. Weitz, Pickering emulsions stabilized by colloidal surfactants: Role of solid particles, Particuology. 64 (2022) 153–163. https://doi.org/10.1016/j.partic.2021.06.004.

[75] W. Li, B. Jiao, S. Li, S. Faisal, A. Shi, W. Fu, Y. Chen, Q. Wang, Recent Advances on Pickering Emulsions Stabilized by Diverse Edible Particles: Stability Mechanism and Applications, Front. Nutr. 9 (2022) 864943. https://doi.org/10.3389/fnut.2022.864943.

[76] B.P. Binks, S.O. Lumsdon, Catastrophic Phase Inversion of Water-in-Oil Emulsions Stabilized by Hydrophobic Silica, Langmuir. 16 (2000) 2539–2547. https://doi.org/10.1021/la991081j.

[77] M. Sarker, E2 protein nanocage as a pickering emulsifier and its applications, Nanyang Technological University, 2018. https://doi.org/10.32657/10356/73892.

[78] I. Capron, O.J. Rojas, R. Bordes, Behavior of nanocelluloses at interfaces, Curr. Opin. Colloid Interface Sci. 29 (2017) 83–95. https://doi.org/10.1016/j.cocis.2017.04.001.

[79] S. Lam, K.P. Velikov, O.D. Velev, Pickering stabilization of foams and emulsions with particles of biological origin, Curr. Opin. Colloid Interface Sci. 19 (2014) 490–500. https://doi.org/10.1016/j.cocis.2014.07.003.

[80] M. Andresen, P. Stenius, Water-in-oil Emulsions Stabilized by Hydrophobized Microfibrillated Cellulose, J. Dispers. Sci. Technol. 28 (2007) 837–844. https://doi.org/10.1080/01932690701341827.

[81] C. Wen, Q. Yuan, H. Liang, F. Vriesekoop, Preparation and stabilization of d-limonene Pickering emulsions by cellulose nanocrystals, Carbohydr. Polym. 112 (2014) 695–700. https://doi.org/10.1016/j.carbpol.2014.06.051.

[82] V. Mikulcová, R. Bordes, V. Kašpárková, On the preparation and antibacterial activity of emulsions stabilized with nanocellulose particles, Food Hydrocoll. 61 (2016) 780–792. https://doi.org/10.1016/j.foodhyd.2016.06.031.

[83] V. Mikulcová, R. Bordes, A. Minařík, V. Kašpárková, Pickering oil-in-water emulsions stabilized by carboxylated cellulose nanocrystals – Effect of the pH, Food Hydrocoll. 80 (2018) 60–67. https://doi.org/10.1016/j.foodhyd.2018.01.034.

[84] L. Bai, S. Lv, W. Xiang, S. Huan, D.J. McClements, O.J. Rojas, Oil-in-water Pickering emulsions via microfluidization with cellulose nanocrystals: 1. Formation and stability, Food Hydrocoll. 96 (2019) 699–708. https://doi.org/10.1016/j.foodhyd.2019.04.038.

[85] I. Capron, B. Cathala, Surfactant-Free High Internal Phase Emulsions Stabilized by Cellulose Nanocrystals, Biomacromolecules. 14 (2013) 291–296. https://doi.org/10.1021/bm301871k.

[86] F. Cherhal, F. Cousin, I. Capron, Structural Description of the Interface of Pickering Emulsions Stabilized by Cellulose Nanocrystals, Biomacromolecules. 17 (2016) 496–502. https://doi.org/10.1021/acs.biomac.5b01413.

[87] A.A.D. Meirelles, A.L.R. Costa, R.L. Cunha, Cellulose nanocrystals from ultrasound process stabilizing O/W Pickering emulsion, Int. J. Biol. Macromol. 158 (2020) 75–84. https://doi.org/10.1016/j.ijbiomac.2020.04.185.

[88] C. Miao, M. Tayebi, W.Y. Hamad, Investigation of the formation mechanisms in high internal phase Pickering emulsions stabilized by cellulose nanocrystals, Philos. Trans. R. Soc. Math. Phys. Eng. Sci. 376 (2018) 20170039. https://doi.org/10.1098/rsta.2017.0039.

[89] S. Varanasi, L. Henzel, L. Mendoza, R. Prathapan, W. Batchelor, R. Tabor, G. Garnier, Pickering Emulsions Electrostatically Stabilized by Cellulose Nanocrystals, Front. Chem. 6 (2018). https://doi.org/10.3389/fchem.2018.00409.

[90] T. Winuprasith, M. Suphantharika, Microfibrillated cellulose from mangosteen (Garcinia mangostana L.) rind: Preparation, characterization, and evaluation as an emulsion stabilizer, Food Hydrocoll. 32 (2013) 383–394. https://doi.org/10.1016/j.foodhyd.2013.01.023.

[91] K. Xhanari, K. Syverud, P. Stenius, Emulsions Stabilized by Microfibrillated Cellulose: The Effect of Hydrophobization, Concentration and O/W Ratio, J. Dispers. Sci. Technol. 32 (2011) 447–452. https://doi.org/10.1080/01932691003658942.

[92] W. Mitbumrung, S. Jain, T. Winuprasith, Properties and stability of Pickering emulsions stabilized by nanofibrillated mangosteen cellulose: Impact of oil type and emulsifier concentration, (2020) 9.

[93] H. Yan, X. Chen, H. Song, J. Li, Y. Feng, Z. Shi, X. Wang, Q. Lin, Synthesis of bacterial cellulose and bacterial cellulose nanocrystals for their applications in the stabilization of olive oil pickering emulsion, Food Hydrocoll. 72 (2017) 127–135. https://doi.org/10.1016/j.foodhyd.2017.05.044.

[94] P. Paximada, E. Tsouko, N. Kopsahelis, A.A. Koutinas, I. Mandala, Bacterial cellulose as stabilizer of o/w emulsions, Food Hydrocoll. 53 (2016) 225–232. https://doi.org/10.1016/j.foodhyd.2014.12.003.

[95] W. Fu, Y. Liu, C. Yang, W.H. Wang, M. Wang, Y.Y. Jia, Stabilization of Pickering Emulsions by Bacterial Cellulose Nanofibrils, Key Eng. Mater. 645–646 (2015) 1247–1254. https://doi.org/10.4028/www.scientific.net/KEM.645-646.1247.

[96] I. Kalashnikova, H. Bizot, B. Cathala, I. Capron, New Pickering Emulsions Stabilized by Bacterial Cellulose Nanocrystals, Langmuir. 27 (2011) 7471–7479. https://doi.org/10.1021/la200971f.

[97] D. Martins, A. Fontão, F. Dourado, M. Gama, Bacterial cellulose as a stabilizer for oil-in-water emulsions, (2018) 2.

[98] X. Zhai, D. Lin, D. Liu, X. Yang, Emulsions stabilized by nanofibers from bacterial cellulose: New potential food-grade Pickering emulsions, Food Res. Int. 103 (2018) 12–20. https://doi.org/10.1016/j.foodres.2017.10.030.

[99] C. Bordes, M. Bolzinger, M. El Achak, F. Pirot, D. Arquier, G. Agusti, Y. Chevalier, Formulation of Pickering emulsions for the development of surfactant-free sunscreen creams, Int. J. Cosmet. Sci. 43 (2021) 432–445. https://doi.org/10.1111/ics.12709.

[100] J. Marto, A. Nunes, A.M. Martins, J. Carvalheira, P. Prazeres, L. Gonçalves, A. Marques, A. Lucas, H.M. Ribeiro, Pickering Emulsions Stabilized by Calcium Carbonate Particles: A New Topical Formulation, Cosmetics. 7 (2020) 62. https://doi.org/10.3390/cosmetics7030062.

[101] M. Sjoo, M. Rayner, M. Wahlgren, Particle-stabilized Emulsions, in: M. Rayner, P. Dejmek (Eds.), Eng. Asp. Food Emuls. Homog., CRC Press, 2015: pp. 101–122. https://doi.org/10.1201/b18436-6.

[102] J. Marto, L.F. Gouveia, L. Gonçalves, B.G. Chiari-Andréo, V. Isaac, P. Pinto, E. Oliveira, A.J. Almeida, H.M. Ribeiro, Design of novel starch-based Pickering emulsions as platforms for skin photoprotection, J. Photochem. Photobiol. B. 162 (2016) 56–64. https://doi.org/10.1016/j.jphotobiol.2016.06.026.

[103] C.C. Daher, I.S. Fontes, R. de O. Rodrigues, G.A. de B. Damasceno, D. dos S. Soares, C.F.S. Aragão, A.P.B. Gomes, M. Ferrari, Development of O/W emulsions containing Euterpe oleracea extract and evaluation of photoprotective efficacy, Braz. J. Pharm. Sci. 50 (2014) 639–652. https://doi.org/10.1590/S1984-82502014000300024.

[104] J. Marto, A. Ascenso, L.M. Gonçalves, L.F. Gouveia, P. Manteigas, P. Pinto, E. Oliveira, A.J. Almeida, H.M. Ribeiro, Melatonin-based pickering emulsion for skin's photoprotection, Drug Deliv. 23 (2016) 1594–1607. https://doi.org/10.3109/10717544.2015.1128496.

[105] S.L. Schneider, H.W. Lim, A review of inorganic UV filters zinc oxide and titanium dioxide, Photodermatol. Photoimmunol. Photomed. 35 (2019) 442–446. https://doi.org/10.1111/phpp.12439.

[106] J. Frelichowska, M.-A. Bolzinger, J.-P. Valour, H. Mouaziz, J. Pelletier, Y. Chevalier, Pickering w/o emulsions: Drug release and topical delivery, Int. J. Pharm. 368 (2009) 7–15. https://doi.org/10.1016/j.ijpharm.2008.09.057.

[107] D. Lee, D. Park, K. Shin, H.M. Seo, H. Lee, Y. Choi, J.W. Kim, ZnO nanoparticles-laden cellulose nanofibers-armored Pickering emulsions with improved UV protection and water resistance, J. Ind. Eng. Chem. 96 (2021) 219–225. https://doi.org/10.1016/j.jiec.2021.01.018.

[108] D. Terescenco, N. Hucher, C. Picard, G. Savary, Sensory perception of textural properties of cosmetic Pickering emulsions, Int. J. Cosmet. Sci. 42 (2020) 198–207. https://doi.org/10.1111/ics.12604.

[109] Y. Kameya, H. Yabe, Optical and Superhydrophilic Characteristics of TiO2 Coating with Subwavelength Surface Structure Consisting of Spherical Nanoparticle Aggregates, Coatings. 9 (2019) 547. https://doi.org/10.3390/coatings9090547.

[110] J. Wang, Y. Sun, M. Yu, X. Lu, S. Komarneni, C. Yang, Emulsions stabilized by highly hydrophilic TiO2 nanoparticles via van der Waals attraction, J. Colloid Interface Sci. 589 (2021) 378–387. https://doi.org/10.1016/j.jcis.2021.01.011.

[111] S. Peito, D. Peixoto, I. Ferreira-Faria, A. Margarida Martins, H. Margarida Ribeiro, F. Veiga, J. Marto, A. Cláudia Paiva-Santos, Nano- and microparticle-stabilized Pickering emulsions designed for topical therapeutics and cosmetic applications, Int. J. Pharm. 615 (2022) 121455. https://doi.org/10.1016/j.ijpharm.2022.121455.

[112] E. Ukaji, T. Furusawa, M. Sato, N. Suzuki, The effect of surface modification with silane coupling agent on suppressing the photo-catalytic activity of fine TiO2 particles as inorganic UV filter, Appl. Surf. Sci. 254 (2007) 563–569. https://doi.org/10.1016/j.apsusc.2007.06.061.

[113] V.S. Saji, ed., Corrosion protection and control using nanomaterials, Woodhead Publ, Oxford, 2012.

[114] Faris Yilmaz, Conducting Polymers., 2016. https://www.doabooks.org/doab?func=fulltext&rid=36560 (accessed June 15, 2021).

[115] H. Shirakawa, E.J. Louis, A.G. MacDiarmid, C.K. Chiang, A.J. Heeger, Synthesis of electrically conducting organic polymers: halogen derivatives of polyacetylene, (CH) x, J. Chem. Soc. Chem. Commun. (1977) 578. https://doi.org/10.1039/c39770000578.

[116] S. Nambiar, J.T.W. Yeow, Conductive polymer-based sensors for biomedical applications, Biosens. Bioelectron. 26 (2011) 1825–1832. https://doi.org/10.1016/j.bios.2010.09.046.

[117] N. K, C.S. Rout, Conducting polymers: a comprehensive review on recent advances in synthesis, properties and applications, RSC Adv. 11 (2021) 5659–5697. https://doi.org/10.1039/D0RA07800J.

[118] R. Kumar, S. Singh, B.C. Yadav, Conducting Polymers: Synthesis, Properties and Applications, 2 (2015) 15.

[119] T.-H. Le, Y. Kim, H. Yoon, Electrical and Electrochemical Properties of Conducting Polymers, Polymers. 9 (2017) 150. https://doi.org/10.3390/polym9040150.

[120] J. Tsukamoto, Recent advances in highly conductive polyacetylene, Adv. Phys. 41 (1992) 509–546. https://doi.org/10.1080/00018739200101543.

[121] J. Tsukamoto, A. Takahashi, K. Kawasaki, Structure and Electrical Properties of Polyacetylene Yielding a Conductivity of 105 S/cm, Jpn. J. Appl. Phys. 29 (1990) 125. https://doi.org/10.1143/JJAP.29.125.

[122] S.Y. Kim, H.-K. Song, Conducting Polymers with Functional Dopants and their Applications in Energy, Environmental Technology, and Nanotechnology, Clean Technol. 21 (2015) 12–21. https://doi.org/10.7464/ksct.2015.21.1.012.

[123] P. Bober, P. Humpolíček, J. Pacherník, J. Stejskal, T. Lindfors, Conducting polyaniline based cell culture substrate for embryonic stem cells and embryoid bodies, RSC Adv. 5 (2015) 50328–50335. https://doi.org/10.1039/C5RA07504A.

[124] M. Šišáková, Y. Asaumi, M. Uda, M. Seike, K. Oyama, S. Higashimoto, T. Hirai, Y. Nakamura, S. Fujii, Dodecyl sulfate-doped polypyrrole derivative grains as a light-responsive liquid marble stabilizer, Polym. J. 52 (2020) 589–599. https://doi.org/10.1038/s41428-020-0307-z.

[125] R. Boddula, P. Srinivasan, Emeraldine Base Form of Polyaniline Nanofibers as New, Economical, Green, and Efficient Catalyst for Synthesis of Z - Aldoximes, J. Catal. 2014 (2014) 1–6. https://doi.org/10.1155/2014/515428.

[126] Zh.A. Boeva, V.G. Sergeyev, Polyaniline: Synthesis, properties, and application, Polym. Sci. Ser. C. 56 (2014) 144–153. https://doi.org/10.1134/S1811238214010032.

[127] P.M. Visakh, Polyaniline-Based Blends, Composites, and Nanocomposites, in: Polyaniline Blends Compos. Nanocomposites, Elsevier, 2018: pp. 1–22. https://doi.org/10.1016/B978-0-12-809551-5.00001-1.

[128] R. Bagherzadeh, M. Gorji, M.S. Sorayani Bafgi, N. Saveh-Shemshaki, Electrospun conductive nanofibers for electronics, in: Electrospun Nanofibers, Elsevier, 2017: pp. 467–519. https://doi.org/10.1016/B978-0-08-100907-9.00018-0.

[129] D.K. Bandgar, G.D. Khuspe, R.C. Pawar, C.S. Lee, V.B. Patil, Facile and novel route for preparation of nanostructured polyaniline (PANi) thin films, Appl. Nanosci. 4 (2014) 27–36. https://doi.org/10.1007/s13204-012-0175-8.

[130] F. de Salas, I. Pardo, H.J. Salavagione, P. Aza, E. Amougi, J. Vind, A.T. Martínez, S. Camarero, Advanced Synthesis of Conductive Polyaniline Using Laccase as Biocatalyst, PLOS ONE. 11 (2016) e0164958. https://doi.org/10.1371/journal.pone.0164958.

[131]J. Stejskal, Colloidal dispersions of conducting polymers, J. Polym. Mater. 18 (2001) 225–258.

[132]Y. Wu, J. Wang, B. Ou, S. Zhao, Z. Wang, S. Wang, Electrochemical Preparation of Polyaniline Nanowires with the Used Electrolyte Solution Treated with the Extraction Process and Their Electrochemical Performance, Nanomaterials. 8 (2018) 103. https://doi.org/10.3390/nano8020103.

[133]J. Stejskal, M. Trchová, P. Bober, P. Humolíček, V. Kašpárková, I. Sapurina, M.A. Shishov, M. Varga, Conducting Polymers: Polyaniline: CONDUCTING POLYMERS: POLYANILINE, in: John Wiley & Sons, Inc. (Ed.), Encycl. Polym. Sci. Technol., John Wiley & Sons, Inc., Hoboken, NJ, USA, 2015: pp. 1–44. https://doi.org/10.1002/0471440264.pst640.

[134]J. Stejskal, R.G. Gilbert, Polyaniline. Preparation of a conducting polymer(IUPAC Technical Report), Pure Appl. Chem. 74 (2002) 857–867. https://doi.org/10.1351/pac200274050857.

[135]B.-J. Kim, S.-G. Oh, M.-G. Han, S.-S. Im, Synthesis and characterization of polyaniline nanoparticles in SDS micellar solutions, Synth. Met. 122 (2001) 297–304. https://doi.org/10.1016/S0379-6779(00)00304-0.

[136]B.-J. Kim, S.-G. Oh, M.-G. Han, S.-S. Im, Preparation of Polyaniline Nanoparticles in Micellar Solutions as Polymerization Medium, Langmuir. 16 (2000) 5841–5845. https://doi.org/10.1021/la9915320.

[137]D. Han, Y. Chu, L. Yang, Y. Liu, Z. Lv, Reversed micelle polymerization: a new route for the synthesis of DBSA–polyaniline nanoparticles, Colloids Surf. Physicochem. Eng. Asp. 259 (2005) 179–187. https://doi.org/10.1016/j.colsurfa.2005.02.017.

[138]F.X. Perrin, T.A. Phan, D.L. Nguyen, Preparation and characterization of polyaniline in reversed micelles of decylphosphonic acid for active corrosion protection coatings, Eur. Polym. J. 66 (2015) 253–265. https://doi.org/10.1016/j.eurpolymj.2015.01.052.

[139]M. Antonietti, R. Basten, S. Lohmann, Polymerization in microemulsions — a new approach to ultrafine, highly functionalized polymer dispersions, Macromol. Chem. Phys. 196 (1995) 441–466. https://doi.org/10.1002/macp.1995.021960201.

[140]P.J. Kinlen, J. Liu, Y. Ding, C.R. Graham, E.E. Remsen, Emulsion Polymerization Process for Organically Soluble and Electrically Conducting Polyaniline, Macromolecules. 31 (1998) 1735–1744. https://doi.org/10.1021/ma971430l.

[141]R. Cruz-Silva, A. Escamilla, M.E. Nicho, G. Padron, A. Ledezma-Perez, E. Arias-Marin, I. Moggio, J. Romero-Garcia, Enzymatic synthesis of pH-responsive polyaniline colloids by using chitosan as steric stabilizer, Eur. Polym. J. 43 (2007) 3471–3479. https://doi.org/10.1016/j.eurpolymj.2007.05.027.

[142] J. Stejskal, I. Sapurina, M. Trchová, Polyaniline nanostructures and the role of aniline oligomers in their formation, Prog. Polym. Sci. 35 (2010) 1420–1481. https://doi.org/10.1016/j.progpolymsci.2010.07.006.

[143] I. Sapurina, J. Stejskal, The mechanism of the oxidative polymerization of aniline and the formation of supramolecular polyaniline structures, Polym. Int. 57 (2008) 1295–1325. https://doi.org/10.1002/pi.2476.

[144] I.Yu. Sapurina, V.I. Frolov, B.M. Shabsel's, J. Stejskal, A Conducting Composite of Polyaniline and Wood, Russ. J. Appl. Chem. 76 (2003) 835–839. https://doi.org/10.1023/A:1026050428908.

[145] M. Atobe, A.-N. Chowdhury, T. Fuchigami, T. Nonaka, Preparation of conducting polyaniline colloids under ultrasonication, Ultrason. Sonochem. 10 (2003) 77–80. https://doi.org/10.1016/S1350-4177(02)00121-9.

[146] J. Stejskal, Conducting polymer hydrogels, Chem. Pap. 71 (2017) 269–291. https://doi.org/10.1007/s11696-016-0072-9.

[147] S. Zaghlol, W.A. Amer, M.H. Shaaban, M.M. Ayad, P. Bober, J. Stejskal, Conducting macroporous polyaniline/poly(vinyl alcohol) aerogels for the removal of chromium(VI) from aqueous media, Chem. Pap. 74 (2020) 3183–3193. https://doi.org/10.1007/s11696-020-01151-z.

[148] P. Humpolíček, K.A. Radaszkiewicz, Z. Capáková, J. Pacherník, P. Bober, V. Kašpárková, P. Rejmontová, M. Lehocký, P. Ponížil, J. Stejskal, Polyaniline cryogels: Biocompatibility of novel conducting macroporous material, Sci. Rep. 8 (2018) 135. https://doi.org/10.1038/s41598-017-18290-1.

[149] Z. Li, L. Gong, Research Progress on Applications of Polyaniline (PANI) for Electrochemical Energy Storage and Conversion, Materials. 13 (2020) 548. https://doi.org/10.3390/ma13030548.

[150] N. Ezzati, E. Asadi, R.M. Leblanc, M.H. Ezzati, S.K. Sharma, Other Applications of Polyaniline-Based Blends, Composites, and Nanocomposites, in: Polyaniline Blends Compos. Nanocomposites, Elsevier, 2018: pp. 279–303. https://doi.org/10.1016/B978-0-12-809551-5.00011-4.

[151] E.N. Zare, P. Makvandi, B. Ashtari, F. Rossi, A. Motahari, G. Perale, Progress in Conductive Polyaniline-Based Nanocomposites for Biomedical Applications: A Review, J. Med. Chem. 63 (2020) 1–22. https://doi.org/10.1021/acs.jmedchem.9b00803.

[152] B. Ferrigno, R. Bordett, N. Duraisamy, J. Moskow, M.R. Arul, S. Rudraiah, S.P. Nukavarapu, A.T. Vella, S.G. Kumbar, Bioactive polymeric materials and electrical stimulation strategies for musculoskeletal tissue repair and regeneration, Bioact. Mater. 5 (2020) 468–485. https://doi.org/10.1016/j.bioactmat.2020.03.010.

[153] B. Guo, P.X. Ma, Conducting Polymers for Tissue Engineering, Biomacromolecules. 19 (2018) 1764–1782. https://doi.org/10.1021/acs.biomac.8b00276.

[154] S. Khorshidi, A. Karkhaneh, Hydrogel/fiber conductive scaffold for bone tissue engineering, J. Biomed. Mater. Res. A. 106 (2018) 718–724. https://doi.org/10.1002/jbm.a.36282.

[155] S. Hosseinzadeh, M. Mahmoudifard, F. Mohamadyar-Toupkanlou, M. Dodel, A. Hajarizadeh, M. Adabi, M. Soleimani, The nanofibrous PAN-PANi scaffold as an efficient substrate for skeletal muscle differentiation using satellite cells, Bioprocess Biosyst. Eng. 39 (2016) 1163–1172. https://doi.org/10.1007/s00449-016-1592-y.

[156] B. Malhotra, C. Dhand, R. Lakshminarayanan, N. Dwivedi, S. Mishra, P. Solanki, M. Venkatesh, R.W. Beuerman, S. Ramakrishna, Polyaniline-based biosensors, Nanobiosensors Dis. Diagn. (2015) 25. https://doi.org/10.2147/NDD.S64841.

[157] G.M. Spinks, V. Mottaghitalab, M. Bahrami-Samani, P.G. Whitten, G.G. Wallace, Carbon-Nanotube-Reinforced Polyaniline Fibers for High-Strength Artificial Muscles, Adv. Mater. 18 (2006) 637–640. https://doi.org/10.1002/adma.200502366.

[158] G.M. Spinks, B. Xi, V.-T. Truong, G.G. Wallace, Actuation behaviour of layered composites of polyaniline, carbon nanotubes and polypyrrole, Synth. Met. 151 (2005) 85–91. https://doi.org/10.1016/j.synthmet.2005.03.006.

[159] L. Wang, Y. Wu, T. Hu, B. Guo, P.X. Ma, Electrospun conductive nanofibrous scaffolds for engineering cardiac tissue and 3D bioactuators, Acta Biomater. 59 (2017) 68–81. https://doi.org/10.1016/j.actbio.2017.06.036.

[160] J. Stejskal, I. Sapurina, Polyaniline: Thin films and colloidal dispersions (IUPAC Technical Report), Pure Appl. Chem. 77 (2005) 815–826. https://doi.org/10.1351/pac200577050815.

[161] J.P. Gonçalves, C.C. de Oliveira, E. da Silva Trindade, I.C. Riegel-Vidotti, M. Vidotti, F.F. Simas, In vitro biocompatibility screening of a colloidal gum Arabic-polyaniline conducting nanocomposite, Int. J. Biol. Macromol. 173 (2021) 109–117. https://doi.org/10.1016/j.ijbiomac.2021.01.101.

[162] P. Bober, P. Humpolíček, T. Syrový, Z. Capáková, L. Syrová, J. Hromádková, J. Stejskal, Biological properties of printable polyaniline and polyaniline–silver colloidal dispersions stabilized by gelatin, Synth. Met. 232 (2017) 52–59. https://doi.org/10.1016/j.synthmet.2017.07.013.

[163] N. Boshkova, N. Tabakova, G. Atanassova, N. Boshkov, Electrochemical Obtaining and Corrosion Behavior of Zinc-Polyaniline (Zn-PANI) Hybrid Coatings, Coatings. 9 (2019) 487. https://doi.org/10.3390/coatings9080487.

[164] K. Kamburova, N. Boshkova, N. Boshkov, T. Radeva, G. Atanasova, Corrosion protection of electrogalvanised steel by application of non-conducting polyaniline-silica particles, Trans. IMF. 99 (2021) 181–187. https://doi.org/10.1080/00202967.2021.1911454.

[165] H. Kebiche, F. Poncin-Epaillard, N. Haddaoui, D. Debarnot, A route for the synthesis of polyaniline-based hybrid nanocomposites, J. Mater. Sci. (2020). https://hal.archives-ouvertes.fr/hal-03015936 (accessed July 17, 2021).

[166] D. Chattopadhyay, S. Banerjee, D. Chakravorty, B.M. Mandal, Ethyl (hydroxyethyl) cellulose stabilized polyaniline dispersions and destabilized nanoparticles therefrom, Langmuir. 14 (1998) 1544–1547.

[167] J. Stejskal, M. Spirkova, A. Riede, M. Helmstedt, P. Mokreva, J. Prokes, Polyaniline dispersions 8. The control of particle morphology, Polymer. 40 (1999) 2487–2492. https://doi.org/10.1016/S0032-3861(98)00478-9.

[168] H. Eisazadeh, K.J. Gilmore, A.J. Hodgson, G. Spinks, G.G. Wallace, Electrochemical production of conducting polymer colloids, Colloids Surf. Physicochem. Eng. Asp. 103 (1995) 281–288. https://doi.org/10.1016/0927-7757(95)03297-Q.

[169] V. Kašpárková, D. Jasenská, Z. Capáková, N. Maráková, J. Stejskal, P. Bober, M. Lehocký, P. Humpolíček, Polyaniline colloids stabilized with bioactive polysaccharides: Non-cytotoxic antibacterial materials, Carbohydr. Polym. 219 (2019) 423–430. https://doi.org/10.1016/j.carbpol.2019.05.038.

[170] A.C. Anbalagan, S.N. Sawant, Biopolymer stabilized water dispersible polyaniline for supercapacitor electrodes, in: Mumbai, India, 2018: p. 140054. https://doi.org/10.1063/1.5029185.

[171] H.H. Darzi, S.G. Larimi, G.N. Darzi, Synthesis, characterization and physical properties of a novel xanthan gum/polypyrrole nanocomposite, Synth. Met. 162 (2012) 236–239. https://doi.org/10.1016/j.synthmet.2011.12.004.

[172] J. Stejskal, I. Sapurina, Polyaniline: Thin films and colloidal dispersions (IUPAC Technical Report), Pure Appl. Chem. 77 (2005) 815–826. https://doi.org/10.1351/pac200577050815.

[173] V.K. Thakur, M.K. Thakur, M.R. Kessler, Handbook of Composites from Renewable Materials, Volume 5, Biodegradable Materials, 2017. https://nbn-resolving.org/urn:nbn:de:101:1-201705033865 (accessed June 29, 2021).

[174] S. Palaniappan, A. John, Polyaniline materials by emulsion polymerization pathway, Prog. Polym. Sci. 33 (2008) 732–758. https://doi.org/10.1016/j.progpolymsci.2008.02.002.

[175] S. Iqbal, S. Ahmad, Recent development in hybrid conducting polymers: Synthesis, applications and future prospects, J. Ind. Eng. Chem. 60 (2018) 53–84. https://doi.org/10.1016/j.jiec.2017.09.038.

[176] C. Dai, C. Chang, H. Chi, H. Chien, W. Su, W. Chiu, Emulsion synthesis of nanoparticles containing PEDOT using conducting polymeric surfactant: Synergy for colloid stability and intercalation doping: Synthesis of Nanoparticles Containing PEDOT, J. Polym. Sci. Part Polym. Chem. 46 (2008) 2536–2548. https://doi.org/10.1002/pola.22585.

[177] T. Syrový, P. Kuberský, I. Sapurina, S. Pretl, P. Bober, L. Syrová, A. Hamáček, J. Stejskal, Gravure-printed ammonia sensor based on organic polyaniline colloids, Sens. Actuators B Chem. 225 (2016) 510–516. https://doi.org/10.1016/j.snb.2015.11.062.

[178] H.-J. Lee, T.-J. Chung, H.-J. Kwon, H.-J. Kim, W.T.Y. Tze, Fabrication and evaluation of bacterial cellulose-polyaniline composites by interfacial polymerization, Cellulose. 19 (2012) 1251–1258. https://doi.org/10.1007/s10570-012-9705-5.

[179] S. Mo, X. Shao, Y. Chen, Z. Cheng, Increasing entropy for colloidal stabilization, Sci. Rep. 6 (2016) 36836. https://doi.org/10.1038/srep36836.

[180] N.V. Blinova, I. Sapurina, J. Klimovič, J. Stejskal, The chemical and colloidal stability of polyaniline dispersions, Polym. Degrad. Stab. 88 (2005) 428–434. https://doi.org/10.1016/j.polymdegradstab.2004.11.014.

[181] L.L. Schramm, E.N. Stasiuk, D.G. Marangoni, 2 Surfactants and their applications, Annu Rep Prog Chem Sect C Phys Chem. 99 (2003) 3–48. https://doi.org/10.1039/B208499F.

[182] J. Stejskal, M. Omastová, S. Fedorova, J. Prokeš, M. Trchová, Polyaniline and polypyrrole prepared in the presence of surfactants: a comparative conductivity study, Polymer. 44 (2003) 1353–1358. https://doi.org/10.1016/S0032-3861(02)00906-0.

[183] N. Kuramoto, A. Tomita, Aqueous polyaniline suspensions: Chemical oxidative polymerization of dodecylbenzene-sulfonic acid aniline salt, Polymer. 38 (1997) 3055–3058. https://doi.org/10.1016/S0032-3861(96)00861-0.

[184] C. DeArmitt, S.P. Armes, Colloidal dispersions of surfactant-stabilized polypyrrole particles, Langmuir. 9 (1993) 652–654. https://doi.org/10.1021/la00027a007.

[185] M.T. Gill, S.E. Chapman, C.L. DeArmitt, F.L. Baines, C.M. Dadswell, J.G. Stamper, G.A. Lawless, N.C. Billingham, S.P. Armes, A study of the kinetics of polymerization of aniline using proton NMR spectroscopy, Synth. Met. 93 (1998) 227–233. https://doi.org/10.1016/S0379-6779(98)00016-2.

[186] S.Y. Luk, W. Lineton, M. Keane, C. DeArmitt, S.P. Armes, Surface composition of surfactant-stabilised polypyrrole colloids, J. Chem. Soc. Faraday Trans. 91 (1995) 905. https://doi.org/10.1039/ft9959100905.

[187] N. Gospodinova, P. Mokreva, T. Tsanov, L. Terlemezyan, A new route to polyaniline composites, Polymer. 38 (1997) 743–746. https://doi.org/10.1016/S0032-3861(96)00698-2.

[188] S.-J. Su, N. Kuramoto, Synthesis of processable polyaniline complexed with anionic surfactant and its conducting blends in aqueous and organic system, Synth. Met. 108 (2000) 121–126. https://doi.org/10.1016/S0379-6779(99)00185-X.

[189] N. Kohut-Svelko, S. Reynaud, J. François, Synthesis and characterization of polyaniline prepared in the presence of nonionic surfactants in an aqueous dispersion, Synth. Met. 150 (2005) 107–114. https://doi.org/10.1016/j.synthmet.2004.12.022.

[190] O.D. Iakobson, O.L. Gribkova, A.A. Nekrasov, V.A. Tverskoi, V.F. Ivanov, P.V. Mel'nikov, E.A. Polenov, A.V. Vannikov, A stable aqueous dispersion of polyaniline and polymeric acid, Prot. Met. Phys. Chem. Surf. 52 (2016) 1005–1011. https://doi.org/10.1134/S207020511606023X.

[191] Z. Kucekova, P. Humpolicek, V. Kasparkova, T. Perecko, M. Lehocký, I. Hauerlandová, P. Sáha, J. Stejskal, Colloidal polyaniline dispersions: Antibacterial activity, cytotoxicity and neutrophil oxidative burst, Colloids Surf. B Biointerfaces. 116 (2014) 411–417. https://doi.org/10.1016/j.colsurfb.2014.01.027.

[192] Y. Li, P. Bober, M. Trchová, J. Stejskal, Colloidal dispersions of conducting copolymers of aniline and p-phenylenediamine for films with enhanced conductometric sensitivity to temperature, J. Mater. Chem. C. 5 (2017) 1668–1674. https://doi.org/10.1039/C6TC05413G.

[193] J. Stejskal, P. Kratochvíl, M. Helmstedt, Polyaniline Dispersions. 5. Poly(vinyl alcohol) and Poly(N-vinylpyrrolidone) as Steric Stabilizers, Langmuir. 12 (1996) 3389–3392. https://doi.org/10.1021/la9506483.

[194] J.C.-C. Wu, S. Ray, M. Gizdavic-Nikolaidis, J. Jin, R.P. Cooney, Effect of polyvinylpyrrolidone on storage stability, anti-oxidative and anti-bacterial properties of colloidal polyaniline, Synth. Met. 217 (2016) 202–209. https://doi.org/10.1016/j.synthmet.2016.03.019.

[195] V.K. Thakur, M.K. Thakur, M.R. Kessler, Handbook of Composites from Renewable Materials, Biodegradable Materials., John Wiley & Sons, Incorporated, Somerset, 2017. http://www.myilibrary.com?id=994745 (accessed July 18, 2021).

[196] J. Stejskal, I. Sapurina, On the origin of colloidal particles in the dispersion polymerization of aniline, J. Colloid Interface Sci. 274 (2004) 489–495. https://doi.org/10.1016/j.jcis.2004.02.053.

[197] P. Beadle, S.P. Armes, S. Gottesfeld, C. Mombourquette, R. Houlton, W.D. Andrews, S.F. Agnew, Electrically conductive polyaniline-copolymer latex composites, Macromolecules. 25 (1992) 2526–2530. https://doi.org/10.1021/ma00035a035.

[198] L. Terlemezyan, M. Mihailov, B. Ivanova, Electrically conductive polymer blends comprising polyaniline, Polym. Bull. 29 (1992) 283–287. https://doi.org/10.1007/BF00944820.

[199] H.-Q. Xie, H. Liu, Z.-H. Liu, J.-S. Guo, Electrically conductive polyaniline/poly(butadiene-co-styrene-co-2-vinylpyridine) latex composites, Angew. Makromol. Chem. 243 (1996) 117–128. https://doi.org/10.1002/apmc.1996.052430110.

[200] T. Lei, K. Aoki, Monodispersed redox submicrometer particles created by polyaniline-coated polystyrene latex, J. Electroanal. Chem. 482 (2000) 149–155. https://doi.org/10.1016/S0022-0728(00)00041-3.

[201] C.-F. Liu, T. Maruyama, T. Yamamoto, Conductive Blends of π-Conjugated Polymers and Thermoplastic Polymers in Latex Form, Polym. J. 25 (1993) 363–372. https://doi.org/10.1295/polymj.25.363.

[202] M. Omastová, F. Simon, Surface characterizations of conductive poly(methyl methacrylate)/polypyrrole composites, J. Mater. Sci. 35 (2000) 1743–1749. https://doi.org/10.1023/A:1004728502591.

[203] A. Yassar, J. Roncali, F. Garnier, Aqueous suspension of conducting material from polypyrrole-coated submicronic latex particles, Polym. Commun. 28 (1987). https://www.semanticscholar.org/paper/Aqueous-suspension-of-conducting-material-from-Yassar-Roncali/de27afcb8a2424994ea50f2edc1401aa6e97b76f (accessed June 22, 2021).

[204] A. Riede, M. Helmstedt, V. Riede, J. Stejskal, Polyaniline dispersions 7. Dynamic light scattering study of particle formation, Colloid Polym. Sci. 275 (1997) 814–820. https://doi.org/10.1007/s003960050153.

[205] J. Stejskal, T. Sulimenko, J. Prokes, I. Sapurina, Polyaniline dispersions 10. Coloured microparticles of variable density prepared using stabilizer mixtures, Colloid Polym. Sci. 278 (2000) 654–658. https://doi.org/10.1007/s003960000312.

[206] M. Gill, F.L. Baines, S.P. Armes, Some observations on the preparation of colloidal polyaniline - silica composites, Synth. Met. 55 (1993) 1029–1033. https://doi.org/10.1016/0379-6779(93)90194-2.

[207] M. Gill, S.P. Armes, D. Fairhurst, S.N. Emmett, G. Idzorek, T. Pigott, Particle size distributions of polyaniline-silica colloidal composites, Langmuir. 8 (1992) 2178–2182. https://doi.org/10.1021/la00045a018.

[208] J. Stejskal, P. Kratochvíl, S.P. Armes, S.F. Lascelles, A. Riede, M. Helmstedt, J. Prokeš, I. Křivka, Polyaniline Dispersions. 6. Stabilization by Colloidal Silica Particles, Macromolecules. 29 (1996) 6814–6819. https://doi.org/10.1021/ma9603903.

[209] S.F. Lascelles, G.P. McCarthy, M.D. Butterworth, S.P. Armes, Effect of synthesis parameters on the particle size, composition and colloid stability of polypyrrole–silica nanocomposite particles, Colloid Polym. Sci. 276 (1998) 893–902. https://doi.org/10.1007/s003960050326.

[210] S. Maeda, R. Corradi, S.P. Armes, Synthesis and Characterization of Carboxylic Acid-Functionalized Polypyrrole-Silica Microparticles, Macromolecules. 28 (1995) 2905–2911. https://doi.org/10.1021/ma00112a042.

[211] S. Maeda, S.P. Armes, Preparation and characterisation of novel polypyrrole–silica colloidal nanocomposites, J. Mater. Chem. 4 (1994) 935–942. https://doi.org/10.1039/JM9940400935.

[212] S. Maeda, S.P. Armes, Surface area measurements on conducting polymer-inorganic oxide nanocomposites, Synth. Met. 73 (1995) 151–155. https://doi.org/10.1016/0379-6779(95)03315-7.

[213] M. Biswas, S. Sinha Ray, Y. Liu, Water dispersible conducting nanocomposites of poly(N-vinylcarbazole), polypyrrole and polyaniline with nanodimensional manganese (IV) oxide, Synth. Met. 105 (1999) 99–105. https://doi.org/10.1016/S0379-6779(99)00049-1.

[214] S.S. Ray, M. Biswas, Water-dispersible conducting nanocomposites of polyaniline and poly(N-vinylcarbazole) with nanodimensional zirconium dioxide, Synth. Met. 108 (2000) 231–236. https://doi.org/10.1016/S0379-6779(99)00258-1.

[215] X. Du, Z. Zhang, W. Liu, Y. Deng, Nanocellulose-based conductive materials and their emerging applications in energy devices - A review, Nano Energy. 35 (2017) 299–320. https://doi.org/10.1016/j.nanoen.2017.04.001.

[216] R.L. Razalli, M.M. Abdi, P.M. Tahir, A. Moradbak, Y. Sulaiman, L.Y. Heng, Polyaniline-modified nanocellulose prepared from Semantan bamboo by chemical polymerization: preparation and characterization, RSC Adv. 7 (2017) 25191–25198. https://doi.org/10.1039/C7RA03379F.

[217] X. Yang, S.K. Biswas, J. Han, S. Tanpichai, M. Li, C. Chen, S. Zhu, A.K. Das, H. Yano, Surface and Interface Engineering for Nanocellulosic Advanced Materials, Adv. Mater. 33 (2021) 2002264. https://doi.org/10.1002/adma.202002264.

[218] F.M. Kelly, J.H. Johnston, T. Borrmann, M.J. Richardson, Functionalised Hybrid Materials of Conducting Polymers with Individual Fibres of Cellulose, Eur. J. Inorg. Chem. 2007 (2007) 5571–5577. https://doi.org/10.1002/ejic.200700608.

[219] M.M. Abdi, R.L. Razalli, P.M. Tahir, N. Chaibakhsh, M. Hassani, M. Mir, Optimized fabrication of newly cholesterol biosensor based on nanocellulose, Int. J. Biol. Macromol. 126 (2019) 1213–1222. https://doi.org/10.1016/j.ijbiomac.2019.01.001.

[220] R.-M. Latonen, A. Määttänen, P. Ihalainen, W. Xu, M. Pesonen, M. Nurmi, C. Xu, Conducting ink based on cellulose nanocrystals and polyaniline for flexographical printing, J. Mater. Chem. C. 5 (2017) 12172–12181. https://doi.org/10.1039/C7TC03729E.

[221] M. Song, H. Yu, J. Zhu, Z. Ouyang, S.Y.H. Abdalkarim, K.C. Tam, Y. Li, Constructing stimuli-free self-healing, robust and ultrasensitive biocompatible hydrogel sensors with conductive cellulose nanocrystals, Chem. Eng. J. 398 (2020) 125547. https://doi.org/10.1016/j.cej.2020.125547.

[222] S. Lyu, Y. Chen, S. Han, L. Guo, Z. Chen, Y. Lu, Y. Chen, N. Yang, S. Wang, Layer-by-layer assembled polyaniline/carbon nanomaterial-coated cellulosic aerogel electrodes for high-capacitance supercapacitor

applications, RSC Adv. 8 (2018) 13191–13199. https://doi.org/10.1039/C8RA01754A.

[223] A.A. Al-Dulaimi, W.D. Wanrosli, Preparation of Colloidal Properties and Water Dispersible Conductive Polypyrrole Nanocomposite of Nanocrystalline Cellulose, Polym. Polym. Compos. 24 (2016) 695–702. https://doi.org/10.1177/096739111602400904.

[224] X. Wu, V.L. Chabot, B.K. Kim, A. Yu, R.M. Berry, K.C. Tam, Cost-effective and Scalable Chemical Synthesis of Conductive Cellulose Nanocrystals for High-performance Supercapacitors, Electrochimica Acta. 138 (2014) 139–147. https://doi.org/10.1016/j.electacta.2014.06.089.

[225] C. Esmaeili, M. Abdi, A. Mathew, M. Jonoobi, K. Oksman, M. Rezayi, Synergy Effect of Nanocrystalline Cellulose for the Biosensing Detection of Glucose, Sensors. 15 (2015) 24681–24697. https://doi.org/10.3390/s151024681.

[226] S. Wang, C. Wei, Y. Gong, J. Lv, C. Yu, J. Yu, Cellulose nanofiber-assisted dispersion of cellulose nanocrystals@polyaniline in water and its conductive films, RSC Adv. 6 (2016) 10168–10174. https://doi.org/10.1039/C5RA19346J.

[227] N.D. Luong, J.T. Korhonen, A.J. Soininen, J. Ruokolainen, L.-S. Johansson, J. Seppälä, Processable polyaniline suspensions through in situ polymerization onto nanocellulose, Eur. Polym. J. 49 (2013) 335–344. https://doi.org/10.1016/j.eurpolymj.2012.10.026.

[228] M.L. Auad, T. Richardson, W.J. Orts, E.S. Medeiros, L.H. Mattoso, M.A. Mosiewicki, N.E. Marcovich, M.I. Aranguren, Polyaniline-modified cellulose nanofibrils as reinforcement of a smart polyurethane: Cellulose nanofibril-reinforced smart polyurethane, Polym. Int. 60 (2011) 743–750. https://doi.org/10.1002/pi.3004.

[229] M.J. Silva, A.O. Sanches, E.S. Medeiros, L.H.C. Mattoso, C.M. McMahan, J.A. Malmonge, Nanocomposites of natural rubber and polyaniline-modified cellulose nanofibrils, J. Therm. Anal. Calorim. 117 (2014) 387–392. https://doi.org/10.1007/s10973-014-3719-1.

[230] W. He, J. Tian, J. Li, H. Jin, Y. Li, Characterization and Properties of Cellulose Nanofiber/ Polyaniline Film Composites Synthesized through in Situ Polymerization, BioResources. 11 (2016) 8535–8547.

[231] L.H.C. Mattoso, E.S. Medeiros, D.A. Baker, J. Avloni, D.F. Wood, W.J. Orts, Electrically Conductive Nanocomposites Made from Cellulose Nanofibrils and Polyaniline, J. Nanosci. Nanotechnol. 9 (2009) 2917–2922. https://doi.org/10.1166/jnn.2009.dk24.

[232] G. Nyström, A. Mihranyan, A. Razaq, T. Lindström, L. Nyholm, M. Strømme, A Nanocellulose Polypyrrole Composite Based on Microfibrillated Cellulose from Wood, J. Phys. Chem. B. 114 (2010) 4178–4182. https://doi.org/10.1021/jp911272m.

[233]P. Bober, J. Liu, K.S. Mikkonen, P. Ihalainen, M. Pesonen, C. Plumed-Ferrer, A. von Wright, T. Lindfors, C. Xu, R.-M. Latonen, Biocomposites of Nanofibrillated Cellulose, Polypyrrole, and Silver Nanoparticles with Electroconductive and Antimicrobial Properties, Biomacromolecules. 15 (2014) 3655–3663. https://doi.org/10.1021/bm500939x.

[234]M. Lay, M.À. Pèlach, N. Pellicer, J.A. Tarrés, K.N. Bun, F. Vilaseca, Smart nanopaper based on cellulose nanofibers with hybrid PEDOT:PSS/polypyrrole for energy storage devices, Carbohydr. Polym. 165 (2017) 86–95. https://doi.org/10.1016/j.carbpol.2017.02.043.

[235]B. Bideau, J. Bras, S. Saini, C. Daneault, E. Loranger, Mechanical and antibacterial properties of a nanocellulose-polypyrrole multilayer composite, Mater. Sci. Eng. C. 69 (2016) 977–984. https://doi.org/10.1016/j.msec.2016.08.005.

[236]D. Müller, J.S. Mandelli, J.A. Marins, B.G. Soares, L.M. Porto, C.R. Rambo, G.M.O. Barra, Electrically conducting nanocomposites: preparation and properties of polyaniline (PAni)-coated bacterial cellulose nanofibers (BC), Cellulose. 19 (2012) 1645–1654. https://doi.org/10.1007/s10570-012-9754-9.

[237]W. Hu, S. Chen, Z. Yang, L. Liu, H. Wang, Flexible Electrically Conductive Nanocomposite Membrane Based on Bacterial Cellulose and Polyaniline, J. Phys. Chem. B. 115 (2011) 8453–8457. https://doi.org/10.1021/jp204422v.

[238]J.A. Marins, B.G. Soares, K. Dahmouche, S.J.L. Ribeiro, H. Barud, D. Bonemer, Structure and properties of conducting bacterial cellulose-polyaniline nanocomposites, Cellulose. 18 (2011) 1285–1294. https://doi.org/10.1007/s10570-011-9565-4.

[239]H. Wang, E. Zhu, J. Yang, P. Zhou, D. Sun, W. Tang, Bacterial Cellulose Nanofiber-Supported Polyaniline Nanocomposites with Flake-Shaped Morphology as Supercapacitor Electrodes, J. Phys. Chem. C. 116 (2012) 13013–13019. https://doi.org/10.1021/jp301099r.

[240]M. Lay, I. González, J.A. Tarrés, N. Pellicer, K.N. Bun, F. Vilaseca, High electrical and electrochemical properties in bacterial cellulose/polypyrrole membranes, Eur. Polym. J. 91 (2017) 1–9. https://doi.org/10.1016/j.eurpolymj.2017.03.021.

[241]D. Müller, C.R. Rambo, D.O.S.Recouvreux, L.M. Porto, G.M.O. Barra, Chemical in situ polymerization of polypyrrole on bacterial cellulose nanofibers, Synth. Met. 161 (2011) 106–111. https://doi.org/10.1016/j.synthmet.2010.11.005.

[242]D. Muller, C.R. Rambo, Luismar.M. Porto, W.H. Schreiner, G.M.O. Barra, Structure and properties of polypyrrole/bacterial cellulose nanocomposites, Carbohydr. Polym. 94 (2013) 655–662. https://doi.org/10.1016/j.carbpol.2013.01.041.

[243]Y. Shao, Z. Fan, M. Zhong, W. Xu, C. He, Z. Zhang, Polypyrrole/bacterial cellulose nanofiber composites for hexavalent chromium removal,

Cellulose. 28 (2021) 2229–2240. https://doi.org/10.1007/s10570-020-03660-2.

[244] J. Xu, L. Zhu, Z. Bai, G. Liang, L. Liu, D. Fang, W. Xu, Conductive polypyrrole–bacterial cellulose nanocomposite membranes as flexible supercapacitor electrode, Org. Electron. 14 (2013) 3331–3338. https://doi.org/10.1016/j.orgel.2013.09.042.

[245] K.L. Chopra, I. Kaur, Thin Film Technology: An Introduction, in: K.L. Chopra, I. Kaur (Eds.), Thin Film Device Appl., Springer US, Boston, MA, 1983: pp. 1–54. https://doi.org/10.1007/978-1-4613-3682-2_1.

[246] V.P. Elanjeitsenni, K.S. Vadivu, B.M. Prasanth, A review on thin films, conducting polymers as sensor devices, Mater. Res. Express. 9 (2022) 022001. https://doi.org/10.1088/2053-1591/ac4aa1.

[247] D. Chinn, J. DuBow, M. Liess, M. Josowicz, J. Janata, Comparison of Chemically and Electrochemically Prepared Polyaniline. Films. 1. Electrical Properties, Chem. Mater. 7 (1995) 1504–1509. https://doi.org/10.1021/cm00056a016.

[248] S.A. Hasoon, Electrochemical polymerization and Optical Vibrations of Polyaniline Films, 3 (2007) 10.

[249] A. de Leon, R.C. Advincula, Conducting Polymers with Superhydrophobic Effects as Anticorrosion Coating, in: Intell. Coat. Corros. Control, Elsevier, 2015: pp. 409–430. https://doi.org/10.1016/B978-0-12-411467-8.00011-8.

[250] M. Rahaman, A. Aldalbahi, M. Almoiqli, S. Alzahly, Chemical and Electrochemical Synthesis of Polypyrrole Using Carrageenan as a Dopant: Polypyrrole/Multi-Walled Carbon Nanotube Nanocomposites, Polymers. 10 (2018) 632. https://doi.org/10.3390/polym10060632.

[251] M. Beygisangchin, S. Abdul Rashid, S. Shafie, A.R. Sadrolhosseini, H.N. Lim, Preparations, Properties, and Applications of Polyaniline and Polyaniline Thin Films—A Review, Polymers. 13 (2021) 2003. https://doi.org/10.3390/polym13122003.

[252] P.-C. Wang, Z. Huang, A.G. MacDiarmid, Critical dependency of the conductivity of polypyrrole and polyaniline films on the hydrophobicity/hydrophilicity of the substrate surface, Synth. Met. 101 (1999) 852–853. https://doi.org/10.1016/S0379-6779(98)01329-0.

[253] I. Sapurina, A.Yu. Osadchev, B.Z. Volchek, M. Trchová, A. Riede, J. Stejskal, In-situ polymerized polyaniline films, Synth. Met. 129 (2002) 29–37. https://doi.org/10.1016/S0379-6779(02)00036-X.

[254] J. Stejskal, O.E. Bogomolova, N.V. Blinova, M. Trchová, I. Šeděnková, J. Prokeš, I. Sapurina, Mixed electron and proton conductivity of polyaniline films in aqueous solutions of acids: beyond the 1000 S cm^{-1} limit: Electron and proton conductivity of PANI films in acids, Polym. Int. 58 (2009) 872–879. https://doi.org/10.1002/pi.2605.

[255] A. Riede, M. Helmstedt, V. Riede, J. Zemek, J. Stejskal, In Situ Polymerized Polyaniline Films. 2. Dispersion Polymerization of Aniline in the Presence

of Colloidal Silica, Langmuir. 16 (2000) 6240–6244. https://doi.org/10.1021/la991414c.

[256] A. Riede, M. Helmstedt, I. Sapurina, J. Stejskal, In Situ Polymerized Polyaniline Films, J. Colloid Interface Sci. 248 (2002) 413–418. https://doi.org/10.1006/jcis.2001.8197.

[257] Y. Koizumi, N. Shida, M. Ohira, H. Nishiyama, I. Tomita, S. Inagi, Electropolymerization on wireless electrodes towards conducting polymer microfibre networks, Nat. Commun. 7 (2016) 10404. https://doi.org/10.1038/ncomms10404.

[258] G. Fomo, T. Waryo, U. Feleni, P. Baker, E. Iwuoha, Electrochemical Polymerization, in: Md.I.H. Mondal (Ed.), Cellul.-Based Superabsorbent Hydrogels, Springer International Publishing, Cham, 2019: pp. 1–28. https://doi.org/10.1007/978-3-319-92067-2_3-1.

[259] A. Yazdanpanah, A. Ramedani, A. Abrishamkar, P.B. Milan, Z.S. Moghadan, N.P.S. Chauhan, F. Sefat, M. Mozafari, Synthetic route of PANI (V): Electrochemical polymerization, in: Fundam. Emerg. Appl. Polyaniline, Elsevier, 2019: pp. 105–119. https://doi.org/10.1016/B978-0-12-817915-4.00006-3.

[260] E. Acosta, Thin Films/Properties and Applications, IntechOpen, 2021. https://doi.org/10.5772/intechopen.95527.

[261] P.M. Martin, ed., Chapter 1 - Deposition Technologies: An Overview, in: Handb. Depos. Technol. Films Coat. Third Ed., William Andrew Publishing, Boston, 2010: pp. 1–31. https://doi.org/10.1016/B978-0-8155-2031-3.00001-6.

[262] P.H. Li, P.K. Chu, Thin film deposition technologies and processing of biomaterials, in: Thin Film Coat. Biomater. Biomed. Appl., Elsevier, 2016: pp. 3–28. https://doi.org/10.1016/B978-1-78242-453-6.00001-8.

[263] M. Li, D. Liu, D. Wei, X. Song, D. Wei, A.T.S. Wee, Controllable Synthesis of Graphene by Plasma-Enhanced Chemical Vapor Deposition and Its Related Applications, Adv. Sci. 3 (2016) 1600003. https://doi.org/10.1002/advs.201600003.

[264] J. Zhang, D.P. Burt, A.L. Whitworth, D. Mandler, P.R. Unwin, Polyaniline Langmuir–Blodgett films: formation and properties, Phys. Chem. Chem. Phys. 11 (2009) 3490. https://doi.org/10.1039/b819809h.

[265] S. Malik, C.C. Tripathi, Thin Film Deposition by Langmuir Blodgett Technique for Gas Sensing Applications, J. Surf. Eng. Mater. Adv. Technol. 03 (2013) 235–241. https://doi.org/10.4236/jsemat.2013.33031.

[266] D. Rawtani, Y.K. Agrawal, Emerging Strategies and Applications of Layer-by-Layer Self-Assembly, Nanobiomedicine. 1 (2014) 8. https://doi.org/10.5772/60009.

[267] Y. Yunus, N.A. Mahadzir, M.N. Mohamed Ansari, T.H. Tg Abd Aziz, A. Mohd Afdzaluddin, H. Anwar, M. Wang, A.G. Ismail, Review of the Common Deposition Methods of Thin-Film Pentacene, Its Derivatives, and

Their Performance, Polymers. 14 (2022) 1112. https://doi.org/10.3390/polym14061112.

[268]B.S. Yilbas, A. Al-Sharafi, H. Ali, Surfaces for Self-Cleaning, in: Self-Clean. Surf. Water Droplet Mobil., Elsevier, 2019: pp. 45–98. https://doi.org/10.1016/B978-0-12-814776-4.00003-3.

[269]A.L. Sharma, P. Kumar, A. Deep, Thermally Evaporated Poly(Aniline-co-Fluoroaniline) Films for Ammonia Sensing, Polym.-Plast. Technol. Eng. 52 (2013) 737–742. https://doi.org/10.1080/03602559.2012.762674.

[270]B. Mishra, P.K. Khare, A Review on Polymer, J. Emerg. Technol. Innov. Res. (2015).

[271]J.M. D'Arcy, H.D. Tran, V.C. Tung, A.K. Tucker-Schwartz, R.P. Wong, Y. Yang, R.B. Kaner, Versatile solution for growing thin films of conducting polymers, Proc. Natl. Acad. Sci. 107 (2010) 19673–19678. https://doi.org/10.1073/pnas.1008595107.

[272]D. Boyne, N. Menegazzo, R.C. Pupillo, J. Rosenthal, K.S. Booksh, Vacuum thermal evaporation of polyaniline doped with camphor sulfonic acid, J. Vac. Sci. Technol. Vac. Surf. Films. 33 (2015) 031510. https://doi.org/10.1116/1.4916990.

[273]A.L. Winck, J.C.V. dos Santos, D.M. Lenz, D.M. Tedesco, Development and characterization of gas sensors using thin films of polyaniline as active layer, Matér. Rio Jan. 23 (2018). https://doi.org/10.1590/s1517-707620180004.0593.

[274]I. Fratoddi, I. Venditti, C. Cametti, M.V. Russo, Chemiresistive polyaniline-based gas sensors: A mini review, Sens. Actuators B Chem. 220 (2015) 534–548. https://doi.org/10.1016/j.snb.2015.05.107.

[275]M.R. Karim, M.M. Alam, M.O. Aijaz, A.M. Asiri, F.S. AlMubaddel, M.M. Rahman, The fabrication of a chemical sensor with PANI-TiO$_2$ nanocomposites, RSC Adv. 10 (2020) 12224–12233. https://doi.org/10.1039/C9RA09315J.

[276]Z. Jin, Y. Su, Y. Duan, An improved optical pH sensor based on polyaniline, Sens. Actuators B Chem. 71 (2000) 118–122. https://doi.org/10.1016/S0925-4005(00)00597-9.

[277]J. Kim, J. Sohn, Y. Jo, H. Woo, J. Han, S. Cho, A.I. Inamdar, H. Kim, H. Im, Drop-casted polyaniline thin films on flexible substrates for supercapacitor applications, J. Korean Phys. Soc. 65 (2014) 1320–1323. https://doi.org/10.3938/jkps.65.1320.

[278]P.R. Deshmukh, S.V. Patil, R.N. Bulakhe, S.N. Pusawale, J.-J. Shim, C.D. Lokhande, Chemical synthesis of PANI–TiO$_2$ composite thin film for supercapacitor application, RSC Adv. 5 (2015) 68939–68946. https://doi.org/10.1039/C5RA09233G.

[279]A. Bessière, C. Duhamel, J.-C. Badot, V. Lucas, M.-C. Certiat, Study and optimization of a flexible electrochromic device based on polyaniline,

Electrochimica Acta. 49 (2004) 2051–2055. https://doi.org/10.1016/j.electacta.2003.12.034.

[280] T.R. Salikhov, Y.M. Yumaguzin, R.B. Salikhov, Electronics applications based on thin polyaniline films, in: 2015 Int. Sib. Conf. Control Commun. SIBCON, IEEE, Omsk, Russia, 2015: pp. 1–3. https://doi.org/10.1109/SIBCON.2015.7147207.

[281] X.H. Huang, J.P. Tu, X.H. Xia, X.L. Wang, J.Y. Xiang, Nickel foam-supported porous NiO/polyaniline film as anode for lithium ion batteries, Electrochem. Commun. 10 (2008) 1288–1290. https://doi.org/10.1016/j.elecom.2008.06.020.

[282] K.-I. Park, H.-M. Song, Y. Kim, S. Mho, W.I. Cho, I.-H. Yeo, Electrochemical preparation and characterization of V2O5/polyaniline composite film cathodes for Li battery, Electrochimica Acta. 55 (2010) 8023–8029. https://doi.org/10.1016/j.electacta.2009.12.047.

[283] C.-W. Peng, K.-C. Chang, C.-J. Weng, M.-C. Lai, C.-H. Hsu, S.-C. Hsu, Y.-Y. Hsu, W.-I. Hung, Y. Wei, J.-M. Yeh, Nano-casting technique to prepare polyaniline surface with biomimetic superhydrophobic structures for anticorrosion application, Electrochimica Acta. 95 (2013) 192–199. https://doi.org/10.1016/j.electacta.2013.02.016.

[284] S. Liu, J. Wang, D. Zhang, P. Zhang, J. Ou, B. Liu, S. Yang, Investigation on cell biocompatible behaviors of polyaniline film fabricated via electroless surface polymerization, Appl. Surf. Sci. 256 (2010) 3427–3431. https://doi.org/10.1016/j.apsusc.2009.12.046.

[285] H. Wang, L. Ji, D. Li, J.-Y. Wang, Characterization of Nanostructure and Cell Compatibility of Polyaniline Films with Different Dopant Acids, J. Phys. Chem. B. 112 (2008) 2671–2677. https://doi.org/10.1021/jp0750957.

[286] P. Rejmontová, Z. Capáková, N. Mikušová, N. Maráková, V. Kašpárková, M. Lehocký, P. Humpolíček, Adhesion, Proliferation and Migration of NIH/3T3 Cells on Modified Polyaniline Surfaces, Int. J. Mol. Sci. 17 (2016) 1439. https://doi.org/10.3390/ijms17091439.

[287] V. Kašpárková, P. Humpolíček, Z. Capáková, P. Bober, J. Stejskal, M. Trchová, P. Rejmontová, I. Junkar, M. Lehocký, M. Mozetič, Cell-compatible conducting polyaniline films prepared in colloidal dispersion mode, Colloids Surf. B Biointerfaces. 157 (2017) 309–316. https://doi.org/10.1016/j.colsurfb.2017.05.066.

[288] D. Jasenská, V. Kašpárková, K.A. Radaszkiewicz, Z. Capáková, J. Pacherník, M. Trchová, A. Minařík, J. Vajďák, T. Bárta, J. Stejskal, M. Lehocký, T.H. Truong, R. Moučka, P. Humpolíček, Conducting composite films based on chitosan or sodium hyaluronate. Properties and cytocompatibility with human induced pluripotent stem cells, Carbohydr. Polym. 253 (2021) 117244. https://doi.org/10.1016/j.carbpol.2020.117244.

[289] Skopalová, Capáková, Bober, Pelková, Stejskal, Kašpárková, Lehocký, Junkar, Mozetič, Humpolíček, In-Vitro Hemocompatibility of Polyaniline

Functionalized by Bioactive Molecules, Polymers. 11 (2019) 1861. https://doi.org/10.3390/polym11111861.

[290] P. Humpolíček, Z. Kuceková, V. Kašpárková, J. Pelková, M. Modic, I. Junkar, M. Trchová, P. Bober, J. Stejskal, M. Lehocký, Blood coagulation and platelet adhesion on polyaniline films, Colloids Surf. B Biointerfaces. 133 (2015) 278–285. https://doi.org/10.1016/j.colsurfb.2015.06.008.

[291] H. Zhang, C. Dou, L. Pal, M. Hubbe, Review of electrically conductive composites and films containing cellulosic fibers or nanocellulose, BioResources. 14 (2019) 7494–7542. https://doi.org/10.15376/biores.14.3.7494-7542.

[292] Z. Zai, M. Yan, C. Shi, L. Zhang, H. Lu, Z. Xiong, J. Ma, Cellulose nanofibrils (CNFs) in uniform diameter: Capturing the impact of carboxyl group on dispersion and Re-dispersion of CNFs suspensions, Int. J. Biol. Macromol. 207 (2022) 23–30. https://doi.org/10.1016/j.ijbiomac.2022.03.001.

[293] X. Qian, Y. Lu, L. Ge, S. Yin, D. Wu, Starch nanocrystals as the particle emulsifier to stabilize caprylic/capric triglycerides-in-water emulsions, Carbohydr. Polym. 245 (2020) 116561. https://doi.org/10.1016/j.carbpol.2020.116561.

[294] P. Severino, S.C. Pinho, E.B. Souto, M.H.A. Santana, Polymorphism, crystallinity and hydrophilic–lipophilic balance of stearic acid and stearic acid–capric/caprylic triglyceride matrices for production of stable nanoparticles, Colloids Surf. B Biointerfaces. 86 (2011) 125–130. https://doi.org/10.1016/j.colsurfb.2011.03.029.

[295] W. Wang, M. Wang, J. Zhang, H. Liu, H. Pan, Cloud point thermodynamics of paclitaxel-loaded microemulsion in the presence of glucose and NaCl, Colloids Surf. Physicochem. Eng. Asp. 507 (2016) 76–82. https://doi.org/10.1016/j.colsurfa.2016.07.086.

[296] J. Stejskal, P. Kratochvíl, N. Radhakrishnan, Polyaniline dispersions 2. UV—Vis absorption spectra, Synth. Met. 61 (1993) 225–231. https://doi.org/10.1016/0379-6779(93)91266-5.

[297] Z. Moosova, M. Pekarova, L.S. Sindlerova, O. Vasicek, L. Kubala, L. Blaha, O. Adamovsky, Immunomodulatory effects of cyanobacterial toxin cylindrospermopsin on innate immune cells, Chemosphere. 226 (2019) 439–446. https://doi.org/10.1016/j.chemosphere.2019.03.143.

[298] O. Vasicek, A. Lojek, V. Jancinova, R. Nosal, M. Ciz, Role of histamine receptors in the effects of histamine on the production of reactive oxygen species by whole blood phagocytes, Life Sci. 100 (2014) 67–72. https://doi.org/10.1016/j.lfs.2014.01.082.

[299] Y.N. Georgiev, B.S. Paulsen, H. Kiyohara, M. Ciz, M.H. Ognyanov, O. Vasicek, F. Rise, P.N. Denev, H. Yamada, A. Lojek, V. Kussovski, H. Barsett, A.I. Krastanov, I.Z. Yanakieva, M.G. Kratchanova, The common lavender (Lavandula angustifolia Mill.) pectic polysaccharides modulate

phagocytic leukocytes and intestinal Peyer's patch cells, Carbohydr. Polym. 174 (2017) 948–959. https://doi.org/10.1016/j.carbpol.2017.07.011.

[300] D. Jasenská, V. Kašpárková, O. Vašíček, L. Münster, A. Minařík, S. Káčerová, E. Korábková, L. Urbánková, J. Vícha, Z. Capáková, E. Falleta, C. Della Pina, M. Lehocký, K. Skopalová, P. Humpolíček, Enzyme-Catalyzed Polymerization Process: A Novel Approach to the Preparation of Polyaniline Colloidal Dispersions with an Immunomodulatory Effect, Biomacromolecules. 23 (2022) 3359–3370. https://doi.org/10.1021/acs.biomac.2c00371.

[301] O. Vašíček, A. Lojek, M. Číž, Serotonin and its metabolites reduce oxidative stress in murine RAW264.7 macrophages and prevent inflammation, J. Physiol. Biochem. 76 (2020) 49–60. https://doi.org/10.1007/s13105-019-00714-3.

[302] X. Yan, X. Chen, Titanium Dioxide Nanomaterials, in: R.A. Scott (Ed.), Encycl. Inorg. Bioinorg. Chem., John Wiley & Sons, Ltd, Chichester, UK, 2015: pp. 1–38. https://doi.org/10.1002/9781119951438.eibc2335.

[303] B. Dréno, A. Alexis, B. Chuberre, M. Marinovich, Safety of titanium dioxide nanoparticles in cosmetics, J. Eur. Acad. Dermatol. Venereol. 33 (2019) 34–46. https://doi.org/10.1111/jdv.15943.

[304] G. Xie, W. Lu, D. Lu, Penetration of titanium dioxide nanoparticles through slightly damaged skin in vitro and in vivo, J. Appl. Biomater. Funct. Mater. 13 (2015) 0–0. https://doi.org/10.5301/jabfm.5000243.

[305] M. Crosera, A. Prodi, M. Mauro, M. Pelin, C. Florio, F. Bellomo, G. Adami, P. Apostoli, G. De Palma, M. Bovenzi, M. Campanini, F. Filon, Titanium Dioxide Nanoparticle Penetration into the Skin and Effects on HaCaT Cells, Int. J. Environ. Res. Public. Health. 12 (2015) 9282–9297. https://doi.org/10.3390/ijerph120809282.

[306] K. Jones, J. Morton, I. Smith, K. Jurkschat, A.-H. Harding, G. Evans, Human in vivo and in vitro studies on gastrointestinal absorption of titanium dioxide nanoparticles, Toxicol. Lett. 233 (2015) 95–101. https://doi.org/10.1016/j.toxlet.2014.12.005.

[307] A. Marucco, M. Prono, D. Beal, E. Alasonati, P. Fisicaro, E. Bergamaschi, M. Carriere, I. Fenoglio, Biotransformation of Food-Grade and Nanometric TiO2 in the Oral–Gastro–Intestinal Tract: Driving Forces and Effect on the Toxicity toward Intestinal Epithelial Cells, Nanomaterials. 10 (2020) 2132. https://doi.org/10.3390/nano10112132.

[308] W. Dudefoi, H. Rabesona, C. Rivard, M. Mercier-Bonin, B. Humbert, H. Terrisse, M.-H. Ropers, In vitro digestion of food grade TiO2 (E171) and TiO2 nanoparticles: physicochemical characterization and impact on the activity of digestive enzymes, Food Funct. 12 (2021) 5975–5988. https://doi.org/10.1039/D1FO00499A.

[309] E. Baranowska-Wójcik, D. Szwajgier, P. Oleszczuk, A. Winiarska-Mieczan, Effects of Titanium Dioxide Nanoparticles Exposure on Human

Health—a Review, Biol. Trace Elem. Res. 193 (2020) 118–129. https://doi.org/10.1007/s12011-019-01706-6.

[310] D.B. Warheit, E.M. Donner, Risk assessment strategies for nanoscale and fine-sized titanium dioxide particles: Recognizing hazard and exposure issues, Food Chem. Toxicol. 85 (2015) 138–147. https://doi.org/10.1016/j.fct.2015.07.001.

[311] J. Wang, G. Zhou, C. Chen, H. Yu, T. Wang, Y. Ma, G. Jia, Y. Gao, B. Li, J. Sun, Acute toxicity and biodistribution of different sized titanium dioxide particles in mice after oral administration, Toxicol. Lett. 168 (2007) 176–185. https://doi.org/10.1016/j.toxlet.2006.12.001.

[312] M.G. Ammendolia, F. Iosi, F. Maranghi, R. Tassinari, F. Cubadda, F. Aureli, A. Raggi, F. Superti, A. Mantovani, B. De Berardis, Short-term oral exposure to low doses of nano-sized TiO 2 and potential modulatory effects on intestinal cells, Food Chem. Toxicol. 102 (2017) 63–75. https://doi.org/10.1016/j.fct.2017.01.031.

[313] L. Zhao, J. Chang, W. Zhai, Effect of Crystallographic Phases of TiO2 on Hepatocyte Attachment, Proliferation and Morphology, J. Biomater. Appl. 19 (2005) 237–252. https://doi.org/10.1177/0885328205047218.

[314] C.-C. Li, S.-J. Chang, M.-Y. Tai, Surface Chemistry and Dispersion Property of TiO2 Nanoparticles: Rapid Communications of the American Ceramic Society, J. Am. Ceram. Soc. 93 (2010) 4008–4010. https://doi.org/10.1111/j.1551-2916.2010.04222.x.

[315] Z.E. Allouni, M.R. Cimpan, P.J. Høl, T. Skodvin, N.R. Gjerdet, Agglomeration and sedimentation of TiO2 nanoparticles in cell culture medium, Colloids Surf. B Biointerfaces. 68 (2009) 83–87. https://doi.org/10.1016/j.colsurfb.2008.09.014.

[316] K. Suttiponparnit, J. Jiang, M. Sahu, S. Suvachittanont, T. Charinpanitkul, P. Biswas, Role of Surface Area, Primary Particle Size, and Crystal Phase on Titanium Dioxide Nanoparticle Dispersion Properties, Nanoscale Res Lett. 6 (2011) 27. https://doi.org/10.1007/s11671-010-9772-1.

[317] M. Kosmulski, The significance of the difference in the point of zero charge between rutile and anatase, Adv. Colloid Interface Sci. 99 (2002) 255–264. https://doi.org/10.1016/S0001-8686(02)00080-5.

[318] B.J. Teubl, C. Schimpel, G. Leitinger, B. Bauer, E. Fröhlich, A. Zimmer, E. Roblegg, Interactions between nano-TiO2 and the oral cavity: Impact of nanomaterial surface hydrophilicity/hydrophobicity, J. Hazard. Mater. 286 (2015) 298–305. https://doi.org/10.1016/j.jhazmat.2014.12.064.

[319] T.M. Sager, D.W. Porter, V.A. Robinson, W.G. Lindsley, D.E. Schwegler-Berry, V. Castranova, Improved method to disperse nanoparticles for *in vitro* and *in vivo* investigation of toxicity, Nanotoxicology. 1 (2007) 118–129. https://doi.org/10.1080/17435390701381596.

[320] Z. Ji, X. Jin, S. George, T. Xia, H. Meng, X. Wang, E. Suarez, H. Zhang, E.M.V. Hoek, H. Godwin, A.E. Nel, J.I. Zink, Dispersion and Stability

Optimization of TiO $_2$ Nanoparticles in Cell Culture Media, Environ. Sci. Technol. 44 (2010) 7309–7314. https://doi.org/10.1021/es100417s.

[321] V. Pareek, A. Bhargava, V. Bhanot, R. Gupta, N. Jain, J. Panwar, Formation and Characterization of Protein Corona Around Nanoparticles: A Review, J. Nanosci. Nanotechnol. 18 (2018) 6653–6670. https://doi.org/10.1166/jnn.2018.15766.

[322] E. Fröhlich, E. Roblegg, Oral uptake of nanoparticles: human relevance and the role of in vitro systems, Arch. Toxicol. 90 (2016) 2297–2314. https://doi.org/10.1007/s00204-016-1765-0.

[323] Y. Sun, T. Zhen, Y. Li, Y. Wang, M. Wang, X. Li, Q. Sun, Interaction of food-grade titanium dioxide nanoparticles with pepsin in simulated gastric fluid, LWT. 134 (2020) 110208. https://doi.org/10.1016/j.lwt.2020.110208.

[324] I.S. Sohal, Y.K. Cho, K.S. O'Fallon, P. Gaines, P. Demokritou, D. Bello, Dissolution Behavior and Biodurability of Ingested Engineered Nanomaterials in the Gastrointestinal Environment, ACS Nano. 12 (2018) 8115–8128. https://doi.org/10.1021/acsnano.8b02978.

[325] Z.J. Deng, G. Mortimer, T. Schiller, A. Musumeci, D. Martin, R.F. Minchin, Differential plasma protein binding to metal oxide nanoparticles, Nanotechnology. 20 (2009) 455101. https://doi.org/10.1088/0957-4484/20/45/455101.

[326] H. Ruh, B. Kühl, G. Brenner-Weiss, C. Hopf, S. Diabaté, C. Weiss, Identification of serum proteins bound to industrial nanomaterials, Toxicol. Lett. 208 (2012) 41–50. https://doi.org/10.1016/j.toxlet.2011.09.009.

[327] M. Pittol, D. Tomacheski, D.N. Simões, V.F. Ribeiro, R.M.C. Santana, Evaluation of the Toxicity of Silver/Silica and Titanium Dioxide Particles in Mammalian Cells, Braz. Arch. Biol. Technol. 61 (2018). https://doi.org/10.1590/1678-4324-2018160667.

[328] M. Rosłon, A. Jastrzębska, K. Sitarz, I. Książek, M. Koronkiewicz, E. Anuszewska, M. Jaworska, J. Dudkiewicz-Wilczyńska, W. Ziemkowska, D. Basiak, A. Rozmys?owska-Wojciechowska, A. Olszyna, The toxicity in vitro of titanium dioxide nanoparticles modified with noble metals on mammalian cells, Int. J. Appl. Ceram. Technol. 16 (2019) 481–493. https://doi.org/10.1111/ijac.13128.

[329] K. Geoffrey, A.N. Mwangi, S.M. Maru, Sunscreen products: Rationale for use, formulation development and regulatory considerations, Saudi Pharm. J. 27 (2019) 1009–1018. https://doi.org/10.1016/j.jsps.2019.08.003.

[330] Ngoc, Tran, Moon, Chae, Park, Lee, Recent Trends of Sunscreen Cosmetic: An Update Review, Cosmetics. 6 (2019) 64. https://doi.org/10.3390/cosmetics6040064.

[331] L.L. Chen, S.Q. Wang, Nanotechnology in Photoprotection, in: Nanosci. Dermatol., Elsevier, 2016: pp. 229–236. https://doi.org/10.1016/B978-0-12-802926-8.00018-5.

[332] M.M. Viana, V.F. Soares, N.D.S. Mohallem, Synthesis and characterization of TiO2 nanoparticles, Ceram. Int. 36 (2010) 2047–2053. https://doi.org/10.1016/j.ceramint.2010.04.006.

[333] A. Wiesenthal, L. Hunter, S. Wang, J. Wickliffe, M. Wilkerson, Nanoparticles: small and mighty: Nanoparticles, Int. J. Dermatol. 50 (2011) 247–254. https://doi.org/10.1111/j.1365-4632.2010.04815.x.

[334] V. Schmitt, M. Destribats, R. Backov, Colloidal particles as liquid dispersion stabilizer: Pickering emulsions and materials thereof, Comptes Rendus Phys. 15 (2014) 761–774. https://doi.org/10.1016/j.crhy.2014.09.010.

[335] H. Lambers, S. Piessens, A. Bloem, H. Pronk, P. Finkel, Natural skin surface pH is on average below 5, which is beneficial for its resident flora, Int. J. Cosmet. Sci. 28 (2006) 359–370. https://doi.org/10.1111/j.1467-2494.2006.00344.x.

[336] S. Wang, C. Wei, Y. Gong, J. Lv, C. Yu, J. Yu, Cellulose nanofiber-assisted dispersion of cellulose nanocrystals@polyaniline in water and its conductive films, RSC Adv. 6 (2016) 10168–10174. https://doi.org/10.1039/C5RA19346J.

[337] Q. Chen, N. Wu, Y. Gao, X. Wang, J. Wu, G. Ma, Alum Pickering Emulsion as Effective Adjuvant to Improve Malaria Vaccine Efficacy, Vaccines. 9 (2021) 1244. https://doi.org/10.3390/vaccines9111244.

[338] Y. Xia, J. Wu, W. Wei, Y. Du, T. Wan, X. Ma, W. An, A. Guo, C. Miao, H. Yue, S. Li, X. Cao, Z. Su, G. Ma, Exploiting the pliability and lateral mobility of Pickering emulsion for enhanced vaccination, Nat. Mater. 17 (2018) 187–194. https://doi.org/10.1038/nmat5057.

[339] M.H. Asfour, H. Elmotasem, D.M. Mostafa, A.A.A. Salama, Chitosan based Pickering emulsion as a promising approach for topical application of rutin in a solubilized form intended for wound healing: In vitro and in vivo study, Int. J. Pharm. 534 (2017) 325–338. https://doi.org/10.1016/j.ijpharm.2017.10.044.

[340] X. Bao, J. Wu, G. Ma, Sprayed Pickering emulsion with high antibacterial activity for wound healing, Prog. Nat. Sci. Mater. Int. 30 (2020) 669–676. https://doi.org/10.1016/j.pnsc.2020.08.001.

[341] K. Raziyeva, Y. Kim, Z. Zharkinbekov, K. Kassymbek, S. Jimi, A. Saparov, Immunology of Acute and Chronic Wound Healing, Biomolecules. 11 (2021) 700. https://doi.org/10.3390/biom11050700.

[342] L.C. Kloth, Electrical Stimulation for Wound Healing: A Review of Evidence From In Vitro Studies, Animal Experiments, and Clinical Trials, Int. J. Low. Extrem. Wounds. 4 (2005) 23–44. https://doi.org/10.1177/1534734605275733.

[343] R. Gharibi, H. Yeganeh, H. Gholami, Z.M. Hassan, Aniline tetramer embedded polyurethane/siloxane membranes and their corresponding

nanosilver composites as intelligent wound dressing materials, RSC Adv. (2014) 10.1039.C4RA11454J. https://doi.org/10.1039/C4RA11454J.

[344] J. Gong, J. Li, J. Xu, Z. Xiang, L. Mo, Research on cellulose nanocrystals produced from cellulose sources with various polymorphs, RSC Adv. 7 (2017) 33486–33493. https://doi.org/10.1039/C7RA06222B.

[345] V. Kašpárková, D. Jasenská, Z. Capáková, N. Maráková, J. Stejskal, P. Bober, M. Lehocký, P. Humpolíček, Polyaniline colloids stabilized with bioactive polysaccharides: Non-cytotoxic antibacterial materials, Carbohydr. Polym. 219 (2019) 423–430. https://doi.org/10.1016/j.carbpol.2019.05.038.

[346] J.-H. Yang, C.-H. Lee, N.A. Monteiro-Riviere, J.E. Riviere, C.-L. Tsang, C.-C. Chou, Toxicity of jet fuel aliphatic and aromatic hydrocarbon mixtures on human epidermal Keratinocytes: evaluation based on in vitro cytotoxicity and interleukin-8 release, Arch. Toxicol. 80 (2006) 508–523. https://doi.org/10.1007/s00204-006-0069-1.

[347] K.A. Traul, A. Driedger, D.L. Ingle, D. Nakhasi, Review of the toxicologic properties of medium-chain triglycerides, Food Chem. Toxicol. 38 (2000) 79–98. https://doi.org/10.1016/S0278-6915(99)00106-4.

[348] W. Hu, S. Chen, Z. Yang, L. Liu, H. Wang, Flexible Electrically Conductive Nanocomposite Membrane Based on Bacterial Cellulose and Polyaniline, J. Phys. Chem. B. 115 (2011) 8453–8457. https://doi.org/10.1021/jp204422v.

[349] M.H. Salehi, H. Golbaten-Mofrad, S.H. Jafari, V. Goodarzi, M. Entezari, M. Hashemi, S. Zamanlui, Electrically conductive biocompatible composite aerogel based on nanofibrillated template of bacterial cellulose/polyaniline/nano-clay, Int. J. Biol. Macromol. 173 (2021) 467–480. https://doi.org/10.1016/j.ijbiomac.2021.01.121.

[350] Z. Lin, Z. Guan, Z. Huang, New Bacterial Cellulose/Polyaniline Nanocomposite Film with One Conductive Side through Constrained Interfacial Polymerization, Ind. Eng. Chem. Res. 52 (2013) 2869–2874. https://doi.org/10.1021/ie303297b.

[351] H. Wang, E. Zhu, J. Yang, P. Zhou, D. Sun, W. Tang, Bacterial Cellulose Nanofiber-Supported Polyaniline Nanocomposites with Flake-Shaped Morphology as Supercapacitor Electrodes, J. Phys. Chem. C. 116 (2012) 13013–13019. https://doi.org/10.1021/jp301099r.

[352] B.-H. Lee, H.-J. Kim, H.-S. Yang, Polymerization of aniline on bacterial cellulose and characterization of bacterial cellulose/polyaniline nanocomposite films, Curr. Appl. Phys. 12 (2012) 75–80. https://doi.org/10.1016/j.cap.2011.04.045.

[353] D.H. Truong, M.S. Dam, E. Bujna, J. Rezessy-Szabo, C. Farkas, V.N.H. Vi, O. Csernus, V.D. Nguyen, N. Gathergood, L. Friedrich, M. Hafidi, V.K. Gupta, Q.D. Nguyen, In situ fabrication of electrically conducting bacterial cellulose-polyaniline-titanium-dioxide composites with the immobilization

of Shewanella xiamenensis and its application as bioanode in microbial fuel cell, Fuel. 285 (2021) 119259. https://doi.org/10.1016/j.fuel.2020.119259.

[354] D. Müller, J.S. Mandelli, J.A. Marins, B.G. Soares, L.M. Porto, C.R. Rambo, G.M.O. Barra, Electrically conducting nanocomposites: preparation and properties of polyaniline (PAni)-coated bacterial cellulose nanofibers (BC), Cellulose. 19 (2012) 1645–1654. https://doi.org/10.1007/s10570-012-9754-9.

[355] E. Alonso, M. Faria, F. Mohammadkazemi, M. Resnik, A. Ferreira, N. Cordeiro, Conductive bacterial cellulose-polyaniline blends: Influence of the matrix and synthesis conditions, Carbohydr. Polym. 183 (2018) 254–262. https://doi.org/10.1016/j.carbpol.2017.12.025.

[356] H.-J. Lee, T.-J. Chung, H.-J. Kwon, H.-J. Kim, W.T.Y. Tze, Fabrication and evaluation of bacterial cellulose-polyaniline composites by interfacial polymerization, Cellulose. 19 (2012) 1251–1258. https://doi.org/10.1007/s10570-012-9705-5.

[357] D.Y. Liu, G.X. Sui, D. Bhattacharyya, Synthesis and characterisation of nanocellulose-based polyaniline conducting films, Compos. Sci. Technol. 99 (2014) 31–36. https://doi.org/10.1016/j.compscitech.2014.05.001.

[358] N.C. Nepomuceno, A.A.A. Seixas, E.S. Medeiros, T.J.A. Mélo, Evaluation of conductivity of nanostructured polyaniline/cellulose nanocrystals (PANI/CNC) obtained via in situ polymerization, J. Solid State Chem. 302 (2021) 122372. https://doi.org/10.1016/j.jssc.2021.122372.

[359] R.L. Razalli, M.M. Abdi, P.M. Tahir, A. Moradbak, Y. Sulaiman, L.Y. Heng, Polyaniline-modified nanocellulose prepared from Semantan bamboo by chemical polymerization: preparation and characterization, RSC Adv. 7 (2017) 25191–25198. https://doi.org/10.1039/C7RA03379F.

[360] D. Zhang, L. Zhang, B. Wang, G. Piao, Nanocomposites of Polyaniline and Cellulose Nanocrystals Prepared in Lyotropic Chiral Nematic Liquid Crystals, J. Mater. 2013 (2013) 1–6. https://doi.org/10.1155/2013/614507.

[361] S. Zhang, G. Sun, Y. He, R. Fu, Y. Gu, S. Chen, Preparation, Characterization, and Electrochromic Properties of Nanocellulose-Based Polyaniline Nanocomposite Films, ACS Appl. Mater. Interfaces. 9 (2017) 16426–16434. https://doi.org/10.1021/acsami.7b02794.

[362] M. Cheng, J. Xia, J. Hu, Q. Liu, T. Wei, Y. Ling, W. Li, B. Liu, Nitrogen and Oxygen Codoped Carbon Anode Fabricated Facilely from Polyaniline Coated Cellulose Nanocrystals for High-Performance Li-Ion Batteries, ACS Appl. Energy Mater. 4 (2021) 9902–9912. https://doi.org/10.1021/acsaem.1c01900.

[363] X. Wang, Y. Tang, X. Zhu, Y. Zhou, X. Hong, Preparation and characterization of polylactic acid/polyaniline/nanocrystalline cellulose nanocomposite films, Int. J. Biol. Macromol. 146 (2020) 1069–1075. https://doi.org/10.1016/j.ijbiomac.2019.09.233.

[364] Q. Wu, Y.-F. Qin, L. Chen, Z.-Y. Qin, Conductive Polyaniline/Cellulose Nanocrystals Composite for Ammonia Gas Detection, in: Comput. Sci. Eng. Technol. CSET2015 Med. Sci. Biol. Eng. MSBE2015, WORLD SCIENTIFIC, Hong Kong, 2016: pp. 670–675. https://doi.org/10.1142/9789814651011_0093.

[365] H. Namazi, M. Baghershiroudi, R. Kabiri, Preparation of Electrically Conductive Biocompatible Nanocomposites of Natural Polymer Nanocrystals With Polyaniline via *In Situ* Chemical Oxidative Polymerization, Polym. Compos. 38 (2017) E49–E56. https://doi.org/10.1002/pc.23943.

[366] G. Cao, X. Gao, L. Wang, H. Cui, J. Lu, Y. Meng, W. Xue, C. Cheng, Y. Tian, Y. Tian, Easily Synthesized Polyaniline@Cellulose Nanowhiskers Better Tune Network Structures in Ag-Based Adhesives: Examining the Improvements in Conductivity, Stability, and Flexibility, Nanomaterials. 9 (2019) 1542. https://doi.org/10.3390/nano9111542.

[367] M.J. Silva, A.O. Sanches, E.S. Medeiros, L.H.C. Mattoso, C.M. McMahan, J.A. Malmonge, Nanocomposites of natural rubber and polyaniline-modified cellulose nanofibrils, J. Therm. Anal. Calorim. 117 (2014) 387–392. https://doi.org/10.1007/s10973-014-3719-1.

[368] M.L. Auad, T. Richardson, W.J. Orts, E.S. Medeiros, L.H. Mattoso, M.A. Mosiewicki, N.E. Marcovich, M.I. Aranguren, Polyaniline-modified cellulose nanofibrils as reinforcement of a smart polyurethane: Cellulose nanofibril-reinforced smart polyurethane, Polym. Int. 60 (2011) 743–750. https://doi.org/10.1002/pi.3004.

[369] L.H.C. Mattoso, E.S. Medeiros, D.A. Baker, J. Avloni, D.F. Wood, W.J. Orts, Electrically Conductive Nanocomposites Made from Cellulose Nanofibrils and Polyaniline, J. Nanosci. Nanotechnol. 9 (2009) 2917–2922. https://doi.org/10.1166/jnn.2009.dk24.

[370] M.J. Silva, A.O. Sanches, L.F. Malmonge, E.S. Medeiros, M.F. Rosa, C.M. McMahan, J.A. Malmonge, Conductive Nanocomposites Based on Cellulose Nanofibrils Coated with Polyaniline-DBSA Via *In Situ* Polymerization, Macromol. Symp. 319 (2012) 196–202. https://doi.org/10.1002/masy.201100156.

[371] G. Xu, D. Xu, J. Zhang, K. Wang, Z. Chen, J. Chen, Q. Xu, Controlled fabrication of PANI/CNF hybrid films: Molecular interaction induced various micromorphologies and electrochemical properties, J. Colloid Interface Sci. 411 (2013) 204–212. https://doi.org/10.1016/j.jcis.2013.08.024.

[372] D.A. Gopakumar, A.R. Pai, Y.B. Pottathara, D. Pasquini, L. Carlos de Morais, M. Luke, N. Kalarikkal, Y. Grohens, S. Thomas, Cellulose Nanofiber-Based Polyaniline Flexible Papers as Sustainable Microwave Absorbers in the X-Band, ACS Appl. Mater. Interfaces. 10 (2018) 20032–20043. https://doi.org/10.1021/acsami.8b04549.

[373] N.D. Luong, J.T. Korhonen, A.J. Soininen, J. Ruokolainen, L.-S. Johansson, J. Seppälä, Processable polyaniline suspensions through in situ polymerization onto nanocellulose, Eur. Polym. J. 49 (2013) 335–344. https://doi.org/10.1016/j.eurpolymj.2012.10.026.

[374] P. Humpolíček, K.A. Radaszkiewicz, V. Kašpárková, J. Stejskal, M. Trchová, Z. Kuceková, H. Vičarová, J. Pacherník, M. Lehocký, A. Minařík, Stem cell differentiation on conducting polyaniline, RSC Adv. 5 (2015) 68796–68805. https://doi.org/10.1039/C5RA12218J.

[375] M. Gizdavic-Nikolaidis, J. Travas-Sejdic, P.A. Kilmartin, G.A. Bowmaker, R.P. Cooney, Evaluation of antioxidant activity of aniline and polyaniline, Curr. Appl. Phys. 4 (2004) 343–346. https://doi.org/10.1016/j.cap.2003.11.044.

[376] E.N. Zare, M.M. Lakouraj, Biodegradable polyaniline/dextrin conductive nanocomposites: synthesis, characterization, and study of antioxidant activity and sorption of heavy metal ions, Iran. Polym. J. 23 (2014) 257–266. https://doi.org/10.1007/s13726-014-0221-3.

[377] R. Karimi-Soflou, S. Nejati, A. Karkhaneh, Electroactive and antioxidant injectable in-situ forming hydrogels with tunable properties by polyethylenimine and polyaniline for nerve tissue engineering, Colloids Surf. B Biointerfaces. 199 (2021) 111565. https://doi.org/10.1016/j.colsurfb.2021.111565.

[378] D. Jasenská, V. Kašpárková, O. Vašíček, L. Münster, A. Minařík, S. Káčerová, E. Korábková, L. Urbánková, J. Vícha, Z. Capáková, E. Falleta, C. Della Pina, M. Lehocký, K. Skopalová, P. Humpolíček, Enzyme-Catalyzed Polymerization Process: A Novel Approach to the Preparation of Polyaniline Colloidal Dispersions with an Immunomodulatory Effect, Biomacromolecules. 23 (2022) 3359–3370. https://doi.org/10.1021/acs.biomac.2c00371.

[379] N. Lin, A. Dufresne, Nanocellulose in biomedicine: Current status and future prospect, Eur. Polym. J. 59 (2014) 302–325. https://doi.org/10.1016/j.eurpolymj.2014.07.025.

[380] M.N.F. Norrrahim, N.M. Nurazzi, M.A. Jenol, M.A.A. Farid, N. Janudin, F.A. Ujang, T.A.T. Yasim-Anuar, S.U.F. Syed Najmuddin, R.A. Ilyas, Emerging development of nanocellulose as an antimicrobial material: an overview, Mater. Adv. 2 (2021) 3538–3551. https://doi.org/10.1039/D1MA00116G.

[381] Z. Kucekova, V. Kasparkova, P. Humpolicek, P. Sevcikova, J. Stejskal, Antibacterial properties of polyaniline-silver films, Chem. Pap. 67 (2013). https://doi.org/10.2478/s11696-013-0385-x.

LIST OF ABBREVIATIONS

ACES	N-(2-acetamido)-2- aminoethanesulfonic acid
AFM	Atomic Force Microscopy
AH	Aniline Hydrochloride
AOT	Sodium Bis-(2-ethylhexyl) Sulfosuccinate
APS	Ammonium Persulfate
ATP	Adenosine Triphosphate
BC	Bacterial Cellulose
BCN	Bacterial Cellulose Nanocrystals
BSA	Bovine Serum Albumin
$CaCl_2$	Calcium Chloride
CAS	Sodium Caseinate
cCNC	Carboxylated Cellulose Nanocrystals
CE	Conventional Emulsification
CI	Creaming Index
CLSM	Confocal Laser Scanning Microscopy
CNC	Cellulose Nanocrystals
CNF	Cellulose Nanofibers
CO_2	Carbon Dioxide
CP	Conducting Polymer
CVD	Chemical Vapor Deposition
DBSA	Dodecylbenzenesulfonic Acid
DLS	Dynamic Light Scattering
DMEM	Dulbecco's Modified Eagle's Medium
DMEM^{Serum}	DMEM Supplemented with Calf Serum
DMF	Dimethylformamide
DOP	*Dendrobium officinale* Polysaccharide
DPPH	1,1-diphenyl-2-picrylhydrazyl
E	Pickering Emulsion
e.g.	*exempli gratia*
ECP	Electrically Conducting Polymer
EE	Encapsulation Efficiency
EHEC	Ethyl(hydroxyethyl) Cellulose
EI	Emulsification Index
etc.	*et cetera*
EU	European Union
ex situ	Out of Place
FBS	Fetal Bovine Serum
$FeCl_3$	Ferric Chloride
FTIR	Fourier Transform Infra Red
GA	Gum Arabic
GIT	Gastrointestinal Tract

H_2O	Water
H_2O_2	Hydrogen Peroxide
HBSS	Hank's Buffered Salt Solution
HCl	Hydrochloric Acid
H_{emuls}	Height of Emulsion Layer
HIPEs	High Internal Phase Emulsions
hiPSC	Human Induced Pluripotent Stem Cells
HLB	Hydrophilic-Lipophilic Balance
HPC	Hydroxypropyl Cellulose
HRP	Horseradish Peroxidase
H_{total}	Total Height of Emulsion
CH	Chitosan
i.e.	*id est*
IEP	Isoelectric Point
IL-6	Inflammatory Cytokine Interleukin 6
in situ	In Its Original Place
in vitro	Withinthe Glass
in vivo	Within the Living
ISO	International Organization for Standardization
IUPAC	International Union of Pure and Applied Chemistry
K_2CO_3	Potassium Carbonate
LB	Langmuir-Blodgett
LbL	Layer-by-Layer
LPS	Lipopolysaccharides
MFC	Microfibrillated Cellulose
MIC	Minimum Inhibitory Concentration
MTT	3-(4,5-dimethylthiazol-2-yl)-2,5-diphenyltetrazolium bromide
n.r.	Not Reported
NaCl	Sodium Chloride
$NaHCO_3$	Sodium Bicarbonate
$NaNO_2$	Sodium Nitrite
NaOH	Sodium Hydroxide
NFC	Nanofibrillated Cellulose
NO	Nitric Oxide
NP	Nanoparticle
O/W	Oil-in-Water
O/W/O	Oil-in-Water-in-Oil
O/W/W	Oil-in-Water-in-Water
OD	Optical Density
OZP	Opsonized Zymosan Particles
PAM	Poly(acrylamide)
PAMPSA	Poly(2-acrylamido-2-methyl-1-propanesulfonate)
PANI	Polyaniline

PBS	Phosphate-Buffered Saline
PBSP	Poly(butadiene-co-styrene-co-2-vinylpyridine)
PCA	Plate Count Agar
PDI	Polydispersity Index
PE	Pickering Emulsion
PECVD	Plasma-Enhanced Chemical Vapor Deposition
PEDOT	Poly(3,4-ethylenedioxythiophene)
PEDOT:PSS	Poly(3,4-ethylenedioxythiophene):(polystyrene sulfonate)
PEO	Poly(ethylene oxide)
PGA	Propylene Glycol Alginate
pH	Potential of Hydrogen
PPy	Polypyrrole
PT	Polythiophene
PU	Polyurethane
PVA	Poly(vinyl alcohol)
PVP	Polyvinylpyrrolidone
ROS	Reactive Oxygen Species
SC	Scavenging Activity
SCDLP	Soybean Casein Digest Lecithin Polysorbate
SD	Standard Deviation
SDBS	Sodium dodecylbenzenesulfonate
SDS	Sodium Dodecyl Sulphate
SEM	Scanning Electron Microscope
SGF	Simulated Gastric Fluid
SGF^{Pepsin}	Simulated Gastric Fluid Supplemented with Pepsin
SH	Sodium Hyaluronate
SIF	Simulated Intestinal Fluid
$SIF^{Pancreatin}$	Simulated Intestinal Fluid Supplemented with Pancreatin
SiO_2	Silicon Dioxide
SPF	Sun Protection Factor
T	Caprylic/capric Triglyceride
TEM	Transmission Electron Microscopy
TEMPO	(2,2,6,6-Tetramethylpiperidin-1-yl)oxyl
TiO_2	Titanium Dioxide
TOCN	TEMPO-Oxidized Cellulose Nanofibers
TPP	Tissue Polystyrene Culture Dishes
TS	Technical Specifications
TSB	Tryptic Soy Broth
U	Undecane
UV	Ultraviolet
UV–vis	Ultraviolet-Visible
V_{emuls}	Volume of Emulsion Layer
V_{encaps}	Volume Fraction of Encapsulated Oil

via	Way
vs.	Versus
V_{total}	Total Volume of Oil Phase
W/O	Water-in-Oil
W/O/W	Water-in-Oil-in-Water
W/W	Water-in-Water
WPI	Whey Protein Isolate
Zn	Zinc
ZnO	Zinc Oxide

LIST OF UNITS

°C	Degree Celsius
CFU mL^{-1}	Colony Forming Units per Millilitre
cm	Centimetre
g	Gram
g cm^{-3}	Grams per Cubic Centimetre
g L^{-1}	Gram per Litre
g mol^{-1}	Gram per Mole
h	Hour
Hz	Herz
kHz	Kilohertz
kV	Kilovolt
L	Liter
M	Molarity (Mole per Litre)
mg	Milligram
mg mL^{-1}	Milligrams per Millilitre
min	Minute
mL	Millilitre
mM	Millimolar
mmol L^{-1}	Millimole per Litre
mN m^{-1}	Millinewton per Metre
mV	Milivolt
N m^{-1}	Newton per Meter
ng mL^{-1}	Nanogram per Millilitre
nm	Nanometre
rpm	Revolutions per Minute
S cm^{-1}	Siemens per Centimetre
S m^{-1}	Siemens per Metre
Sec	Second
U mL^{-1}	Units per Millilitre
vol%	Percentage by Volume
W	Watt
wt%	Percentage by Mass
µg g^{-1}	Microgram per Gram
µg mL^{-1}	Microgram per Millilitre
µL	Microlitre
µm	Micrometre
µM	Micromole
µmol L^{-1}	Micromole per Litre

LIST OF SYMBOLS

%	Percent
$<$	Less Than
$>$	Greater Than
°	Degree
θ	Contact Angle
cos	Cosinus
D[4,3]	Volume Mean Diameter
p	Para
r	Radius
β	Beta
γ^{AB}	Polar Parts of Surface Energy
γ^{LW}	Dispersive Parts of Surface Energy
γ^{ow}	Interfacial Tension at Oil/Water
γ^{tot}	Total Surface Energy
ΔGd	Minimum Desorption Energy
ζ	Zeta Potential
λ	Wavelength
π	Pi Covalent Bond
ρ	Density

LIST OF FIGURES

LIST OF TABLES

LIST OF PUBLICATIONS

Publications in journal with impact factors

1. **Korábková, E.**; Kašpárková, V.; Jasenská, D.; Moricová, D.; Daďová, E.; Truong, T.H.; Capáková, Z.; Vícha, J.; Pelková, J.; Humpolíček, P. Behaviour of Titanium Dioxide Particles in Artificial Body Fluids and Human Blood Plasma. *Int. J. Mol. Sci.* 2021, **22**, 10614.

2. **Korábková, E.**; Kašpárková, V.; Vašíček, O.; Víchová Z.; Káčerová, S.; Valášková, K.; Urbánková, L.; Vícha, J.; Munster, L.; Skopalová, K.; Humpolíček, P. Pickering Emulsions as an Effective Route for the Preparation of Bioactive Composites: A Study of Nanocellulose/polyaniline Particles with Immunomodulatory Effect. *Submitted manuscript, under review.*

3. **Korábková, E.**; , Boeva, Z.; Radaszkiewiczc, K. A.; Skopalová, K.; Kašpárková, V.; Xu, W.; Pacherník, J.; Minařík, A.; Lindfors, T.; Humpolíček, P. Stimuli-Responsive Conductive Thin Film Composites of Conducting Polymers and Cellulose Nanocrystals for Tissue Engineering. *Submitted manuscript.*

4. **Korábková, E.**; Kašpárková, V.; Pacherník, J.; Minařík, A.; Valášková, K.; Káčerová, S.; Özaltin, K.; Moučka, R; Humpolíček, P. Conducting Composite Films Based on Polyaniline and Nanocellulose. *Prepared to submit.*

5. Urbánková, L.; Kašpárková, V.; Egner, P.; Rudolf, O; **Korábková, E**. Caseinate-Stabilized Emulsions of Black Cumin and Tamanu Oils: Preparation, Characterization and Antibacterial Activity. *Polymers.* 2019, **11**, 1951.

6. Truong, T.H.; Musilová, L.; Kašpárková, V.; Jasenská, D.; Ponížil, P.; Minařík, A.; **Korábková, E.**; Münster, L.; Hanulíková, B.; Mráček, A.; Rejmontová, P.; Humpolíček, P. New approach to prepare cytocompatible 3D scaffolds via the combination of sodium hyaluronate and colloidal particles of conductive polymers. *Scientific Reports.* 2022, **12**, 8065.

7. Jasenská, D.; Kašpárková, V.; Vašíček, O.; Münster, L.; Minařík, A.; Káčerová, S.; **Korábková, E.**; Urbánková, L.; Vícha, J.; Capáková, Z.; Falletta, E.; Della Pina, C.; Lehocký, M.; Skopalová, K.; Humpolíček, P. Enzyme-Catalysed Polymerization Process: A Novel Approach to the Preparation of Polyaniline Colloidal Dispersions with Immunomodulatory Effect. *Biomacromolecules.* 2022, **23**, 4958.

Conference proceedings

1. **Korábková, E.**, D. Jasenská, T. H. Truong, J. Vajďák, Z. Capáková, V. Kašpárková, P. Humpolíček. Composite films of conducting polyaniline prepared in colloidal dispersion mode. In: *9th International Colloids Conference*. 2018, Sitges, Spain.

2. **Korábková, E.**, V. Kašpárková, A. Minařík, K. Valášková, S. Káčerová, K. Özaltin, R. Moučka, P. Humpolíček. Conducting composite films based on polyaniline and nanocellulose. In: *11th International Colloids Conference*. 2022, Lisbon, Portugal.

CURRICULUM VITAE

Personal information

Name: Eva Korábková
Date of birth: 02/12/1991
Address: Na Oborách 422, 373 11 Ledenice, Czech Republic
Nationality: Czech
Email: e_korabkova@utb.cz

Work experience

01/2018 – 06/2018   **Tomas Bata University in Zlin, Centre of Polymer Systems**
Performing and Evaluating Experiments – Synthesis of Conducting Polymers, Working with Fundamental Tests in Laboratory of Microbiology
Internship

08/2017 – 09/2017   **Tomas Bata University in Zlin, Faculty of Technology**
Preparation and Characterization of Emulsions
Internship

12/2015 – 09/2016   **Schwan Cosmetics CR, s.r.o., Český Krumlov**
Quality Control in Production of Cosmetics
Internship

09/2015   **Nobilis Tilia, s.r.o., Krásná Lípa**
Preparation of Cosmetic Emulsions
Internship

Education

2018 – Present   **Doctoral's degree**
Tomas Bata University in Zlin, Centre of Polymer Systems
Study Program: Materials Science and Engineering Subject: Biomatrials and Biocomposites
Dissertation Topic: Dispersion Systems Based on Nanoparticles

2016 – 2018   **Master's degree**
Tomas Bata University in Zlin, Faculty of Technology
Field of Study: Technology of Fat, Detergent and Cosmetics Production
Master Thesis: Formulation of Pickering Emusions for Topical Application

2012 – 2016   **Bachelor's degree**
Tomas Bata University in Zlin, Faculty of Technology
Field of Study: Technology and Economics of Fat, Cosmetics and Production Detergent

Projects

IGA/CPS/2022/001 – Preparation of Advanced Biomaterials and Their Application: Member of Project Team

JUNG-2020-007 – Development of Biopolymer-Based Hydrogels for Microextrusion: Member of Project Team

IGA/CPS/2021/001 – Biocompatibility of Materials: Member of Project Team

GAČR 20-28732S – Colloidal Systems for Topical Formulations. Pickering Emulsions and Colloids Based on Polymers: Member of Project Team

IGA/CPS/2020/001 – Biocompatibility and Antimicrobial Activity of Materials Member of Project Team

GAČR 19-16861S – Interactions of Biomaterials with Stem Cells in Simulated *in vivo* Conditions: Member of Project Team

IGA/CPS/2019/004 – Biological Properties of Polymers: Member of Project Team

Pedagogic activities

Participation in Teaching of Laboratory Classes:
- Chemistry and Technology of Fats I
- Cosmetic Ingredients
- Sensory Analysis of Cosmetics

Training

05/2019	**Training Course Malvern Panalytical, Phenom a 3P Instruments**
	Malvern Panalytical − velikost, tvar, koncentrace, zeta potenciál a složení částic
	Phenom (Thermo Scientific) − stolní rastrovací elektronové mikroskopy s automatizačním SW
	3P Instruments − sorpce plynů a par, měrný povrch, skeletální hustota, Altamira – chemisorpce
10/2021	**HR Mobility**
	Laboratory of Molecular Science and Engineering, Åbo Akademi University, Turku, Finland

Topic: Electropolymerization of Conducting Polymers in Presence of Biopolymer-Based Stabilizers

11/2021	**Erasmus+ Programme Internship**
	Laboratory of Molecular Science and Engineering, Åbo Akademi University, Turku, Finland
	Topic: Electropolymerization of Conducting Polymers in Presence of Biopolymer-Based Stabilizers

Certifications

- Certificate of Attendance at the Training Session for Internal Auditor of Hazard Analysis and Critical Control Points (HACCP) systém (Konfirm, spol. s r.o., Brno)
- Certificate of Attendance at the Training Session for Internal Auditors of Quality Management Systems Standard ISO 9001:2015 (Konfirm, spol. s r.o., Brno)

Eva Korábková

Dispersion systems based on nanoparticles
Disperzní systémy na bázi nanočástic

Doctoral thesis

This publication has not undergone any proofreading or editorial review.

Year of publication 2023